



INSTITUTO SUPERIOR TÉCNICO

**Development of new photocatalysts for
pharmaceuticals photodegradation by advanced
oxidation processes**

João Rafael Policarpo Ribeiro

Thesis to obtain the Master of Science Degree in

Integrated Master's in Chemical Engineering

Supervisors

Professor João Paulo Costa Tomé

Professor Elisabete Clara Bastos do Amaral Alegria

Examination Committee

Chairperson: Professor Luísa Margarida Dias Ribeiro de Sousa Martins

Supervisor: Professor João Paulo Costa Tomé

Members of the committee:

Dr. Flávio Alberto da Silva Figueira

Dr. Bruno Gonçalo Martins Rocha

April 2022

Acknowledgments

First of all, I would like to express the sincerest form of gratitude for my supervisors Dr. João Tomé and Dr. Elisabete Alegria, not only for the incredible warm welcome I received but also for their guidance, their availability to enlighten me when I had doubts, for the scientific expertise they shared with me, and for the motivation they conferred me, every step of the way. It was absolutely essential for the completion of the task at hand, and I am incredibly grateful.

I would also like to thank PhD students Sara Fernandes and Sandra Beirão for the warm welcome, the help in the first few weeks of this project and for telling me what to expect from the world of organic synthesis. In particular to Sandra Beirão I would like to say thanks for showing me the ropes around a laboratory of organic chemistry and how to work safely and independently.

To Dr. Mohamed Soliman, I sincerely thank him for the help with the Powder X-Ray analysis and for his kind words of support, his advice, and his availability to always help me in whatever form I needed help.

I am most grateful to Dr. Flávio Figueira and Dr. Filipe Paz for sharing with me their expertise in the field of Metal-Organic frameworks and how to navigate the challenging world of synthesis and characterization of this class of material.

I would like to express my deepest gratitude to my colleague and dear friend Mónica Bernardino, who was in the laboratory with me, day in and day out for over a year. Without your company this would have been a much worse experience and your help was invaluable to me.

To my partner, and my love, Catarina Coelho, goes a big acknowledgement. Her unconditional love and support, as well as her relentless believe in my capacity to do a good job gave me the strength and confidence to carry on.

I would also like to leave my appreciation and acknowledgment to all my friends in particular to Rita Boto Pereira, Eduardo Gameiro, Manuel Pinho, and Rui Almeida. University can be an incredibly challenging experience that not always feels rewarding. However, your friendship made it an experience I will never forget and that I will cherish. Thanks guys!

Quero deixar também uma palavra de apreço aos meus pais. Sem o seu amor, os seus sacrifícios, a sua determinação em dar-me tudo o que eles não tiverem oportunidade de ter e a sua fé inabalável em mim, eu não estaria onde estou hoje. Espero que tenha conseguido deixá-los orgulhosos do meu percurso até aqui e prometo fazer tudo o que estiver ao meu alcance para que se mantenham assim. Muito obrigado Fernanda e Carlos.

Finally, I would like to express my gratitude towards the Fundação para a Ciência e a Tecnologia (FCT), Portugal, for the financial support through the project Ref. PTDC/QUI-QIN/29778/2017.

Resumo

A presença de poluentes farmacêuticos em ambiente aquático, constitui atualmente, um enorme perigo para a saúde humana e para o ambiente. Dessa forma, é imperativo desenvolver métodos “verdes” de tratamento de águas, capazes de eliminar totalmente, ou pelo menos transformar estes poluentes em compostos menos perigosos.

O objetivo desta dissertação consistiu em desenvolver redes metalo-orgânicas baseadas em porfirinas (Por-MOFs), com capacidade para atuar como fotocatalisadores em processos de oxidação avançada na degradação de dois compostos farmacêuticos: paracetamol e 17 β -estradiol. Os processos de oxidação avançada já demonstraram eficácia na oxidação de compostos orgânicos, sem formação de produtos secundários perigosos, constituindo assim um método “verde” de tratamento de águas. Os Por-MOFs são uma classe de materiais com propriedades únicas e aplicações em várias áreas científicas e tecnológicas incluindo em fotocatalise.

Durante este projeto foram desenvolvidos dois Por-MOFs de zircônio baseados na tetraquis(4-carboxifenil)porfirina. Os materiais foram caracterizados por Raio-X de pós e a sua atividade (foto)catalítica foi testada na degradação dos fármacos supramencionados. Os estudos catalíticos investigaram a influência de parâmetros como a concentração de catalisador, o efeito de um agente oxidante e o pH. Os resultados demonstraram que valores alcalinos de pH são essenciais para promover a oxidação dos substratos estudados.

Esta dissertação inclui também a preparação de MOFs baseados nas porfirinas tetra-piridil e tetra-S-piridil, como ligandos orgânicos. Os materiais foram caracterizados por Raio-X de pós e utilizados na oxidação catalítica de álcoois secundários assistida por micro-ondas. Infelizmente, os primeiros ensaios revelaram que os materiais híbridos eram pouco estáveis nas condições estudadas.

Palavras-Chave: Tratamento de águas residuais, Poluentes farmacêuticos, Processos de Oxidação Avançada, Fotocatálise, Redes Metalo-Orgânicas, Porfirinas

Abstract

Pharmaceutical pollutants, present in waste, surface, and ground waters, constitute nowadays a serious hazard for human health, as well as a threat to the environment. It is therefore imperative to develop green methods for the treatment of these water bodies, in order to eliminate or at least transform these pollutants into less hazardous compounds.

The goal of this dissertation was to develop new porphyrin based MOFs (Por-MOFs) capable of acting as photocatalysts in Advanced Oxidation Processes (AOPs) for the degradation of two pharmaceutical compounds: paracetamol and 17 β -estradiol. AOPs have shown the capacity to oxidize most organic compounds, without forming hazardous secondary products, constituting a green method of wastewater treatment. Por-MOFs are a class of materials with a myriad of unique properties which has applications in multiple scientific and technological fields, including photocatalysis.

In this project we developed two zirconium Por-MOFs based on tetrakis(4-carboxyphenyl)porphyrin which were characterized by Powder X-Ray diffraction and then tested as (photo)catalysts in the oxidation of the aforementioned pharmaceuticals. The catalytic studies investigated the influence of parameters such as the load of catalyst, the effect of an oxidant agent and the pH. Results indicated that the oxidation of the pharmaceutical substrates was favoured in alkaline reaction medium.

We also reported the preparation of tetra-pyridyl and tetra-S-pyridyl based MOFs, characterized by Powder X-Ray diffraction, for catalytic micro-wave assisted oxidation of secondary alcohols. Preliminary results showed that the hybrid materials have little chemical stability under the reaction conditions used, indicating the necessity for further investigation of optimum reactions conditions.

Keywords: Wastewater treatment, Pharmaceutical Pollutants, Advanced Oxidation Processes (AOPs), Photocatalysis, Metal-Organic Frameworks (MOFs), Porphyrins

Index

Acknowledgments	iii
Resumo	v
Abstract	vii
List of Tables	xi
List of Figures	xiii
List of Schemes	xvii
Abbreviations and Acronyms	xix
1. Introduction	1
1.1 Pharmaceuticals in aquatic environment.....	1
1.2 Metal-Organic Frameworks (MOFs).....	6
1.3 Porphyrins.....	9
1.4 Porphyrin-based MOFs: a unique type of materials	12
2. Synthesis of porphyrin-based MOFs	15
2.1 Objective	15
2.2 Synthesis of the free-base porphyrins	16
2.3 Synthesis of metallic porphyrin complexes	17
2.4 Preparation of porphyrin and metalloporphyrin based MOFs	21
3. Oxidation of pharmaceuticals by Advanced Oxidation Processes	29
3.1 General Overview	29
3.2 Photostability and singlet oxygen production of porphyrins and zirconium Por-MOFs	29
3.3 Photooxidation of paracetamol	32
3.4 Photooxidation of 17 β -estradiol	45
3.5 Oxidation of pharmaceuticals in dark conditions	53
4. Preparation of tetra-pyridyl and tetra-S-pyridyl based MOFs as catalysts for microwave-assisted oxidation of secondary alcohols.....	57
4.1 General Overview	57
4.2 Synthesis of copper porphyrin complexes.....	58
4.3 Preparation of tetra-pyridyl and tetra-S-pyridyl based MOFs.....	58

5.	Conclusions and Outlook.....	63
6.	Experimental Section.....	65
6.1	Materials and Equipment.....	65
6.2	Synthesis of porphyrins and metallic porphyrin complexes	66
6.3	Preparation of porphyrin based MOFs	68
6.4	Catalytic Studies	68
6.5	Synthesis of tetra-pyridyl and tetra-S-pyridyl metallic porphyrin complexes	71
6.6	Preparation of tetra-pyridyl and tetra-S-pyridyl Por-MOFs.....	71
7.	References	73
8.	Appendices	83
8.1	Appendix A: characterization of porphyrins and metalloporphyrins	83
8.2	Appendix B: Photocatalytic studies with the metalloporphyrin Mn(III)TPP(COOH) ₄ and its respective Por-MOF	87
8.3	Appendix C: Catalytic studies in dark conditions.....	89
8.4	Appendix D: Characterization of tetra-pyridyl and tetra-S-pyridyl metalloporphyrins.....	91
8.5	Communications	92

List of Tables

Table 3.1. Values of pH before and after irradiation for each study, as well as the main results from each reaction.	40
Table 3.2. Main reaction conditions and results of the photocatalytic studies for PCM degradation performed with the MOF catalyst $\text{H}_2\text{TPP}(\text{COOH})_4\text{Zr}_4$	41
Table 3.3. Main reaction conditions and results of the photocatalytic studies for E2 degradation performed with the MOF catalyst $\text{H}_2\text{TPP}(\text{COOH})_4\text{Zr}_4$	48

List of Figures

Figure 1.1. Classification of water treatment processes. ^{15–17}	2
Figure 1.2. Modified Jablonski diagram, and schematic photocatalytic mechanism, using a PS as photocatalyst. ^{23,28}	5
Figure 1.3. Summary of the MOFs multiple applications.....	8
Figure 1.4. Summary of the advantages and disadvantages of solvothermal synthesis and slow diffusion MOFs synthesis methods. Adapted from Silva, Patrícia. <i>et al.</i> (2015). ⁴²	9
Figure 1.5. The Porphyrin macrocycle.....	10
Figure 1.6. Nomenclature systems for the unsubstituted porphyrin macrocycle by a) Hans Fischer and b) IUPAC. ⁶³	10
Figure 2.1. Structures and designations of the porphyrins explored in this project.....	15
Figure 2.2. Structure of the metalloporphyrin ZnTPPF₁₆(SC₆H₄COOH)₄	18
Figure 2.3. a) : Powder X-ray diffraction data of MOF H₂TPP(COOH)₄Zr₄ ; b) : . UV-Vis spectra of porphyrin H₂TPP(COOH)₄ (3) and its respective zirconium MOF, both in methanol.	23
Figure 2.4. a) : Powder X-ray diffraction data of MOF Mn(III)TPP(COOH)₄Zr₄ ; b) : UV-Vis spectra of porphyrin Mn(III)TPP(COOH)₄ (7) and its respective zirconium MOF, both in methanol.	23
Figure 2.5. a) : Powder X-ray diffraction data of MOF H₂TPPF₁₆(SC₆H₄COOH)₄Zr₄ ; b) : UV-Vis spectra of porphyrin H₂TPPF₁₆(SC₆H₄COOH)₄ and its respective zirconium MOF in methanol.....	24
Figure 3.1. UV-Vis spectra of the photostability test of porphyrins a) : H₂TPP(COOH)₄ (3) and b) : Mn(III)TPP(COOH)₄ (7).	30
Figure 3.2. Comparative photooxidation of DPBF (16.5 μM) in a DMF/distilled water (9:1) solution or suspension with or without homogeneous photosensitizers H₂TPP(COOH)₄ (3) and Mn(III)TPP(COOH)₄ (7), (0.67 μM) and heterogeneous photosensitizers H₂TPP(COOH)₄Zr₄ (20.9 μM) and Mn(III)TPP(COOH)₄Zr₄ (19.0 μM).	32
Figure 3.3. UV-Vis spectra of an aqueous solution of paracetamol (130 μM, 20 ppm) under white light (18 mW/cm ²) irradiation, at predetermined periods of time.....	33
Figure 3.4. UV-Vis spectra of the reaction mixture of paracetamol (pH 8.5) (130 μM, 20 ppm) and H₂TPP(COOH)₄ (3) (13 μM, 10% molar ratio) with pH = 8.5, under white light irradiation (18 mW/cm ²) and the respective samples analyzed after predetermined periods of time (30-180 min).	34
Figure 3.5. UV-Vis spectra of the reaction mixture of paracetamol (130 μM, 20 ppm) and H₂TPP(COOH)₄ (3) (13 μM, 10% molar ratio) with pH = 8.5 and the respective samples analyzed after predetermined periods of irradiation with white light (18 mW/cm ²), for a) : the first 30 minutes of irradiation; and b) : the last 35 minutes of irradiation.	35
Figure 3.6. UV-Vis spectra of aqueous solutions of paracetamol (20 ppm), <i>p</i> -aminophenol (20 ppm), <i>p</i> -nitrophenol (20 ppm), hydroquinone (20 ppm) and benzoquinone (10 ppm).....	36
Figure 3.7. Paracetamol oxidation mechanism by photocatalysis. ^{106,107}	36

Figure 3.8. Deacylation paracetamol oxidation mechanism by photocatalysis, proposed by Edgar Moctezuma <i>et al.</i> ¹⁰³	37
Figure 3.9. UV-Vis spectra of aqueous solutions of paracetamol (130 μM , 20 ppm) and $\text{H}_2\text{TPP}(\text{COOH})_4$ (3) (13 μM , 10% molar ratio).with pH = 9.5 and pH = 11 and the samples analyzed at different times of irradiation with white light (18 mW/cm ²).....	38
Figure 3.10. UV-Vis spectra of paracetamol (130 μM , 20 ppm) and $\text{H}_2\text{TPP}(\text{COOH})_4$ (13 μM , 10% molar ratio) in solutions with pH=5.5 and pH = 7.0 and of the samples analyzed at different times of irradiation with white light (18 mW/cm ²).	39
Figure 3.11. UV-Vis spectra of paracetamol (130 μM , 20 ppm) and $\text{H}_2\text{TPP}(\text{COOH})_4$ (3) (13 μM , 10% molar ratio) in a solution with pH=2.5 and of the samples analyzed at different times of irradiation with white light (18 mW/cm ²).....	40
Figure 3.12. UV-Vis spectra of the aqueous solutions of paracetamol (130 μM , 20 ppm) and the MOF catalyst $\text{H}_2\text{TPP}(\text{COOH})_4\text{Zr}_4$: a):12.96 μM (10% molar ratio) and b): 60,05 μM (50% molar ratio) and the samples analyzed after predetermined periods of irradiation with white light (18 mW/cm ²).....	42
Figure 3.13. UV-Vis spectra of the aqueous solutions of paracetamol (130 μM , 20 ppm), the MOF catalyst $\text{H}_2\text{TPP}(\text{COOH})_4\text{Zr}_4$: a): 12.96 μM (10% molar ratio) and b): 60,05 μM (50% molar ratio); and H_2O_2 (1.3×10^{-3} M) and the samples analyzed after predetermined periods of irradiation with white light (18 mW/cm ²).....	43
Figure 3.14. UV-Vis spectra of the aqueous solution (pH = 8) of paracetamol (130 μM , 20 ppm) and the MOF catalyst $\text{H}_2\text{TPP}(\text{COOH})_4\text{Zr}_4$ (60,05 μM , 50% molar ratio) and the samples analyzed after predetermined periods of irradiation with white light (18 mW/cm ²).	44
Figure 3.15. UV-Vis spectra of a methanol solution of 17 β -estradiol (E2) (147 μM , 40 ppm) under white light (18 mW/cm ²) and the respective samples analyzed after predetermined periods of irradiation. ...	45
Figure 3.16. a): UV-Vis spectra of the reaction mixture of E2 (147 μM , 40 ppm) and $\text{H}_2\text{TPP}(\text{COOH})_4$ (3) (14.7 μM , 10% molar ratio) under white light irradiation (18 mW/cm ²), for 180 minutes, and the samples analyzed after predetermined periods of time; b): Evolution of the concentration of E2 in the reaction mixture over time, based on HPLC data.	46
Figure 3.17. HPLC results from the sample of the reaction mixture consisting of a methanol solution of E2 (147 μM) and the porphyrin $\text{H}_2\text{TPP}(\text{COOH})_4$ (3) (14.7 μM , 10% molar ratio) analyzed before irradiation (t = 0 minutes).....	47
Figure 3.18. HPLC results from the sample of the reaction mixture consisting of a methanol solution of E2 (147 μM) and the porphyrin $\text{H}_2\text{TPP}(\text{COOH})_4$ (3) (14.7 μM , 10% molar ratio) analyzed after 60 minutes of irradiation. The red circles indicate the possible sub products of the oxidation of E2.	47
Figure 3.19. UV-Vis spectra of the reaction mixture of E2 (147 μM , 40 ppm) and $\text{H}_2\text{TPP}(\text{COOH})_4\text{Zr}_4$: a): 14.7 μM , 10% molar ratio and b): 73.5 μM , 50% molar ratio; under white light irradiation (18 mW/cm ²), for 270 minutes, and the respective samples analyzed after predetermined periods of time.	48
Figure 3.20. UV-Vis spectra of the reaction mixture of E2 (147 μM , 40 ppm), $\text{H}_2\text{TPP}(\text{COOH})_4\text{Zr}_4$ (73.5 μM , 50% molar ratio) and H_2O_2 (1.47×10^{-3} M) under white light irradiation (18 mW/cm ²), for 90 minutes, and the respective samples analyzed after predetermined periods of time.	49

Figure 3.21. a): UV-Vis spectra of the reaction mixture of E2 (147 μ M, 40 ppm) and H₂TPP(COOH)₄Zr₄ (73.5 μ M, 50% molar ratio) (pH \sim 8) under white light irradiation (18 mW/cm ²), for 180 minutes, and the respective samples analyzed after predetermined periods of time; b): Evolution of the concentration of E2 in the reaction mixture over time, based on HPLC data.	50
Figure 3.22. HPLC results from the sample of the reaction mixture consisting of a methanol solution of E2 (147 μ M) and the MOF H₂TPP(COOH)₄Zr₄ (73.5 μ M), with pH \sim 8 analyzed before irradiation (t = 0 minutes).	51
Figure 3.23. HPLC results from the sample of the reaction mixture consisting of a methanol solution of E2 (147 μ M) and the MOF H₂TPP(COOH)₄Zr₄ (73.5 μ M), with pH \sim 8 analyzed after 180 minutes of irradiation. The red circles indicate the possible sub products of the oxidation of E2.	51
Figure 3.24. UV-Vis spectra of the MOF catalyst H₂TPP(COOH)₄Zr₄ during the photooxidation of E2 at pH 8.	52
Figure 3.25. UV-Vis spectra of the reaction mixture of Mn(III)TPP(COOH)₄ (7) (molar ratio catalyst/substrate = 0.1) and H ₂ O ₂ (molar ratio oxidant/substrate = 10) and a): PCM (130 μ M, 20 ppm), b): E2 (40 ppm, 147 μ M). The reactions were left in the dark with stirring for 180 min and the respective samples analyzed after predetermined periods of time.	54
Figure 3.26. UV-Vis spectra of the reaction mixture of Mn(III)TPP(COOH)₄Zr₄ (catalyst/substrate molar ratio = 0.5) and H ₂ O ₂ (oxidant/substrate molar ratio = 10) and a): PCM (130 μ M, 20 ppm), b): E2 (40 ppm, 147 μ M). The reactions were left in the dark with stirring for 80 min and the respective samples analyzed after predetermined periods of time.	55
Figure 4.1. Structure and designation of the porphyrins explored in this section.	57
Figure 4.2. Powder X-ray diffraction data of MOF CuTPyPCu₄	59
Figure 4.3. Powder X-ray diffraction data of MOF CuTPPF₁₆(Spy)₄Cu₄	60
Figure 8.1. UV-Vis spectra of porphyrin H₂TPPF₁₆(SC₂H₄COOH)₄ (1) in methanol.	83
Figure 8.2. UV-Vis spectra of porphyrin H₂TPPF₁₆(SC₆H₄COOH)₄ (2) in methanol.	84
Figure 8.3. UV-Vis spectra of metalloporphyrin ZnTPPF₁₆(SC₂H₄COOH)₄ (5) in methanol.	84
Figure 8.4. UV-Vis spectra of metalloporphyrin Mn(III)TPP(COOH)₄ (7) in methanol.	85
Figure 8.5. UV-Vis spectra of metalloporphyrin Mn(III)TPPF₁₆(SC₆H₄COOH)₄ (8) in methanol.	85
Figure 8.6. UV-Vis spectra of metalloporphyrin Fe(III)CITPPF₁₆(SC₂H₄COOH)₄ (9) in methanol.	86
Figure 8.7. UV-Vis spectra of the reaction solutions with PCM (130 μ M, 20 ppm) and a): the metalloporphyrin Mn(III)TPP(COOH)₄ (7) (13 μ M) and b): the Por-MOF Mn(III)TPP(COOH)₄Zr₄ (13 μ M). The solutions were irradiated for 180 minutes, and samples were analyzed at predetermined periods of time.	87
Figure 8.8. UV-Vis spectra of the reaction solutions with E2 (147 μ M, 40 ppm) and a): the metalloporphyrin Mn(III)TPP(COOH)₄ (7) (14.7 μ M) and b): the Por-MOF Mn(III)TPP(COOH)₄Zr₄ (14.7 μ M). The solutions were irradiated for 210 minutes, and samples were analyzed at predetermined periods of time.	88
Figure 8.9. UV-Vis spectra of the control reaction with PCM (130 μ M, 20 ppm) and the porphyrin catalyst Mn(III)TPP(COOH)₄ (7) (13 μ M, molar ratio catalyst/substrate = 0.1), left under vigorous stirring and dark conditions for 3 hours.	89

Figure 8.10. UV-Vis spectra of the control reaction with PCM (130 μM , 20 ppm) and H_2O_2 (1300 μM , molar ratio oxidant/substrate = 10) as oxidant agent, left under vigorous stirring and dark conditions for 3 hours.....	90
Figure 8.11. UV-Vis spectra of the control reaction with E2 (147 μM , 40 ppm) and the porphyrin catalyst Mn(III)TPP(COOH)₄ (7) (14.7 μM , molar ratio catalyst/substrate = 0.1), left under vigorous stirring and dark conditions for 4 hours.	90
Figure 8.12. UV-Vis spectra of the control reaction with E2 (147 μM , 40 ppm) and H_2O_2 (1470 μM , molar ratio oxidant/substrate = 10) as oxidant agent, left under vigorous stirring and dark conditions for 3 hours.	90
Figure 8.13. UV-Vis spectra of metalloporphyrin CuTPyP (13) in a mixture of dichloromethane and methanol (85:15).	91
Figure 8.14. UV-Vis spectra of metalloporphyrin CuTPPF₁₆(SPy)₄ (14) in a mixture of dichloromethane and methanol (85:15).	91

List of Schemes

- Scheme 2.1 16
- Scheme 2.2 17
- Scheme 2.3 18
- Scheme 2.4 19
- Scheme 2.5 19
- Scheme 2.6 20
- Scheme 2.7 22
- Scheme 2.8 22
- Scheme 2.9 24
- Scheme 2.10 25
- Scheme 2.11 26
- Scheme 3.1 31
- Scheme 4.1 58
- Scheme 4.2 59
- Scheme 4.3 60
- Scheme 4.4 61
- Scheme 4.5 61
- Scheme 4.6 62

Abbreviations and Acronyms

AOP - Advanced Oxidation Processes

CN - Coordination Network

CP - Coordination Polymer

DBB - *o*-dibenzoylbenzene

DMF - *N,N'*-Dimethylformamide

DPBF - Diphenylbenzofurane

E2 - 17 β -estradiol

HPLC - High Performance Liquid Chromatography

IUPAC - International Union of Pure Applied Chemistry

MIL – Materials Institute Lavoisier

MOF – Metal-Organic Framework

MW - Microwave

NMR - Nuclear Magnetic Resonance

PBU – Primary Building Unit

PC - Pharmaceutical Compound

PCM – Paracetamol

PCN – Porous Coordination Network

PDI – Photodynamic Inactivation

PDT - Photodynamic Therapy

Por-MOFs - Porphyrin Metal-Organic Frameworks

PS - Photosensitizer

ROS - Reactive Oxygen Species

SBU - Secondary Building Unit

SNU – Seoul National University

THF - Tetrahydrofuran

TLC - Thin Layer Chromatography

TMS - Tetramethylsilane

UV-Vis - Ultraviolet-visible

XRD - X-Ray Diffraction

1. Introduction

1.1 Pharmaceuticals in aquatic environment

The continuous technological and scientific advances the world as witness in recent decades, have allowed the existence of a wide range of pharmaceuticals used to treat many different types of medical conditions. Despite being an overwhelmingly positive aspect of modern society, it also represents an environmental problem since an increasing volume of pharmaceutical compounds (PCs) is being detected in aquatic environments.¹⁻³ PCs are considered to be pseudopersistent organic pollutants as a result of their continuous discharge into the environment as well as how difficult their removal by common water treatment methods tends to be.^{3,4} Despite being found in relatively low concentrations, usually from ng/L to µg/L, in both surface and wastewaters as well as in groundwater, a wide range of effects of this type of contaminants and how they disrupt the aquatic environment, namely the fauna and flora, has been reported.⁴⁻⁹ In addition, these pollutants also represent a threat to human health.¹⁰ The presence of antibiotics in the aquatic environment is one of the main areas of concern since their presence has been associated with the surge of bacterial species resistant to antibiotics.¹¹⁻¹⁴ Based on this it is possible to affirm that there is a necessity of treating surface, waste and groundwaters in order to transform these organic pollutants into less hazardous compounds or remove them completely from the aquatic environment.

1.1.1 Water treatment for removal of pharmaceutical compounds

The array of conventional water treatment processes can be classified as primary, secondary, or tertiary. Primary treatments are based in physical separation processes designed to remove large sediments, heavier solids, oils, and greases. Secondary treatments consist of biological processes, capable of removing organic pollutants both soluble and insoluble. Tertiary treatments are essentially chemical processes with the goal of disinfecting water so it can be safely utilized for human consumption.¹⁵⁻¹⁷ **Figure 1.1** shows a scheme with the multiple processes which fall under each classification.

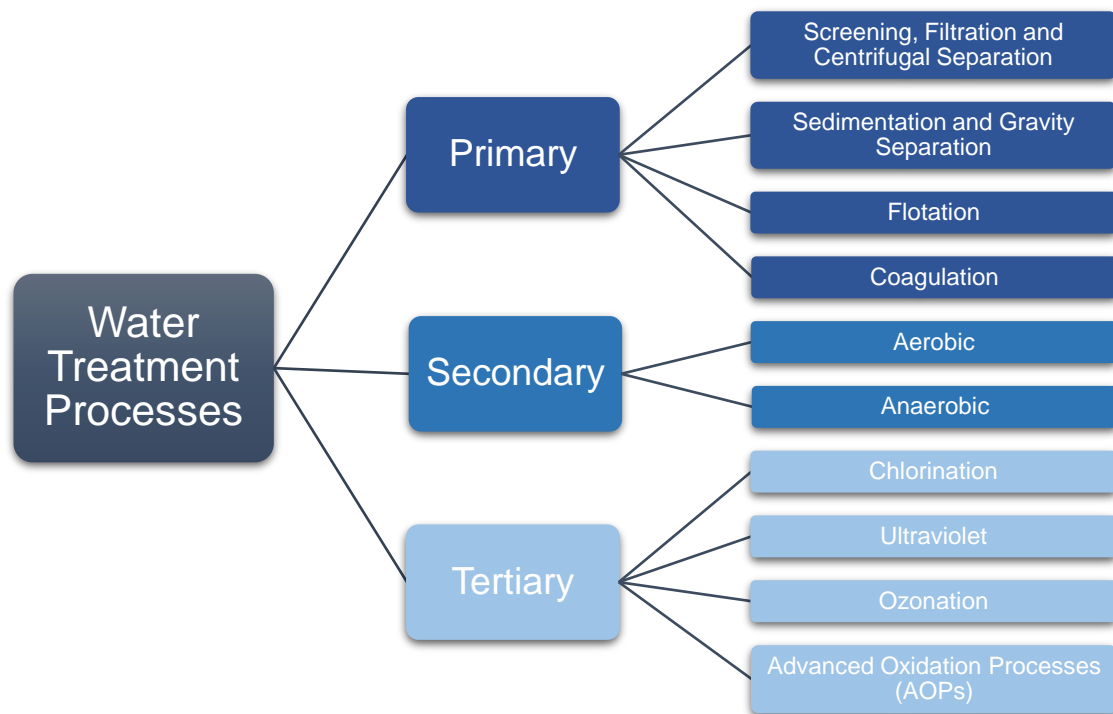


Figure 1.1. Classification of water treatment processes.^{15–17}

The primary and secondary treatments available are not suited or at least ideal to remove or decompose PCs. Nevertheless, some PCs, such as diclofenac or ketoprofen can be removed by biological processes.¹⁵ The chemical processes are the most effective method for the removal of PCs from water. Amongst the different treatments chlorination is the most commonly utilized. This is a consequence of its simple application as well as its capability to inactivate pollutants and its low cost. Despite its strengths, this method of purification of water has its disadvantages mainly the requirement of high dosages of chlorine which can be harmful for human health.^{15,16,18} In light of these facts other technologies have been explored in recent years such as ultraviolet irradiation, ozonation or advanced oxidation processes (AOPs).

While ultraviolet irradiation and ozonation are valid methods for the removal of PCs from water, AOPs are regarded as a technology with tremendous potential for this application and will be the focus of this project. In the next subsection the basic concepts, merits, and hurdles yet to overcome of this technology will be discussed in more detail.

1.1.2 Advanced Oxidation Processes (AOPs)

AOPs consist of chemical reactions capable of producing highly reactive oxidizing species, which have the capacity to oxidize and mineralize most organic compounds.^{19,20} There is a wide range of AOPs in existence that goes from ozone-based methods to UV-based, as well as electrochemical, physical and catalytical AOPs.¹⁹ The treatment of organic wastewater is the main application of this type of process and, when compared to other methods, AOPs demonstrate advantages such as high efficiency of mineralization as well as the limited formation of secondary pollutants. Nevertheless, AOPs have some disadvantages, with the biggest challenges being their establishment as a common method for wastewater treatment in large industrial scale and their high costs, at least for now.^{15,21,22} This technology has been explored for other applications, particularly in the field of air purification.²³

From the different types of AOPs already in existence, this project will focus in the catalytical reactions, which can be conducted in the absence or presence of light. Both catalytic reactions can occur either in homogenous or heterogeneous conditions, dependent on whether the catalyst and the substrate are in the same phase or not.¹⁵ Heterogeneous catalysts offer an undeniable advantage when compared to their homogeneous counterparts, mainly based on their capacity to be reused in multiple catalytic cycles, oftentimes, without significant loss of activity. This allows the reduction of costs even with slightly lower oxidation rates. For this reason, heterogeneous catalysis has been widely explored in recent years, not only for wastewater treatment but also in multiple other applications, with photocatalysis following this trend as well.²⁴

The most common heterogeneous photocatalytic process consists in activating semiconductors with UV irradiation.²⁵ This will set in motion a mechanism in which electron-hole pairs will be generated in the valence band of the semiconductor. The generated holes can, in turn, react either with water present in the medium or with hydroxyl groups to generate hydroxyl radicals.²⁵ Several semiconductors such as, titanium dioxide (TiO₂), zinc oxide (ZnO), tungsten trioxide (WO₃) or vanadate (VO₄) have been reported as effective photocatalysts demonstrating advantages, such as: very low toxicity, easily tunable properties, and low cost.^{15,26} The most explored semiconductor is TiO₂ with multiple studies of its photocatalytic activity having been reported.^{15,20,26} Despite its advantages and vast potential, TiO₂ catalysts have some limitations mainly the poor depth of penetration by the radiation in the semiconductors suspension. This is a consequence of the scattering of light by the opaque particles of the photocatalyst.¹⁵ Furthermore, TiO₂ catalysts absorb only UV radiation (300-400 nm) which precludes the use of the “free of charge” solar irradiation.^{20,27}

Another photocatalysis method consists of utilizing photosensitizers (PS) which absorb visible light and can react with molecular oxygen to form reactive oxygen species (ROS) such as singlet oxygen (¹O₂) and hydroxyl (•OH), peroxy (•OOR) and superoxide anion (•O₂⁻) radicals.^{15,28} The process starts by exposing the PS to irradiation. The absorption of photons (hν) by a ground singlet state (S₀) PS will promote an electron to one of two vibrational levels: S₁^{*} (first excited singlet state) or S₂^{*} (second excited singlet state), depending on the energy of the photons. From this point, multiple phenomena can be

responsible for the dissipation of energy by the electron originating different vibrational levels. Internal conversion from S_2^* as well as vibrational relaxation of S_1^* will lead to the occupation of the lowest vibrational level of S_1^* . It is from this vibrational level that all other processes occur. This is stated by *Kasha's* rule. Processes such as fluorescence, non-radiative relaxation and quenching will yield S_0 . On the other hand, intersystem crossing will yield the first excited triplet state, T_1^* . When compared with S_1^* , T_1^* has a much longer lifetime (10^{-12} s to 10^{-6} s and 10^{-7} s to 10^{-2} s, respectively), thus explaining why most of the intermolecular photoreactions of excited molecules occur from T_1^* , whereas the lifetime of S_1^* only allows intramolecular reactions.^{23,28}

This photodynamic method covers two reaction mechanisms that start in the vibrational level T_1^* , the type I and type II mechanisms. The type I mechanism consists of reactions of transference of electrons from the PS to molecular oxygen, that can be described by **equations 1-4**, yielding multiple ROS. In contrast, the type II mechanism consists of energy transfer from the PS to molecular oxygen upon collision between the two, yielding singlet oxygen. This mechanism is described by **equations 5 and 6**.¹⁵

Type I mechanism



Type II mechanism



The well-known *Jablonski* diagram is an accurate schematic representation of the mechanism of photocatalysis using photosensitizers as catalysts (**Figure 1.2**).^{23,28}

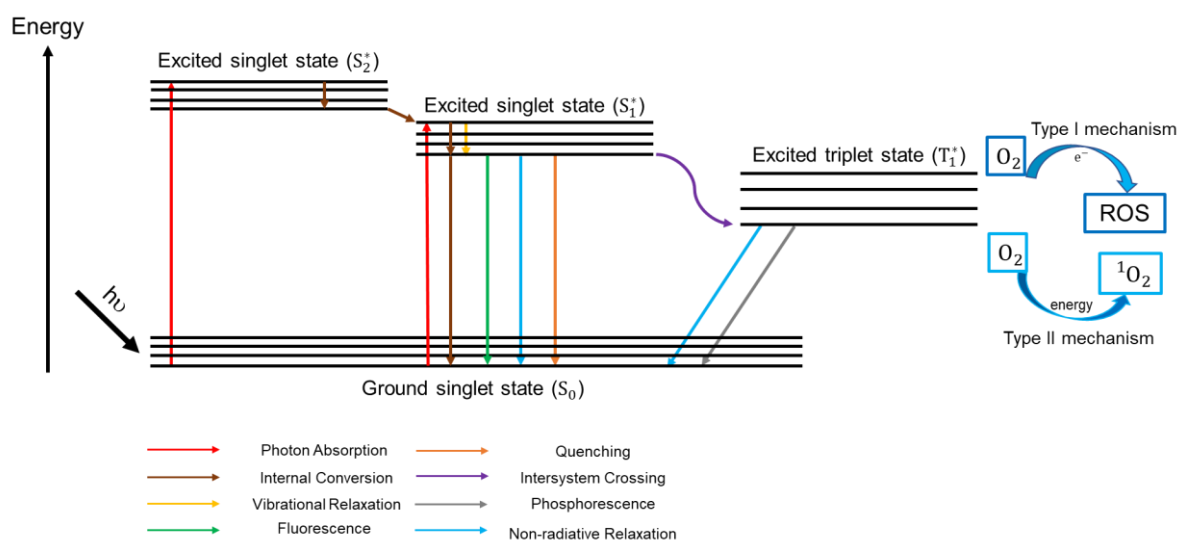


Figure 1.2. Modified *Jablonski* diagram, and schematic photocatalytic mechanism, using a PS as photocatalyst.^{23,28}

This photocatalysis method, based on photosensitizers, has been widely explored in cancer photodynamic therapy (PDT)²⁹, in photoinactivation of microorganisms (PDI)^{30,31} as well as in organic synthesis³², to enumerate some. In addition, its potential to be used as a tertiary wastewater treatment has attracted interest from scientists all around the world in recent years. This methodology is capable of oxidizing organic compounds without originating other hazardous sub products. On top of that, multiple PS can be activated with sunlight avoiding the use of UV-lamps which have much higher rates of energy consumption. These two facts demonstrate why this approach is considered a green method of chemical wastewater treatment.^{15,28}

The preparation of efficient and inexpensive catalysts is utterly essential to the development of photocatalytic AOPs for wastewater treatment. If in the field of semiconductors, TiO_2 has been established as the best and most efficient catalyst, when it comes to photosensitizers, multiple dyes have been explored. From amongst the different options, porphyrins have been piquing the interest of the scientific community.³³ These organic macrocycles have unique photochemical properties which can be easily manipulated. In addition, porphyrins can be immobilized on solid materials to form heterogeneous catalysts which conjugates their photochemical properties with the possibility of their reuse in multiple catalytic cycles. Heterogeneous porphyrin catalysts supported on materials such as zeolites, polymers, nanoparticles, and oxides have been reported.³⁴

Metal-Organic frameworks (MOFs) are another type of material that can be utilized as a porphyrin based heterogeneous PS in photocatalytic AOPs for wastewater treatment. This class of materials has a wide range of interesting functionalities, not only for water remediation but also for multiple other applications as well.³⁵

1.2 Metal-Organic Frameworks (MOFs)

The concept of MOFs was first introduced by Dr. Omar M. Yaghi and his research group in 1995.³⁶ Dr Yaghi and co-workers reported the synthesis of a new material consisting of a symmetric organic molecule which could bind metal ions thus forming a layered, porous, and crystalline structure. This publication established the definition of MOFs as crystalline, porous compounds formed by organic ligands coordinated with metal ions. This definition has been widely accepted by the inorganic chemistry scientific community being utilized in multiple publications over the years.^{37–39} Nevertheless, in recent years, interest in this class of materials has increased significantly even amongst non-specialized public. As a direct result of the growing interest in MOFs, and to avoid ambiguity or confusion with other terms such as coordination polymer (CP) or coordination network (CN), the International Union of Pure Applied Chemistry (IUPAC) has published a recommendation on the definition of these three terms.⁴⁰ According to the 2013 publication by Batten, S. R. *et al.*⁴⁰ MOFs are defined as coordination networks with organic ligands, containing potential voids. This is a broader definition that establishes MOFs and CNs as subsets of CPs. Given the nature of this project, it made sense to adopt a more specific definition that could facilitate the interpretation of the characteristics which are essential to the preparation of MOFs. For that reason, for the remaining of this project, MOFs will be considered to be crystalline and porous materials formed by organic linkers coordinated with metal ions.

The metallic centers and the organic linkers are considered to be the MOFs' primary building units (PBUs) and the number of possible combinations between these are nearly endless. As a consequence, it is possible to prepare MOFs with specific characteristics, useful for predetermined applications. This constitutes the primary motive which explains the exponential interest growth in this class of materials in the last two decades. Furthermore, it has been reported that the properties of a MOF are closely related to the organic PBU.⁴¹ Bearing this in mind, the synthesis of new organic PBUs, or the modification of previous existent ones, allows for the preparation of MOFs with distinct and tailor made properties for a myriad of different applications.⁴²

MOFs have picked up popularity in the field of gas storage as well as capture and removal of gas molecules due to their typical high porosity.^{43,44} Hydrogen (H₂) and methane (CH₄) are considered promising alternatives for the other conventional fuels thereby making their storage essential. A large assortment of MOFs has been synthesized with the propose of facilitating the storage of these gases. Previously described families of MOFs such as PCNs⁴⁵, SNU_s⁴⁶ and MIL_s⁴⁷ have demonstrated great hydrogen storage capacity. When it comes to the storage of methane, MOFs as for instance MIL-101⁴⁸, NU-111⁴⁹ or PCN-14⁵⁰ have shown to be effective materials. With regards to capture of gases, specifically carbon dioxide (CO₂), porous materials, such as MOFs have long been considered a viable option to prevent its release into the atmosphere. The porosity of MOFs allows these materials to trap CO₂ in its channels functioning like gas adsorbers. Some examples of MOFs which have been reported as good CO₂ adsorbers are MOF-177⁵¹, MOF-200⁵² and MOF-210.⁵²

Another field in which MOFs have been significantly explored is luminescence. Due to their crystalline character MOFs with relevant optical properties have been synthesized. The emission of light from these materials can be originated either from the organic PBU or by specific metallic centers such as lanthanides and transition metals. The use of luminescent MOFs has been reported in areas such as biomedicine and nanotechnology⁵², in addition to its common use as sensors⁵³. MOFs have also been reported as promising metal corrosion inhibitors as a consequence of their properties, mainly their high surface areas.⁵⁴

As stated in the previous section of this chapter, MOFs are very interesting materials in the field of heterogeneous catalysis. The most popular heterogeneous catalysts utilized in industrial environment are zeolites.⁴² This class of materials has a large scope of applications related to heterogeneous catalysis, which is a consequence of its unique properties. Nevertheless, zeolites have shown some limitations over the years and, consequently, other materials have been explored with the objective of suppressing those limitations. MOFs are one of those materials and have been studied in multiple catalytic reactions.⁵⁵

The catalytic activity of MOFs is modulated by three distinct factors: i) the metal active sites; ii) the functional organic PBUs' reactivity and iii) the inherent porosity of the material. MOFs constituted by catalytic active metal ions include materials with just one type of metal which provides both catalytic activity as well as the structure, and with multiple different types of metals. In the latter case, one of the metals is responsible for the structural configuration of the MOF whereas the other one acts as a catalytic active site. MOFs whose activity is a consequence of a catalytic active organic linker are less explored. This is a consequence of the necessity of having the reactive functional groups available to interact with the intended substrate. However, the metal ions have a tendency to interact with these organic groups, therefore it is difficult to synthesize MOFs with these characteristics. Finally, there have been reports of MOFs whose catalytic activity is not related to neither the metallic nor the organic PBUs but instead, to the porosity of the material.⁵⁵

MOFs with metal active sites have been utilized as heterogeneous catalysts in hydrogenation reactions, in the oxidation of a wide range of organic substrates, in oxidation of CO to CO₂, in carbonyl cyanosilylation, in hydrodesulfurization and also in photocatalysis, amongst multiple other processes.^{42,55}

With regards to photocatalysis, MOFs have attracted the scientific community's attention, as of late due, to the possibility of combining the effects of adsorbent and photocatalyst in the removal of dyes and other organic contaminants from waste waters, including pharmaceutical compounds.⁵⁶ The MOF family MIL, in particular, has been significantly explored in this field. The MOF MIL-53(Fe), for instance, showed great photo-reactivity in the degradation of the organic dye rhodamine B, in a system of catalyst plus visible light irradiation and hydrogen peroxide as oxidant agent.⁵⁷ The same material showed to be capable of decomposing the pharmaceuticals clofibric acid and carbamazepine, with photodegradation yields of up to 90%, under visible light irradiation.⁵⁸ Dongbo Wang *et al.* tested the MOFs Fe-MIL-100 and Fe-MIL-101 in the photodegradation of tetracycline.⁵⁹ MOF Fe-MIL-100 was able to decompose

only ca. 58% of the substrate whereas Fe-MIL-101 had a degradation efficiency around 97%, under visible light irradiation.

In summary, the vast versatility MOFs possess allied to their multiple possible applications, justifies the increasing scientific and industrial interest in this type of material (**Figure 1.3**).

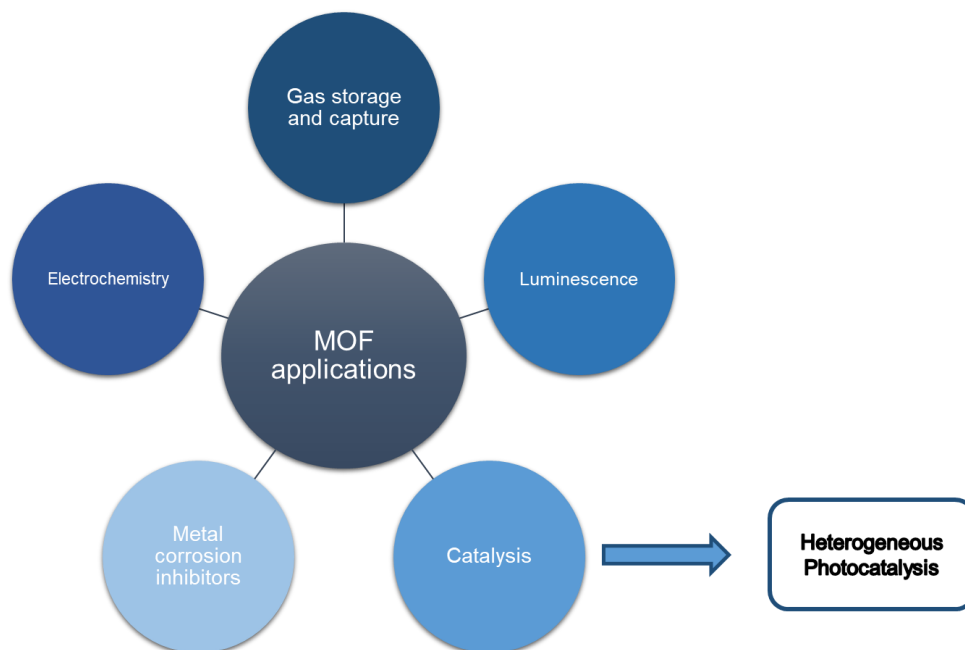


Figure 1.3. Summary of the MOFs multiple applications.

The preparation of a MOF is a complex process involving multiple pieces. The proper selection of the PBUs is of crucial importance. In addition, parameters such as the pressure, the temperature, the reaction time, and pH, all play an essential role in the synthesis of a MOF. In order to obtain MOFs with different properties, several synthetic methods have been successfully employed. Solvothermal synthesis is the default method with the majority of MOFs being prepared via this method, including the materials prepared during the development of this dissertation. The procedure starts by preparing the reaction mixture with the PBUs as well as a solvent, hence the name. The most commonly used solvents are water (in which case the method is called hydrothermal synthesis), and some organic solvents for instance, *N,N'*-dimethylformamide (DMF) and tetrahydrofuran (THF). The mixture is transferred to a closed system, usually an autoclave, and put in an oven for a predetermined period of time, often multiple days. The temperatures in this type of synthesis range between 80 °C and 250 °C, which normally means that the reaction takes place at temperatures higher than the boiling point of the solvent.⁴²

Another popular method for the preparation of MOFs is called slow diffusion and consists of preparing a saturated solution with both the metallic and organic PBUs as well as an organic solvent. The reaction then takes place at low or ambient temperatures, in a system opened to the air, for long periods of time (ranging between a few days to several weeks or months). This method involves the slow evaporation of the solvent and is ideal for obtaining mono-crystals. This is of the utmost importance

when trying to synthesize new materials since it allows for characterization via single-crystal X-ray diffraction. **Figure 1.4** shows a summary of the main advantages and disadvantages of the two most popular methods of MOF preparation. Other previously reported successful methods of synthesizing MOFs are one-pot, micro-wave assisted, mechanochemical, ultrasonic and electrochemical synthesis.⁴²

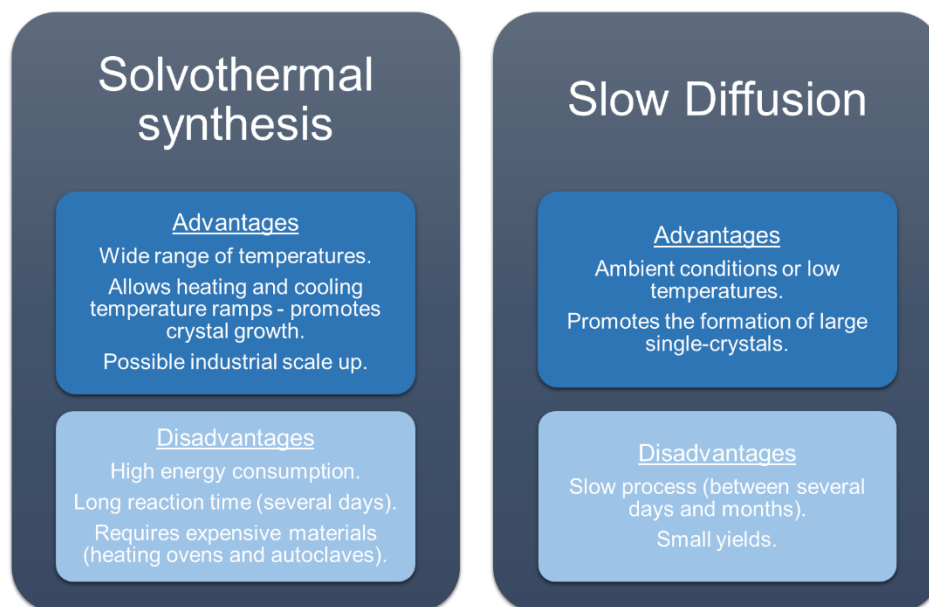


Figure 1.4. Summary of the advantages and disadvantages of solvothermal synthesis and slow diffusion MOFs synthesis methods. Adapted from Silva, Patrícia. *et al.* (2015).⁴²

1.3 Porphyrins

Porphyrins constitute a large class of organic molecules who all share a core unit which consists of an aromatic macrocyclic ring composed by four modified pyrrole subunits linked together by four methine bridging groups (**Figure 1.5**).⁶⁰ The porphyrin structure was first proposed by William Küster in 1912⁶¹ but it was only in 1929, when Hans Fischer successfully synthesized heme, an iron porphyrin precursor to hemoglobin, that this molecule concept became established by the scientific community.⁶⁰ Porphyrins are pigments, usually purple, with crystalline and fluorescent character which can be found either in nature or synthesized in laboratorial settings.⁶⁰

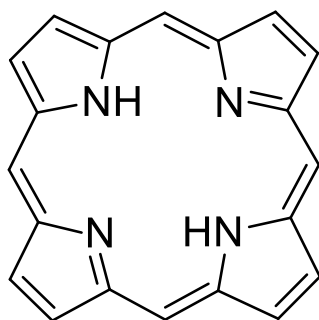


Figure 1.5. The Porphyrin macrocycle.

The first nomenclature system for porphyrins was proposed by Hans Fischer in 1938.⁶² According to Fischer's nomenclature, the external carbon atoms of the pyrrole rings are called β -pyrrolic and are numbered from 1 to 8. This nomenclature designates the methine bridges as *meso* positions and attributes them the Greek letters, alpha (α), beta (β), gamma (γ) and delta (δ). This system allowed for a straightforward and intuitive identification of simple porphyrins. However, with the increased complexity of porphyrins, due to their substituents the system became difficult to apply correctly. As a consequence, the IUPAC recommended a new nomenclature system in 1986.⁶³ The nomenclature as recommended by IUPAC consists of numbering all the non-hydrogen atoms of the porphyrin macrocycle from 1 to 24. It is important to note that, the porphyrin is tautomeric concerning the hydrogen atoms which are not involved in the conjugated system, meaning that these hydrogen atoms may be linked to any two of the nitrogen atoms. As a result, the representation of one of the tautomeric forms does not exclude the other forms. Nevertheless, regarding the nomenclature system proposed by IUPAC, the hydrogen atoms are linked to the nitrogen atoms numbered as 21 and 23. **Figure 1.6** shows a comparison between the two nomenclatures described.

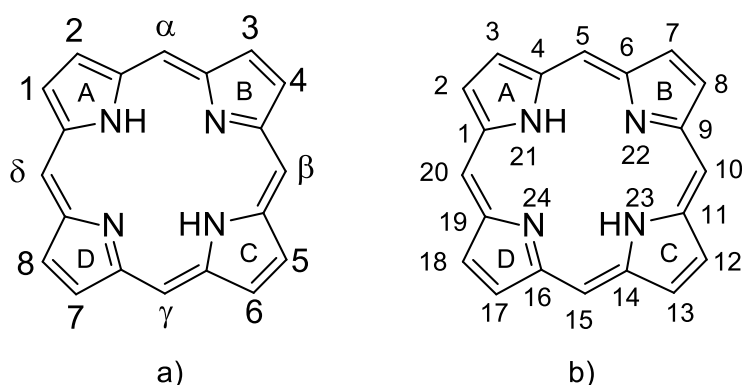


Figure 1.6. Nomenclature systems for the unsubstituted porphyrin macrocycle by a) Hans Fischer and b) IUPAC.⁶³

The nitrogen atoms present in the core of the porphyrin have the ability to bind metal ions. This originates a special subset of porphyrins called metalloporphyrins. These molecules can act as CPs due to the capacity of the metal ions to bind to linkers of the aromatic ring. This means that, whereas porphyrins are flat molecules, metalloporphyrins are not.⁶⁰ The previously mentioned heme is a metalloporphyrin with iron as the metal ion accommodated in its core. This metalloporphyrin has a critical role in human life by being a precursor to hemoglobin but it is not the only essential metalloporphyrin for life as we know it. Chlorophyll is a green pigment, present in plants, responsible for the photosynthesis process. The main structure of chlorophyll is a metalloporphyrin with magnesium as its central metal ion.⁶⁰

The synthesis of porphyrins is a field that has been extensively explored through the years. New porphyrins can be synthesized via three main routes including performing modifications in pigments found in nature such as hemoglobin and chlorophyll, by organic synthesis with pyrrole precursors and by functionalization of previously reported porphyrins.^{64,65} Regarding the characterization of this type of molecules a plethora of techniques can be applied. Nuclear magnetic resonance (NMR) and ultraviolet-visible (UV-Vis) spectroscopy are two of these techniques that show some identifiable characteristics of porphyrins. In the ¹H NMR spectrum, the hydrogen atoms linked to the nitrogen atoms in the core of the porphyrin, as well as the β -pyrrolic and *meso* protons, have a characteristic resonance signal (-2 to -3 ppm, 8-9 ppm and 10-11 ppm, respectively) when compared to the resonance signal originated by the internal standard's tetramethylsilane (TMS) protons which is 0 ppm.⁶⁶ This confers porphyrins with a typical NMR spectrum that allows their quick identification. When it comes to UV-Vis spectroscopy, porphyrins also have a unique spectrum which consists of an intense band designated by Soret band at around 400 nm, and four bands with less intensity called Q bands at the visible light region between 450 nm and 700 nm. With regards to the UV-Vis spectrum of metalloporphyrins, it has been established that the introduction of the metal ion in the core of the porphyrin results in the depletion of between one and two Q bands.⁶⁷

The unique properties and the possibility for modification and functionalization of porphyrins raised the interest of the scientific community for the possible applications of these dyes. Porphyrins have been widely explored in the fields of photomedicine (in particular in cancer PDT)^{68,69}, chemical sensors^{70,71}, solar cells^{72,73}, and catalysis^{74,75}. It is worth mentioning that the presence of porphyrins with catalytic functions in nature has led scientists to pursue the synthesis of porphyrins with similar characteristics introducing this class of organic molecule as exquisite biomimetic catalysts.^{76,77}

1.4 Porphyrin-based MOFs: a unique type of materials

Porphyrin-based MOFs are a unique class of materials in which porphyrins are the organic PBU of the hybrid structure. The first report of a Por-MOF dates from 1991, when Abrahams' research group published the synthesis of an infinite 3D structure with the metalloporphyrin [tetrakis(*p*-pyridyl)porphyrinate]Pd(II) as organic linker coordinate by Cd(II) metal ions nodes.⁷⁸ Since then, the interest in this type of MOF has grown significantly. The reason behind this growth is based on the fact that the properties of a MOF are very closely related to the organic PBU, as was previously stated⁴¹, and in the case of Por-MOFs, the organic PBUs have fascinating properties that are not only incredibly compatible with MOF construction (as for instance their rigid molecular structure and large dimensions) but also confer the MOF with unique capabilities, as a consequence of their tunable substituents and metalation site in their core.⁷⁹

Despite being extremely promising materials, Por-MOFs are not yet as widely explored as other classes of MOFs. This is a consequence of the difficulties the scientific community has found when trying to prepare Por-MOFs. A significant number of Por-MOFs is unable to retain its structural integrity after solvent removal thereby explaining the struggle that synthesizing a stable material capable of maintaining its crystallinity represents.⁸⁰ Nevertheless, researchers have been developing strategies aimed specifically at constructing stable Por-MOFs with tailored properties based on their respective organic and metallic PBUs. From the multiple strategies available crystal engineering, the pillar-layered strategy, the construction of nanoscopic metal-organic polyhedral cages and post-synthetic modification deserve to be mentioned.⁸⁰

Por-MOFs have been explored in the fields of guest molecules adsorption, separation, and storage (due to their porosity and large surface area, and in the case of metalloporphyrins due to their metal centers that provide additional accessibility to guest molecules), as well as in the fields of nano-thin film, light harvesting and catalysis.⁸⁰

Multiple types of catalysis with Por-MOFs have been explored. One of the most relevant is biomimetic catalysis.^{81,82} Metalloporphyrins possess similar catalytic activity and substrate selectivity to some natural enzymes, therefore they are capable of mimicking them. Heme, in particular, is a protein whose characteristics scientists have been trying to replicate in Por-MOFs. Ma and his research group have reported a Por-MOF consisting of the tetrakis(4-carboxyphenyl)porphyrin ($H_2TPP(COOH)_4$) metalated with iron (III) with a zirconium based secondary building unit, called MMPF-6.⁸² This material showed relevant catalytic activity when compared to the heme protein. The Por-MOF PCN-222(Fe) was also tested in catalytic studies by Zhou's research group and showed satisfactory results.⁸³ Ultimately, the synthesis of Por-MOFs with the intent of mimicking the heme protein has been considered a better strategy than loading heme on supports such as zeolites or clays, since the MOFs are capable of retaining more active sites.⁸⁰

Photocatalysis is another important genre of catalytic reactions in which Por-MOFs are interesting since, porphyrins, when in homogeneous phase have great photocatalytic activity as a

consequence of their conjugated aromatic electron system.⁸⁰ Furthermore, the incorporation of photocatalytic active metal ions, such as zinc into the core of the porphyrin, originates metalloporphyrins with significant potential in this field. When these properties are combined with the MOFs' typical high porosity and surface area, as well as the possibility of being reutilized in multiple catalytic cycles, it becomes simple to understand why Por-MOFs are being explored in photocatalysis. In addition, in homogeneous phase reactions, metalloporphyrins usually face degradation by reacting with singlet oxygen. In heterogeneous conditions this obstacle is often averted.⁸⁰

Por-MOFs have been significantly explored in the field of photocatalysis for the oxidation of organic compounds, for instance phenol and sulfides, as reported by Wu and co-workers after testing a MOF based on the Sn^{IV}TPyP metalloporphyrin which bridges Zn metal ions.⁸⁴ Zang and co-workers also reported the photocatalytic activity of a Por-MOF in the oxidation of sulfides.⁸⁵ The Por-MOF in question is based on the organic ligand H₁₀TBCPPP (tetrakis(3,5-bis[(4-carboxy)-phenyl]phenyl)porphyrin) and has four [In(COO)₄]⁻ secondary building units (SBUs). More recently, Pereira, Carla *et. al.* reported the photo-oxidation of a mustard-gas simulant (2-chloroethyl sulfide) using Por-MOFs as catalysts.⁸⁶ The MOF was built with porphyrin H₁₀TPPA (5, 10, 15, 20-tetrakis(*p*-phenylphosphonic acid)porphyrin) and exhibited a selectivity control toward the decomposition of bis-2-chloroethylsulfide, avoiding this way the formation of the toxic product bis-2-chloroethylsulfone. In 2019, Jiang, Z. W. *et. al.* reported the synthesis of porphyrin-based 2D lanthanide MOFs, capable of photooxidation of 1,5-dihydroxynaphthalene.⁸⁷ The MOFs were prepared via a microwave-assisted method with tetrakis(4-carboxyphenyl)porphyrin (H₂TPP(COOH)₄) being utilized as organic ligand.

As previously stated, the main goal of this dissertation was to develop novel Por-MOFs, capable of photodegradation of PCs present in water via advanced oxidation processes. However, this is a field in which Por-MOFs have not been extensively explored yet, contrary to the efforts done in the same field with porphyrin sensitizers in homogeneous conditions.⁸⁸ Nevertheless, it is possible to find some studies reporting the use of the free base or metalated H₂TPP(COOH)₄ porphyrin supported on solid materials, either on graphitic carbon nitride (g-C₃N₄) or TiO₂. Murphy and co-workers reported the photodegradation of famotidine using the H₂TPP(COOH)₄-TiO₂ composite as catalyst.⁸⁹ Mineralization of the pharmaceutical compound was not achieved, but rather the degradation into other intermediates, mainly the S-oxide of famotidine. The same catalyst was tested in the photodegradation of tamsulosin and solifenacin, with no success, proving the selectivity of the catalyst to determined substrates. Ma's research group reported a ZnTPP(COOH)₄ based MOF, supported on g-C₃N₄ capable of photodegrading methylene blue and tetracycline with decomposition yields above 90% and 80%, respectively.⁹⁰

In this dissertation we report the synthesis of zirconium based Por-MOFs and the catalytic assays investigating their effectiveness as heterogeneous catalysts in advanced oxidation processes for the photodegradation of the pharmaceutical compounds paracetamol and 17 β -estradiol, with the intention of further exploring the potential of porphyrin based MOFs in the field of water remediation.

2. Synthesis of porphyrin-based MOFs

2.1 Objective

The main goal of this project was to synthesize new porphyrin-based zirconium MOFs in which the organic linkers would be the porphyrins 5,10,15,20-tetrakis(4-carboxyethylthio-2,3,5,6-tetrafluorophenyl)porphyrin ($\text{H}_2\text{TPPF}_{16}(\text{SC}_2\text{H}_4\text{COOH})_4$, **1**) and 5,10,15,20-tetrakis(4-carboxyphenylthio-2,3,5,6-tetrafluorophenyl)porphyrin ($\text{H}_2\text{TPPF}_{16}(\text{SC}_6\text{H}_4\text{COOH})_4$, **2**). Another objective was the synthesis of the previously reported PCN-222^{83,91} which consists of a class of zirconium MOFs with porphyrin tetrakis(4-carboxyphenyl)porphyrin ($\text{H}_2\text{TPP}(\text{COOH})_4$, **3**) or derivatives as the organic linker. These materials would then be tested and compared as photocatalysts in the photodegradation of pharmaceutical compounds in water. For that reason, we started by synthesizing **1** and **2** from the commercially available 5,10,15,20-tetrakis(pentafluorophenyl)porphyrin ($\text{H}_2\text{TPPF}_{20}$, **4**). Porphyrin **3** is commercially available, which means it was not necessary to synthesize. **Figure 2.1** shows the structures of each porphyrin as well as the designations utilized in this document.

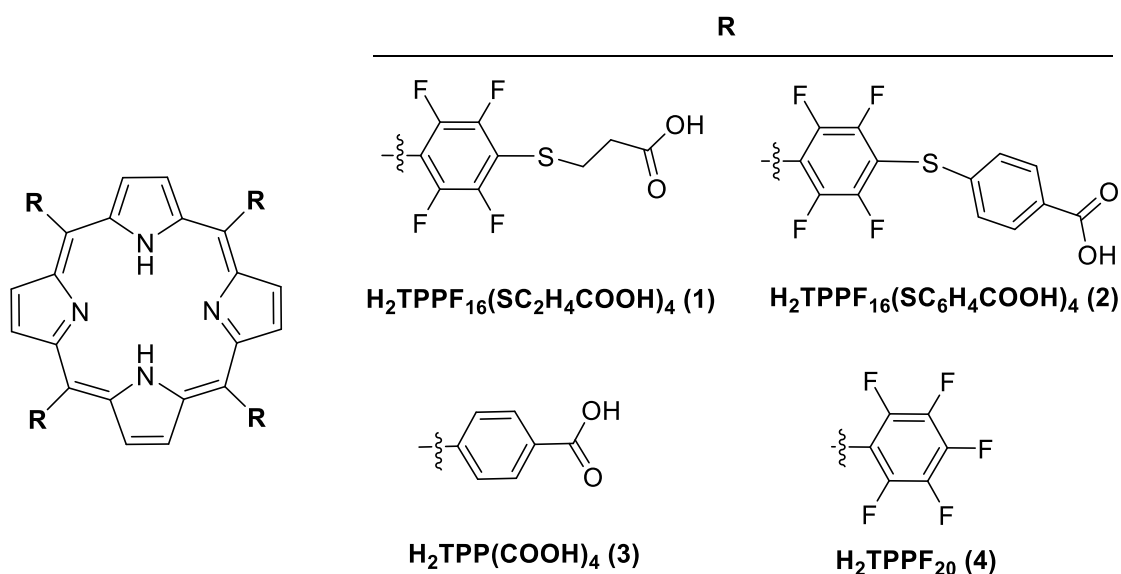
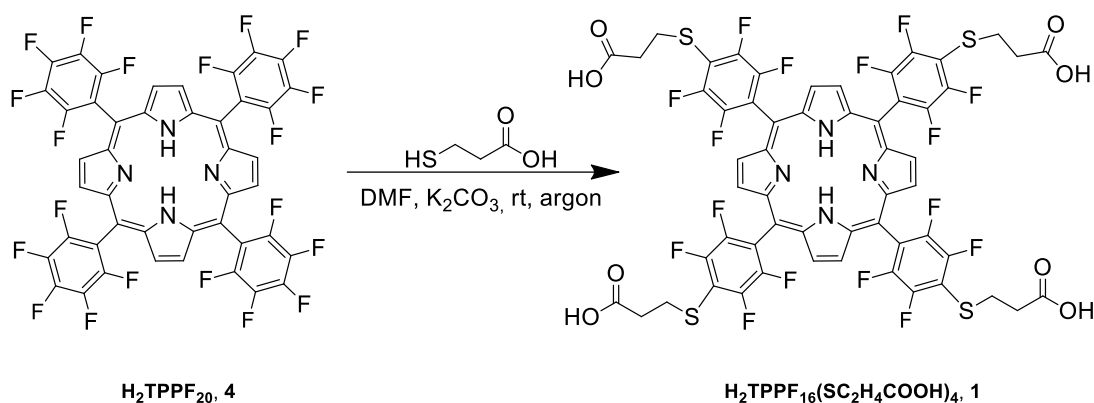


Figure 2.1. Structures and designations of the porphyrins explored in this project.

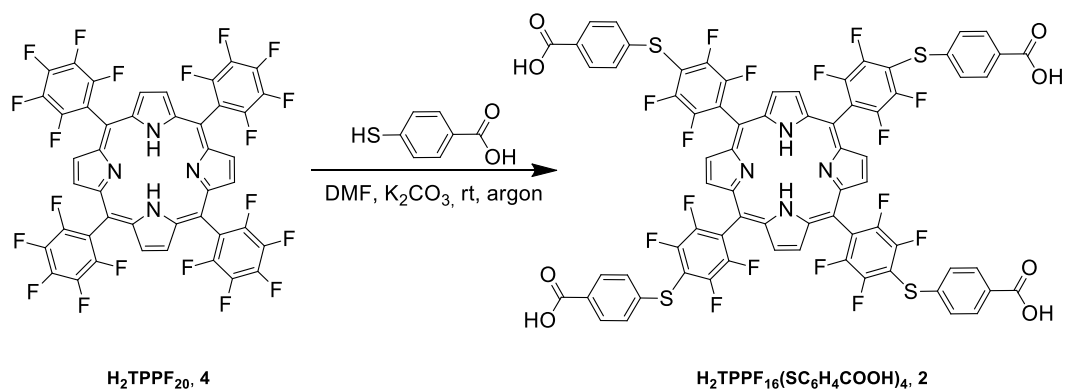
2.2 Synthesis of the free-base porphyrins

Porphyrins $\text{H}_2\text{TPPF}_{16}(\text{SC}_2\text{H}_4\text{COOH})_4$ (**1**) and $\text{H}_2\text{TPPF}_{16}(\text{SC}_6\text{H}_4\text{COOH})_4$ (**2**) were the first to be synthesized. The process was initiated by purifying porphyrin $\text{H}_2\text{TPPF}_{20}$ (**4**) on a silica chromatography column using a mixture of petroleum ether and dichloromethane (3:1) as eluent. Once the porphyrin was purified the reaction was carried out using a procedure adapted from Lourenço *et al.*⁹² where 3-mercaptopropionic acid and potassium carbonate in excess, were added to a DMF solution of $\text{H}_2\text{TPPF}_{20}$ (**4**), under oxygen free conditions (**Scheme 2.1**). In order to infer if the reaction was completed it was controlled by analytical thin layer chromatography (TLC) with a mobile phase of a hexane/dichloromethane (2:1) mixture. The reaction mixture was then neutralized with citric acid which led to the porphyrin's precipitation. The solid was separated by filtration and recrystallized in a mixture of methanol and chloroform. The porphyrin $\text{H}_2\text{TPPF}_{16}(\text{SC}_2\text{H}_4\text{COOH})_4$ (**1**) was isolated in 96.6% yield.



Scheme 2.1

The procedure for the synthesis of $\text{H}_2\text{TPPF}_{16}(\text{SC}_6\text{H}_4\text{COOH})_4$ (**2**) followed the same protocol as the synthesis for $\text{H}_2\text{TPPF}_{16}(\text{SC}_2\text{H}_4\text{COOH})_4$ (**1**). The difference was the acid added, that now was the 4-mercaptobenzoic acid (**Scheme 2.2**). This reaction had the same work-up as the one previously described and the porphyrin $\text{H}_2\text{TPPF}_{16}(\text{SC}_6\text{H}_4\text{COOH})_4$ (**2**) was isolated in 68.9% yield.



Scheme 2.2

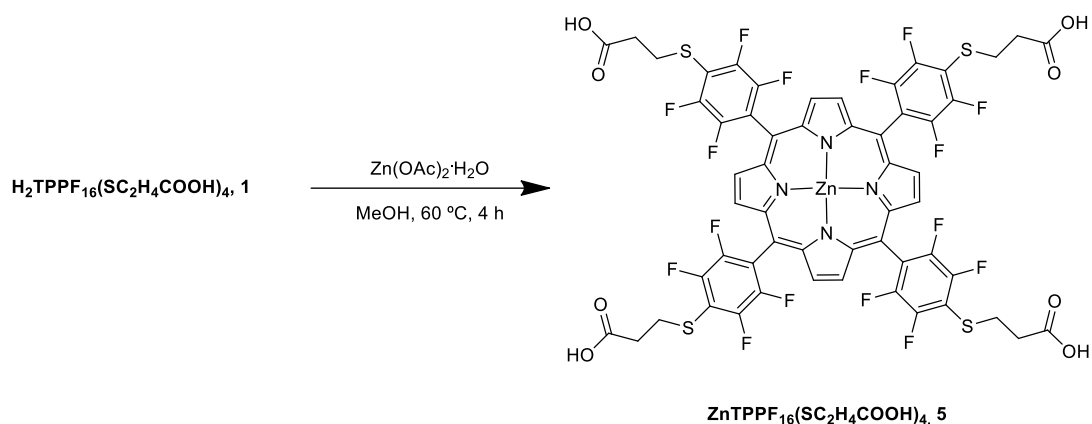
The obtained porphyrins were characterized by ^1H NMR, UV-Vis and mass spectrometry, being the results aligned with the literature (see **Appendix A** for the UV-Vis spectra of these porphyrins).⁹²

2.3 Synthesis of metallic porphyrin complexes

As mentioned in **Chapter 1**, metal ions, once introduced in the porphyrin's core, give to the latter different properties which can improve their effectiveness as catalysts. Bearing that in mind, metallic complexes of porphyrins **1-3** were synthesized using three different metal ions: i) zinc(II); ii) manganese(III) and iii) iron(III). The metals manganese and iron were chosen since previous research found that metalloporphyrin based catalysts with these metals were significantly effective and selective in oxidation reactions.^{93,94} As for the reason behind the choice of the metal zinc, previous work showed that zinc complexes had great photocatalytic activity, which would obviously be a valuable characteristic for this project.^{28,75,95}

2.3.1 Synthesis of zinc porphyrin complexes

At this point, the goal was to obtain porphyrin $\text{ZnTPPF}_{16}(\text{SC}_2\text{H}_4\text{COOH})_4$ (**5**) (**Scheme 2.3**). For that the free base porphyrin $\text{H}_2\text{TPPF}_{16}(\text{SC}_2\text{H}_4\text{COOH})_4$ (**1**) and zinc acetate were used. The reaction followed a procedure adapted from typical porphyrin metalation reactions,^{96,97} but it is worth noting that once the zinc acetate was added the free base porphyrin lost its solubility in the solvent and the reaction occurred in suspension. This can be explained by the fact that the addition of the base turned the porphyrin to its carboxylate state which in turn diminishes its solubility in methanol.



Scheme 2.3

In addition to $\text{ZnTPPF}_{16}(\text{SC}_2\text{H}_4\text{COOH})_4$ (**5**) the zinc complex of porphyrin $\text{H}_2\text{TPPF}_{16}(\text{SC}_6\text{H}_4\text{COOH})_4$ (**2**), $\text{ZnTPPF}_{16}(\text{SC}_6\text{H}_4\text{COOH})_4$ (**6**) (**Figure 2.2**) was also utilized in the preparation of MOFs. This material was not synthesized during the development of this project however, it was kindly provided by Dr. Sara Fernandes.

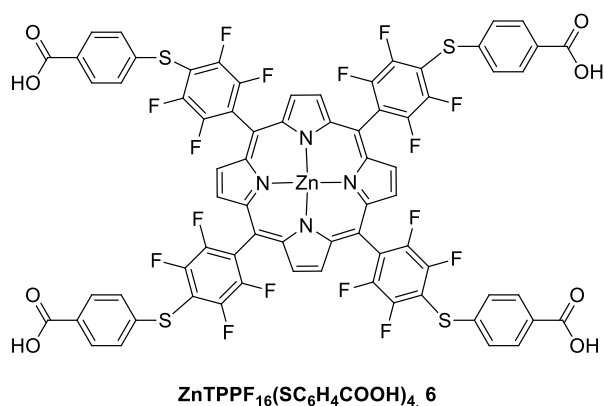
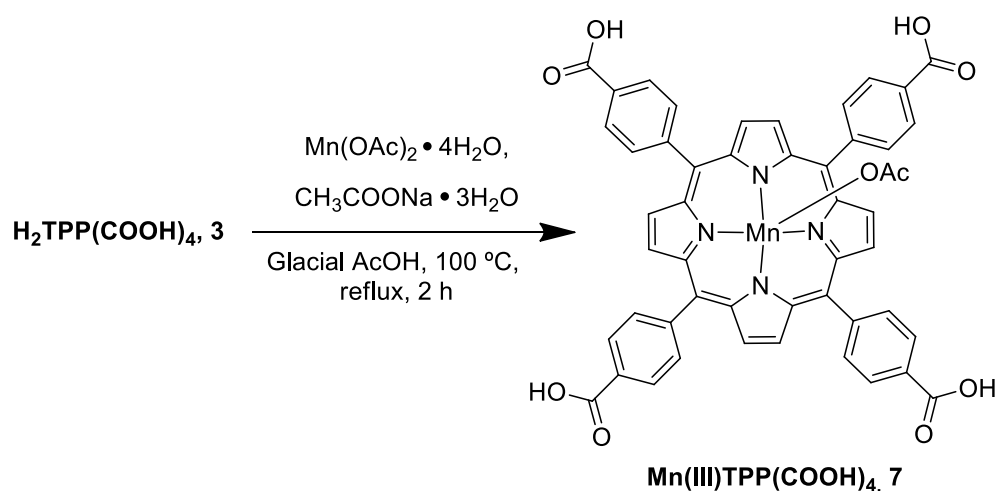


Figure 2.2. Structure of the metalloporphyrin $\text{ZnTPPF}_{16}(\text{SC}_6\text{H}_4\text{COOH})_4$.

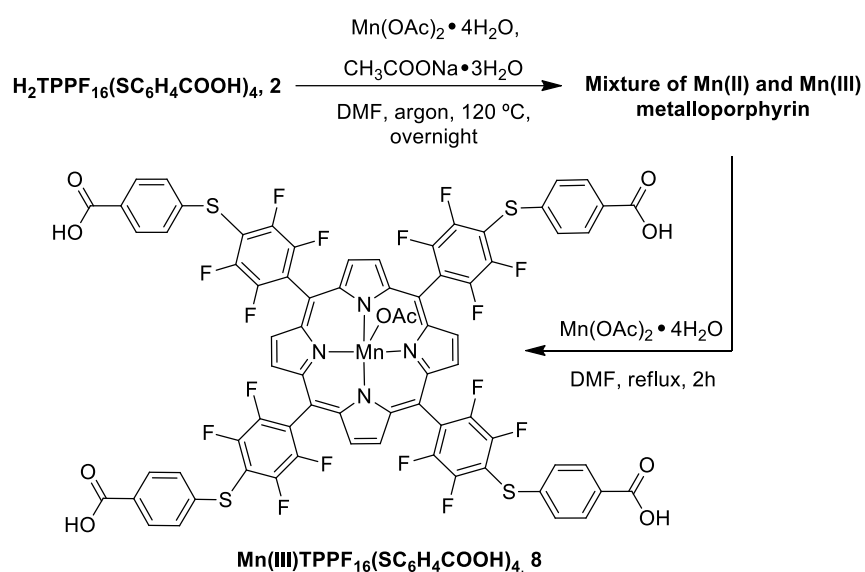
2.3.2 Synthesis of manganese porphyrin complexes

Manganese porphyrin complexes were attempted with porphyrins $\text{H}_2\text{TPPF}_{16}(\text{SC}_6\text{H}_4\text{COOH})_4$ (**2**) and $\text{H}_2\text{TPP}(\text{COOH})_4$ (**3**). The synthesis of $\text{Mn(III)TPP}(\text{COOH})_4$ (**7**) followed the procedure described in **Scheme 2.4**, which was adapted from Piccirillo, Giusi. *et al.* (2021).⁹⁸ The reaction was controlled by UV-Vis spectroscopy.



Scheme 2.4

The metallic complex **Mn(III)TPPF₁₆(SC₆H₄COOH)₄ (8)** was synthesized following the procedure by Castro, Kelly *et al.* (2015)⁹⁴ utilizing the same manganese salt but with DMF as solvent. The reaction was performed overnight, in a glass reactor closed under argon at 120 °C and in suspension (**Scheme 2.5**). The reaction was controlled by UV-Vis spectroscopy and showed a mixture between what we believe to be the metalloporphyrin with manganese in different oxidation states, namely II and III. For that reason, the reaction was left opened to air for an entire day in an attempt to oxidize manganese from oxidation state II to III. After this, the reaction mixture was analyzed by UV-Vis and showed no significant alteration. At this point, a different path was taken and more manganese acetate was added, and the reaction mixture was left at 140 °C for approximately two hours. After this the UV-Vis analysis showed the complete conversion to manganese(III).

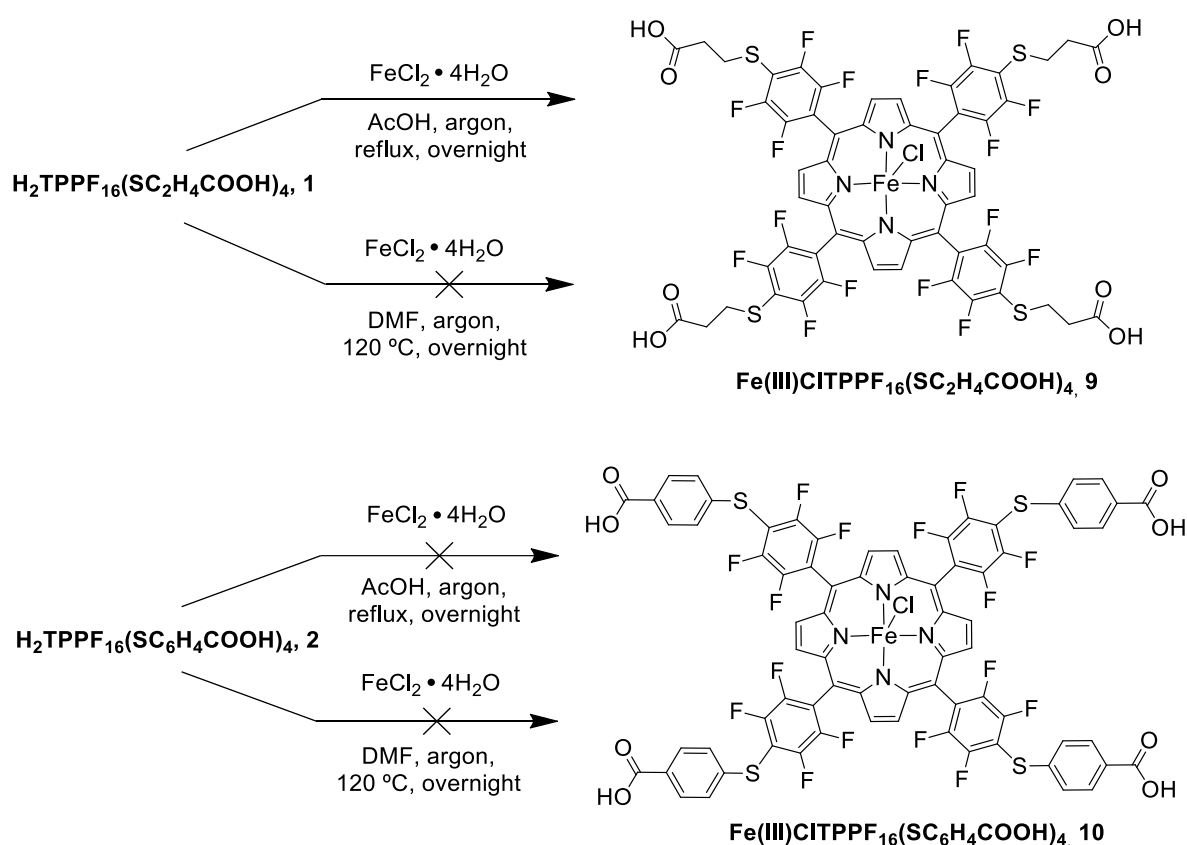


Scheme 2.5

2.3.3 Synthesis of iron porphyrin complexes

The preparation of iron porphyrin complexes of porphyrins $\text{H}_2\text{TPPF}_{16}(\text{SC}_2\text{H}_4\text{COOH})_4$ (**1**) and $\text{H}_2\text{TPPF}_{16}(\text{SC}_6\text{H}_4\text{COOH})_4$ (**2**) was attempted via two different reaction pathways which were previously reported.^{94,99} One of the pathways consisted of adding iron chloride tetrahydrate to each of the porphyrins, using acetic acid as solvent and having the reaction closed under an argon atmosphere and left overnight at reflux (118 °C) (**Scheme 2.6**). Before performing the work-up the reaction mixtures were left open to the air with agitation to ensure that any iron with oxidation state II would be oxidize to III. This method allowed us to obtain the metalloporphyrin $\text{Fe(III)CITPPF}_{16}(\text{SC}_2\text{H}_4\text{COOH})_4$ (**9**). However, we were not able to synthesize $\text{Fe(III)CITPPF}_{16}(\text{SC}_6\text{H}_4\text{COOH})_4$ (**10**) via this method.

The second pathway changed the solvent from acetic acid to DMF and performed the reaction at 120 °C. The remaining conditions were kept the same. Unfortunately, utilizing this method, neither reaction with porphyrins $\text{H}_2\text{TPPF}_{16}(\text{SC}_2\text{H}_4\text{COOH})_4$ (**1**) nor $\text{H}_2\text{TPPF}_{16}(\text{SC}_6\text{H}_4\text{COOH})_4$ (**2**) resulted in the desired metallic complexes (**Scheme 2.6**).



Scheme 2.6

All metalloporphyrins prepared and described in this chapter were characterized by UV-Vis. The characterization of metalloporphyrins $\text{ZnTPPF}_{16}(\text{SC}_2\text{H}_4\text{COOH})_4$ (**5**) and $\text{Fe(III)CITPPF}_{16}(\text{SC}_2\text{H}_4\text{COOH})_4$

(9) is very similar to the free base $\text{H}_2\text{TPPF}_{16}(\text{SC}_2\text{H}_4\text{COOH})_4$ (1).⁹² The results for the remaining metalloporphyrins were in alignment with what can be found in the literature (see **Appendix A** for details).^{94,100}

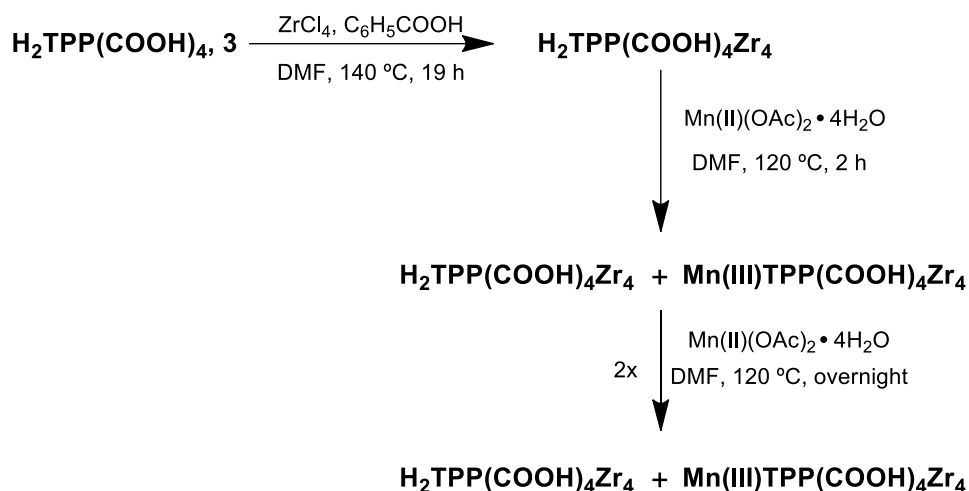
2.4 Preparation of porphyrin and metalloporphyrin based MOFs

In this project the preparation of MOFs employed a solvothermal method in which the reaction mixture was left in a glass reactor with slow agitation. The reactions took place in an oil bath at temperatures ranging from 120 to 140 °C. Typically, solvothermal synthesis of MOFs is performed in autoclaves inside ovens. However, it was decided that the reactions would be conducted in glass reactors, in an oil bath, to easily follow the evolution of the reaction visually as well as decide when to stop them.

The general procedure followed was adapted from Feng, D. *et al.* (2012).⁸³ However, during the preparation of the different MOFs we faced multiple obstacles which were tackled by changing experimental conditions such as the temperature or the duration of the reactions, the solvent and other reagents. Despite all these variables two things were deemed essential and were performed for every reaction. One of them was to assure that all the reactants were thoroughly dissolved before heating the reaction mixture. In order to accomplish this, all reaction mixtures were put in an ultrasonic bath for a few seconds prior to their heating. The other was to thoroughly wash the obtained solid after the reaction was finished with solvents which could dissolve the base porphyrin and metal salts. This way it was ensured that there would not be a mixture of porphyrin, salts, and MOF in the obtained solid. The different MOFs prepared and attempted will be described.

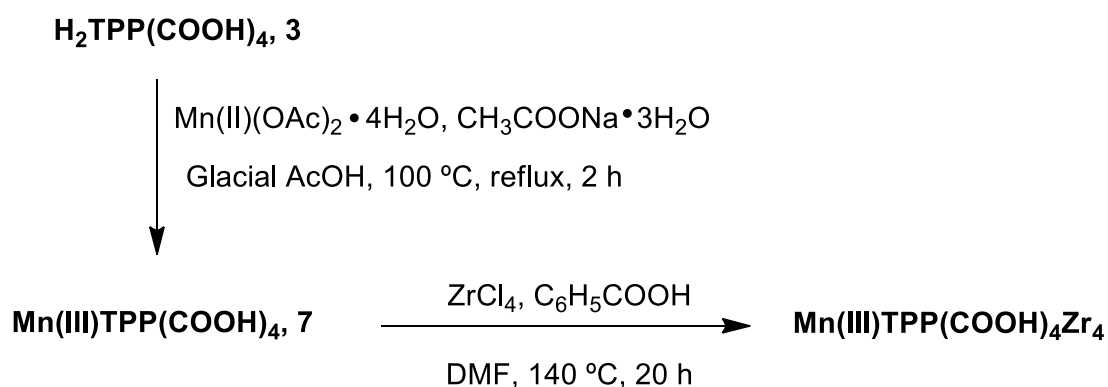
2.4.1 Preparation of $\text{H}_2\text{TPP}(\text{COOH})_4$ based MOFs

Two materials correspondent to the previously reported class of MOFs PCN-222^{79,83} were prepared from the base porphyrin $\text{H}_2\text{TPP}(\text{COOH})_4$ (3). MOF $\text{H}_2\text{TPP}(\text{COOH})_4\text{Zr}_4$ (**Scheme 2.7**) and MOF $\text{Mn(III)TPP}(\text{COOH})_4\text{Zr}_4$ (**Scheme 2.8**) were prepared in the reaction conditions presented below. For the preparation of $\text{Mn(III)TPP}(\text{COOH})_4\text{Zr}_4$ two different reaction pathways were attempted. Firstly, we attempted to perform the direct metalation of MOF $\text{H}_2\text{TPP}(\text{COOH})_4\text{Zr}_4$, however, this post-synthesis reaction produced a mixture between the wanted MOF and the starting material (**Scheme 2.7**).



Scheme 2.7

The second attempt to prepare the Mn(III) MOF started by synthesizing the metalloporphyrin **Mn(III)TPP(COOH)₄ (7)** and then use it as the organic linker for the preparation of the desired MOF **Mn(III)TPP(COOH)₄Zr₄** (**Scheme 2.8**). The reactions conditions were similar to the ones used to prepare **H₂TPP(COOH)₄Zr₄**.



Scheme 2.8

After the reactions were completed, the obtained solid materials were washed four times with ethanol, being centrifuged and decanted each time. The solids were then left in acetone for a night before finally being harvested with quantitative yields.

Both the free base and Mn(III) solids (**Figure 2.3** and **Figure 2.4**, respectively) were characterized by Powder XRD and by UV-Vis spectroscopy. This data shows crystalline materials that kept the porphyrin's absorption characteristics, which means the synthesis of these Por-MOFs was successful.

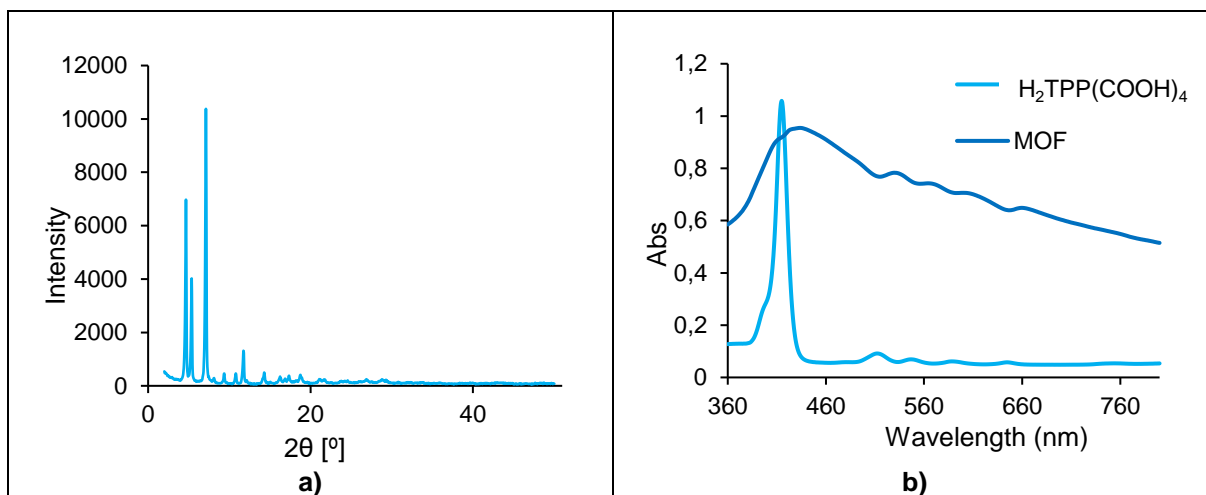


Figure 2.3. a): Powder X-ray diffraction data of MOF $\text{H}_2\text{TPP}(\text{COOH})_4\text{Zr}_4$; **b):** UV-Vis spectra of porphyrin $\text{H}_2\text{TPP}(\text{COOH})_4$ (3) and its respective zirconium MOF, both in methanol.

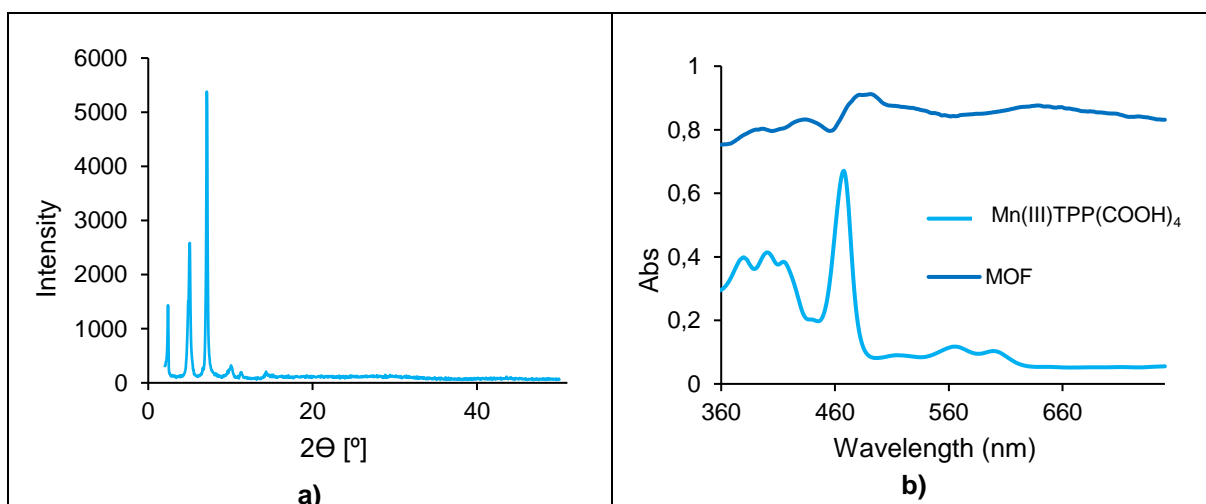
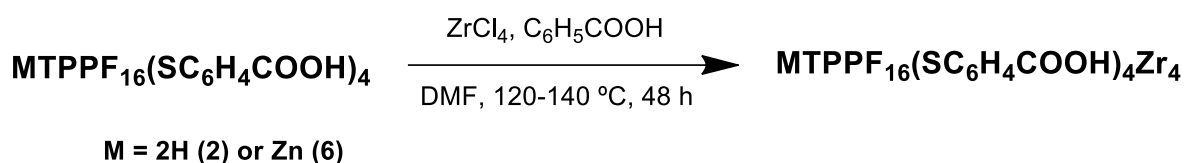


Figure 2.4. a): Powder X-ray diffraction data of MOF $\text{Mn}(\text{III})\text{TPP}(\text{COOH})_4\text{Zr}_4$; **b):** UV-Vis spectra of porphyrin $\text{Mn}(\text{III})\text{TPP}(\text{COOH})_4$ (7) and its respective zirconium MOF, both in methanol.

2.4.2 Preparation of $\text{H}_2\text{TPPF}_{16}(\text{SC}_6\text{H}_4\text{COOH})_4$ based MOFs

Similar conditions were applied to prepare zirconium MOFs $\text{H}_2\text{TPPF}_{16}(\text{SC}_6\text{H}_4\text{COOH})_4\text{Zr}_4$ and $\text{ZnTPPF}_{16}(\text{SC}_6\text{H}_4\text{COOH})_4\text{Zr}_4$ (Scheme 2.9) based on free-base and Zn porphyrin $\text{TPPF}_{16}(\text{SC}_6\text{H}_4\text{COOH})_4$ (2), respectively. We started by preparing $\text{H}_2\text{TPPF}_{16}(\text{SC}_6\text{H}_4\text{COOH})_4\text{Zr}_4$, following the same procedure used in the previously prepared MOFs with the difference being the time of the reaction (48 h).



Scheme 2.9

The obtained solid was filtrated to remove the DMF and was then washed with a mixture of dichloromethane/methanol (85:15) and then methanol. The solid was characterized by Powder XRD and UV-Vis spectroscopy (**Figure 2.5**). The results showed once again the successful preparation of a Por-MOF with crystalline character that kept the absorption characteristics of the porphyrin linker.

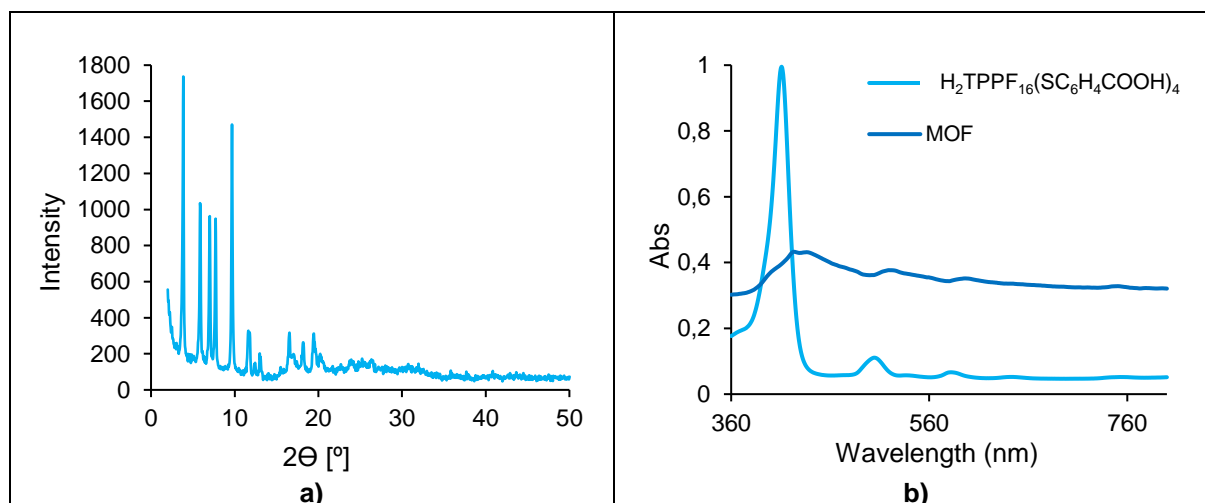


Figure 2.5. a): Powder X-ray diffraction data of MOF $\text{H}_2\text{TPPF}_{16}(\text{SC}_6\text{H}_4\text{COOH})_4\text{Zr}_4$; **b):** UV-Vis spectra of porphyrin $\text{H}_2\text{TPPF}_{16}(\text{SC}_6\text{H}_4\text{COOH})_4$ and its respective zirconium MOF in methanol.

This was a very exciting result because from our bibliographic search a zirconium MOF with porphyrin $\text{H}_2\text{TPPF}_{16}(\text{SC}_6\text{H}_4\text{COOH})_4$ (**2**) as organic linker seems to have not been previously reported, which meant it was a new material. However, upon multiple attempts to replicate the procedure, we kept failing to reobtain $\text{H}_2\text{TPPF}_{16}(\text{SC}_6\text{H}_4\text{COOH})_4\text{Zr}_4$. For that reason, the preparation of this material was attempted changing multiple variables. The first attempt consisted of changing the temperature of the reaction from 140 °C to 120 °C. From this alteration came no successful results. Secondly, we tried adding different bases, maintaining the remaining conditions as the original synthesis, in order to deprotonate the carboxylic acids of porphyrin $\text{H}_2\text{TPPF}_{16}(\text{SC}_6\text{H}_4\text{COOH})_4$ (**2**) so that it could coordinate the zirconium cations. Two different bases were tried namely potassium carbonate and sodium acetate but neither of the attempts resulted in the desired material. In these two syntheses the amount of base added was correspondent to 4 molar equivalents of the amount of porphyrin. Suspecting that it could be an insufficient amount of base we tried yet another preparation of this MOF this time adding an amount of base correspondent to 170 molar equivalents of the amount of porphyrin. This attempt also did not

result in $\text{H}_2\text{TPPF}_{16}(\text{SC}_6\text{H}_4\text{COOH})_4\text{Zr}_4$. After all these failed attempts we moved on to the synthesis of other MOFs.

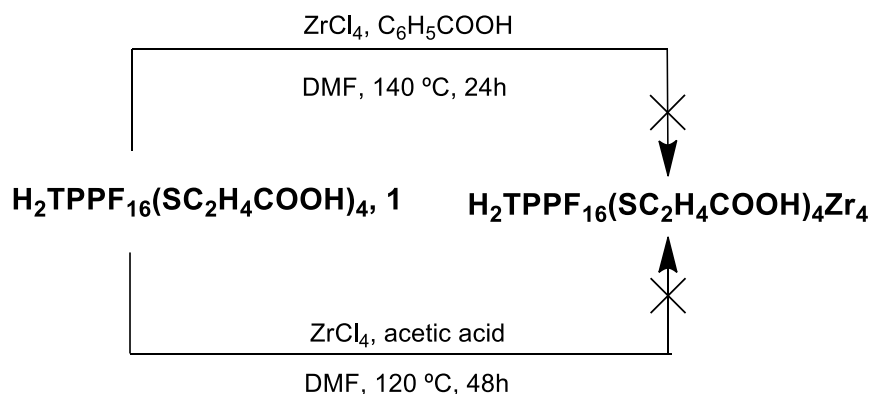
For the preparation of corresponding zinc porphyrin MOF derivative, $\text{ZnTPPF}_{16}(\text{SC}_6\text{H}_4\text{COOH})_4\text{Zr}_4$, three attempts were made. The first one in the exact same conditions in which $\text{H}_2\text{TPPF}_{16}(\text{SC}_6\text{H}_4\text{COOH})_4\text{Zr}_4$ was firstly obtained (see **Scheme 2.8**). A second attempt in which only the temperature of the reaction was changed from 140 °C to 120 °C was performed and finally a third attempt in which the conditions from **Scheme 2.9** were replicated with the exception of the amount of zirconium chloride added which was changed to double the amount. Unfortunately, none of this synthesis resulted in the desired MOF $\text{ZnTPPF}_{16}(\text{SC}_6\text{H}_4\text{COOH})_4\text{Zr}_4$.

2.4.3 Preparation of $\text{H}_2\text{TPPF}_{16}(\text{SC}_2\text{H}_4\text{COOH})_4$ based MOFs

In this section the attempts to prepare MOFs $\text{H}_2\text{TPPF}_{16}(\text{SC}_2\text{H}_4\text{COOH})_4\text{Zr}_4$, $\text{ZnTPPF}_{16}(\text{SC}_2\text{H}_4\text{COOH})_4\text{Zr}_4$ and $\text{Fe(III)TPPF}_{16}(\text{SC}_6\text{H}_4\text{COOH})_4\text{Zr}_4$ from the corresponding free-base and metalated porphyrins (**Scheme 2.10** and **Scheme 2.11**) are described.

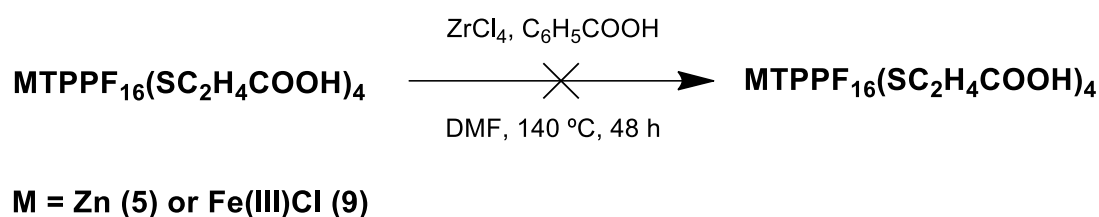
For the preparation of $\text{H}_2\text{TPPF}_{16}(\text{SC}_2\text{H}_4\text{COOH})_4\text{Zr}_4$ two attempts were made (**Scheme 2.10**). The first one consisted in replicating most of the conditions described in **Scheme 2.9**. The exception was the time of the reaction. Since visually it was possible to see that a significant amount of solid had precipitated after 24 hours, the reaction was stopped and the solid was washed with a solution of dichloromethane and methanol (15%) and then with methanol. Unfortunately, the obtained solid did not have crystalline character and so a different reaction pathway was attempted.

The second reaction had acetic acid instead of benzoic acid, albeit in the same proportions. The temperature was also changed from 140 °C to 120 °C and the reaction took 48 hours. **Scheme 2.10** shows both pathways attempted. After this period the reaction received the exact same work-up as for the first attempt. Once again, the obtained solid was not crystalline and so we moved on to attempt the preparation of other MOFs.



Scheme 2.10

The attempts at the preparation of MOFs **ZnTPPF₁₆(SC₂H₄COOH)₄Zr₄** and **Fe(III)TPPF₁₆(SC₆H₄COOH)₄Zr₄** (**Scheme 2.11**) were done simultaneously and with the same protocol. Mixtures of metalloporphyrins **ZnTPPF₁₆(SC₂H₄COOH)₄** (**5**) and **Fe(III)CITPPF₁₆(SC₂H₄COOH)₄** (**9**), benzoic acid and zirconium chloride anhydrous were thoroughly dissolved in DMF and put in closed glass reactors. The reactors were heated to 140 °C during 48 hours in an oil bath. The obtained solids were then washed three times with ethanol and were left in acetone for one night after which they were dried and analyzed by Powder XRD. The obtained materials were amorphous, similarly to what was verified for the free base porphyrin.



Scheme 2.11

With the intent of summarizing this chapter we lay down the main conclusions drawn from the work of synthesis. The synthesis of porphyrins **H₂TPPF₁₆(SC₂H₄COOH)₄** (**1**) and **H₂TPPF₁₆(SC₆H₄COOH)₄** (**2**) consisted of the nucleophilic aromatic substitution of the four *para*-fluorine atoms of porphyrin **H₂TPPF₂₀** (**4**) by 3-mercaptopropionic acid and 4-mercaptopbenzoic acid, respectively. From previous work with these porphyrins it was known they possessed interesting photochemical and physical properties to act as photocatalysts.⁹² In addition to this, for the best of our knowledge, the preparation of Por-MOFs with these materials as organic linkers had not been previously reported. This made the proposition of developing these materials rather exciting. Unfortunately, it was not possible to come up with definitive procedures for the syntheses of MOFs based on porphyrins **1** and **2** nor on their metallic complexes. During the development of this project, it was possible to understand that the synthesis of MOFs, specially from large organic ligands, such as porphyrins, is incredibly complex with a wide range of variables being crucial to the success of the reaction, from temperature to time of reaction or even the acid utilized. As per the nature of the project it was not possible to attempt more reaction pathways. However, an extensive range of attempts varying multiple reaction conditions could possibly result in more successful outcomes. Nevertheless, it was possible to reproduce the synthesis of MOFs from the free base porphyrin **H₂TTP(COOH)₄** (**3**) and its manganese metallic complex **Mn(III)TTP(COOH)₄** (**7**), which were explored as (photo)catalysts in the degradation of pharmaceutical compounds.

Regarding the synthesis of metallic complexes, it was clear that the introduction of ion metals, in the porphyrin's core and obtaining a specific oxidation state is also a significant challenge. The fact that more often than not the result of the reactions would be a mixture of the metallic complex with

multiple oxidation states forced us to attempt multiple approaches in order to obtain the metallic complex with the right oxidation state. This was worth it however, since metalloporphyrins from metals zinc, iron and manganese were obtained with satisfactory yields.

3. Oxidation of pharmaceuticals by Advanced Oxidation Processes

3.1 General Overview

Nowadays, the need to optimize and implement “greener” methods for treatment of surface and waste waters for the removal of pharmaceutical compounds, is tremendous, as it was previously explained in **Chapter 1**. The oxidation of this type of pollutants via AOPs is one of such methods and will be explored in this chapter.

Pharmaceuticals such as paracetamol (PCM) and 17 β -estradiol (E2) are fairly widespread in modern society and for that reason it is becoming increasingly common to find them in waste and surface waters alike.^{28,101–104} In addition, the accumulation of this type of pollutants in aquatic environment represents dangerous potential effects on both fauna and flora, as well as to human health. For those reasons, these two compounds were applied as models of pharmaceutical pollutants to test the activity of our synthesized porphyrins and zirconium-porphyrin MOFs as catalysts for their photodegradation.

The photooxidation of these pharmaceuticals was explored in the presence of both the heterogeneous MOF catalysts $\text{H}_2\text{TPP}(\text{COOH})_4\text{Zr}_4$ and $\text{Mn}(\text{III})\text{TPP}(\text{COOH})_4\text{Zr}_4$ and their corresponding base porphyrins $\text{H}_2\text{TPP}(\text{COOH})_4$ (**3**) and $\text{Mn}(\text{III})\text{TPP}(\text{COOH})_4$ (**7**), which act as homogeneous catalysts, all in batch mode. Before the oxidation studies, the photostability of the porphyrins and the capacity of both heterogeneous and homogeneous catalysts to generate singlet oxygen were attested.

3.2 Photostability and singlet oxygen production of porphyrins and zirconium Por-MOFs

In order to utilize porphyrins $\text{H}_2\text{TPP}(\text{COOH})_4$ (**3**) and $\text{Mn}(\text{III})\text{TPP}(\text{COOH})_4$ (**7**) as catalysts for paracetamol (PCM) and 17 β -estradiol (E2) degradation, stock solutions (500 μM) were prepared using a mixture of distilled water and an aqueous saturated solution of potassium bicarbonate (9:1). The pH value of each stock solution was 10.68 and 9.38, respectively. For the photostability tests the porphyrins were exposed to visible white light (18 mW/cm^2) for periods of 4 hours and the results were analyzed by UV-Vis spectroscopy. **Figure 3.1.a**) shows that $\text{H}_2\text{TPP}(\text{COOH})_4$ (**3**) suffers some decrease in absorbance of the Soret band ($\lambda \sim 414 \text{ nm}$). Considering relative values, based on the absorbance values of the Soret band at the beginning of the test and at the end, the concentration decay was approximately 30%. This result can be attributed to some aggregation phenomena of effective

photodegradation during the four hours of irradiation, since previously reported work states that this porphyrin tends to form aggregates in aqueous solutions.¹⁰⁵ Contrarily, porphyrin **Mn(III)TPP(COOH)₄** (**7**) did not change its concentration under the same irradiation conditions of the free base precursor (**Figure 3.1.b**). So, the observed decrease in the first one is, most probably, related to a lower solubility.

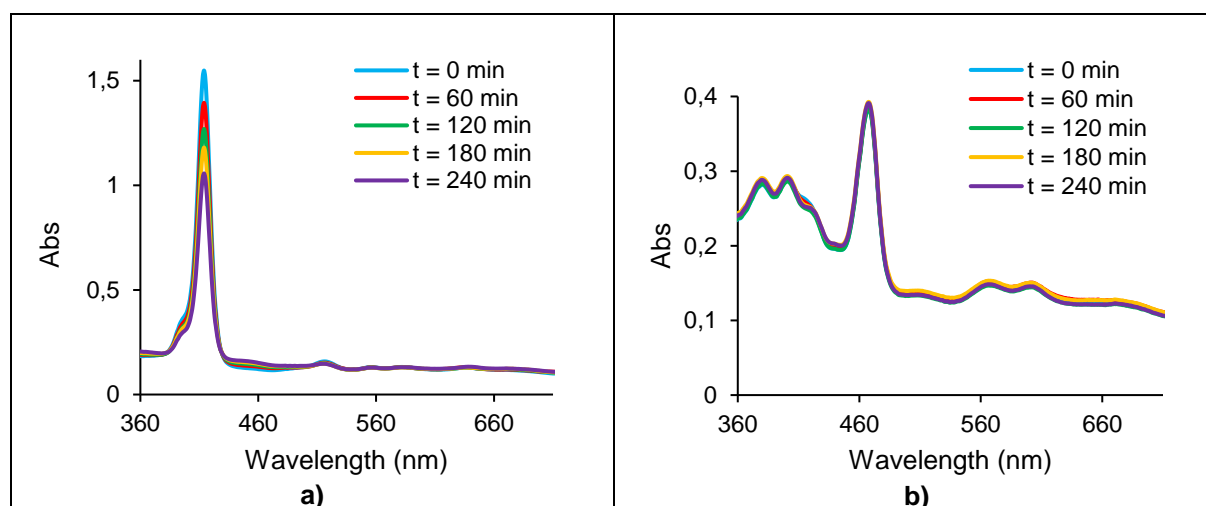
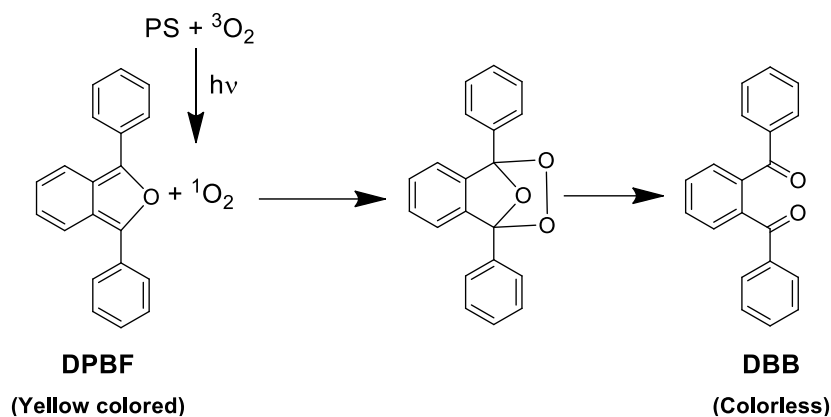


Figure 3.1. UV-Vis spectra of the photostability test of porphyrins **a): H₂TPP(COOH)₄** (**3**) and **b): Mn(III)TPP(COOH)₄** (**7**).

The photostability of the MOF catalysts was not studied by UV-Vis spectroscopy since their heterogeneous nature results in variable results of absorbance at each UV-Vis analysis. For this reason, the stability of the materials was controlled visually. During the catalytic studies the MOFs showed to be stable, under the reaction conditions, with the only exception of studies with variation of pH. These results will be later discussed in more detail.

The singlet oxygen assay was performed using 1,3-diphenylisobenzofuran (DPBF) as a ¹O₂ scavenger. DPBF reacts with ¹O₂ and is oxidized to *o*-dibenzoylbenzene (DBB) (**Scheme 3.1**) losing its characteristic yellow color and becoming colorless during the process. Furthermore, DPBF has its peak absorption at approximately 415 nm which means the depletion of DPBF can be followed by UV-Vis analysis by comparing its absorption before and after irradiation.²⁸



Scheme 3.1

To this end, five solutions of DPBF (16.5 μM) were prepared in a mixture of DMF and distilled water (90:10). To four of them were added the four catalysts studied: porphyrins **H₂TPP(COOH)₄ (3)** and **Mn(III)TPP(COOH)₄ (7)** (0.67 μM) and the MOFs **H₂TPP(COOH)₄Zr₄ (20.9 μM)** and **Mn(III)TPP(COOH)₄Zr₄ (19.0 μM)** and the remaining solution was the control with just DPBF. All prepared solutions were irradiated at room temperature, for a period of 21 minutes, with white light (18 mW/cm²). The light was filtered through a cut-off filter for wavelengths inferior to 550 nm. The reactions were controlled by UV-Vis in pre-determined intervals of time.

The results of the study show that the porphyrin **H₂TPP(COOH)₄ (3)** has the capacity to generate ¹O₂ since in its presence, approximately 50% of DPBF was decomposed (**Figure 3.2**). On the other hand, the metallic complex **Mn(III)TPP(COOH)₄ (7)** does not have the capacity to generate ¹O₂ based on the residual depletion of DPBF during the reaction in its presence.

The results of the study with the two MOFs are in line with their respective base porphyrins (**Figure 3.2**). The MOF **H₂TPP(COOH)₄Zr₄** shows capacity to generate ¹O₂ albeit less than its base porphyrin, since during the same period and with a bigger concentration of catalyst the depletion of DPBF remained at approximately 34% (compared to the 50% obtained with **H₂TPP(COOH)₄ (3)**). This result was also expected based on what can be found on the literature regarding the comparison between the photocatalytic activity of this type of heterogeneous catalysts and their respective homogeneous precursors.²⁸ The **Mn(III)TPP(COOH)₄Zr₄** MOF showed no capacity to generate ¹O₂ as shown by the residual depletion of DPBF which is in alignment with what had been previously verified with its base metalloporphyrin.

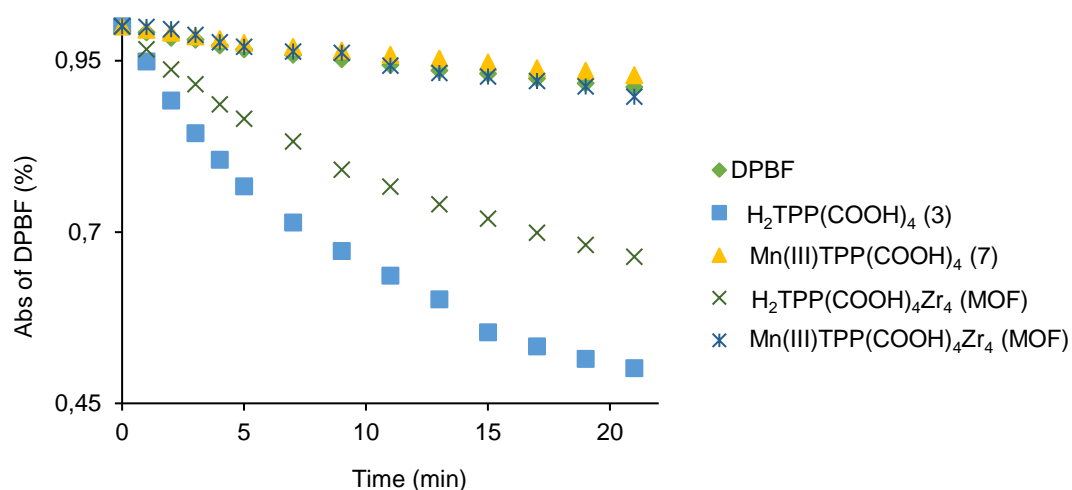


Figure 3.2. Comparative photooxidation of DPBF (16.5 μM) in a DMF/distilled water (90:10) solution or suspension with or without homogeneous photosensitizers **H₂TPP(COOH)₄ (3)** and **Mn(III)TPP(COOH)₄ (7)**, (0.67 μM) and heterogeneous photosensitizers **H₂TPP(COOH)₄Zr₄** (20.9 μM) and **Mn(III)TPP(COOH)₄Zr₄** (19.0 μM).

Despite suffering a slight decrease in its concentration in the solution, perhaps due to aggregation phenomena, when exposed to white light for long periods of time, porphyrin **H₂TPP(COOH)₄ (3)** was still tested as a photocatalyst since it showed capacity to generate singlet oxygen. In addition to this, it was possible to verify that, during the catalytic studies, when in the reaction mixture with the substrate the porphyrin is more stable and able to maintain its catalytic activity. The MOF **Mn(III)TPP(COOH)₄Zr₄** and its base metalloporphyrin showed to have no capacity to generate singlet oxygen. For that reason, they were tested in oxidation reactions without a light source in addition to the photocatalytic studies (which served as control and can be found in **Appendix B**), since it was expected that these materials would have no catalytic effect during the latter.

3.3 Photooxidation of paracetamol

The photooxidation of paracetamol was firstly tested with porphyrin **H₂TPP(COOH)₄ (3)**. The studies consisted in a first assessment of whether or not the porphyrin was capable of oxidizing the medicinal substrate, followed by a study of potential degradation mechanisms as well as an investigation on the effect of the reaction mixture pH value. Once these studies were concluded, the MOF catalyst **H₂TPP(COOH)₄Zr₄** was tested, and the studies focused on finding optimum reaction conditions. In this section it will be possible to see the main results obtained, as well as the conclusions drawn, based on those results.

Before performing the photocatalytic degradation of paracetamol (PCM), its stability in aqueous solution, under white light irradiation was tested. For that, an aqueous solution of paracetamol (20 ppm, 130 μM) was irradiated with white light (18 mW/cm^2) for a period of 3 h and the solution analyzed by UV-Vis spectroscopy at predetermined periods of time (**Figure 3.3**). It is possible to see that the UV-Vis spectrum maintains the characteristic peak of paracetamol with maximum absorbance at 243 nm without any depletion during the 3 h irradiation period, showing that paracetamol is, indeed, stable under the irradiation tested conditions.

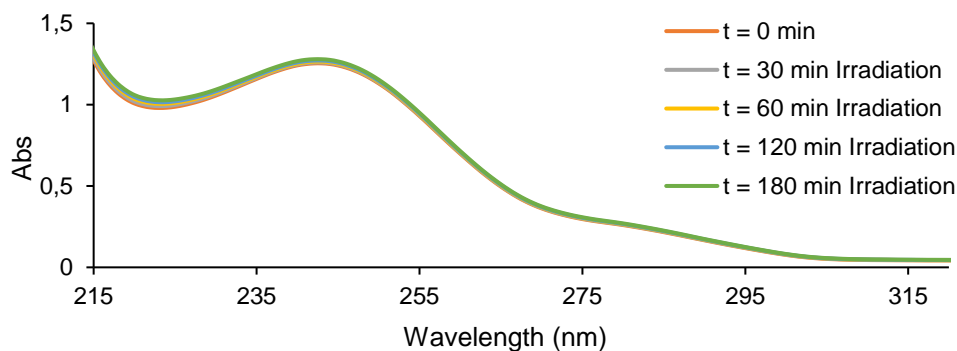


Figure 3.3. UV-Vis spectra of an aqueous solution of paracetamol (130 μM , 20 ppm) under white light (18 mW/cm^2) irradiation, at predetermined periods of time.

3.3.1 Photooxidation of paracetamol with $\text{H}_2\text{TPP}(\text{COOH})_4$

To evaluate the photocatalytic performance of $\text{H}_2\text{TPP}(\text{COOH})_4$ (**3**) on paracetamol degradation, an aqueous solution of the latter (130 μM , 20 ppm) and the porphyrin (13 μM) was irradiated with white light (18 mW/cm^2) for 180 minutes and followed by UV-Vis spectroscopy. The addition of the catalyst originated a slight shift of PCM's absorbance band from 243 nm to 248 nm. Furthermore, after just 30 minutes of irradiation paracetamol's absorbance band disappeared and a new peak of absorption appears at approximately 270 nm (**Figure 3.4**). This points to the substrate's degradation and possible formation of sub products.

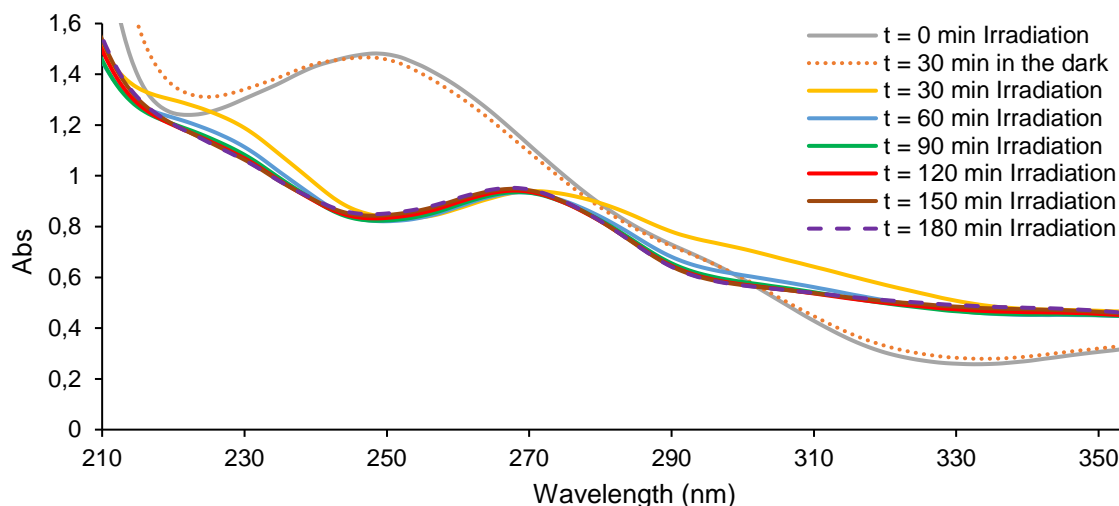


Figure 3.4. UV-Vis spectra of the reaction mixture of paracetamol (130 μ M, 20 ppm) and $\text{H}_2\text{TTP}(\text{COOH})_4$ (**3**) (13 μ M, 10% molar ratio) with pH = 8.5, under white light irradiation (18 mW/cm²) and the respective samples analyzed after predetermined periods of time (30-180 min).

Considering that under these conditions the catalyst seems to be able to oxidize paracetamol quite quickly, the same reaction was then repeated, but now diminishing the irradiation time to 50 minutes and the samples were analyzed by UV-Vis spectroscopy every 5 minutes (**Figure 3.5**). The objective of this study was to follow the degradation of paracetamol over time and not just its immediate oxidation. However, after only 5 minutes of irradiation paracetamol's UV-Vis band at 248 nm disappears and a new peak appears around 290 nm, which points to the formation of an intermediate sub product, from now on designated as P1 (**Figure 3.5.a**). P1's concentration increases in the reaction mixture for 15 minutes.

After 30 minutes P1 starts to disappear, and a new product with corresponding band at approximately 270 nm seems to be formed, from now on designated as P2 (**Figure 3.5.b**). These results are in alignment with that observed in the previous study with a sub product with λ_{max} at approximately 270 nm being formed after approximately one hour of reaction.

The results obtained in these two reactions allowed us to conclude that the porphyrin $\text{H}_2\text{TTP}(\text{COOH})_4$ is able to decompose paracetamol in aqueous solution under white light irradiation in just 5 minutes and that two different sub products are formed during the first 50 minutes of reaction. This led to the next objective of this investigation which was the identification of the possible products that were formed.

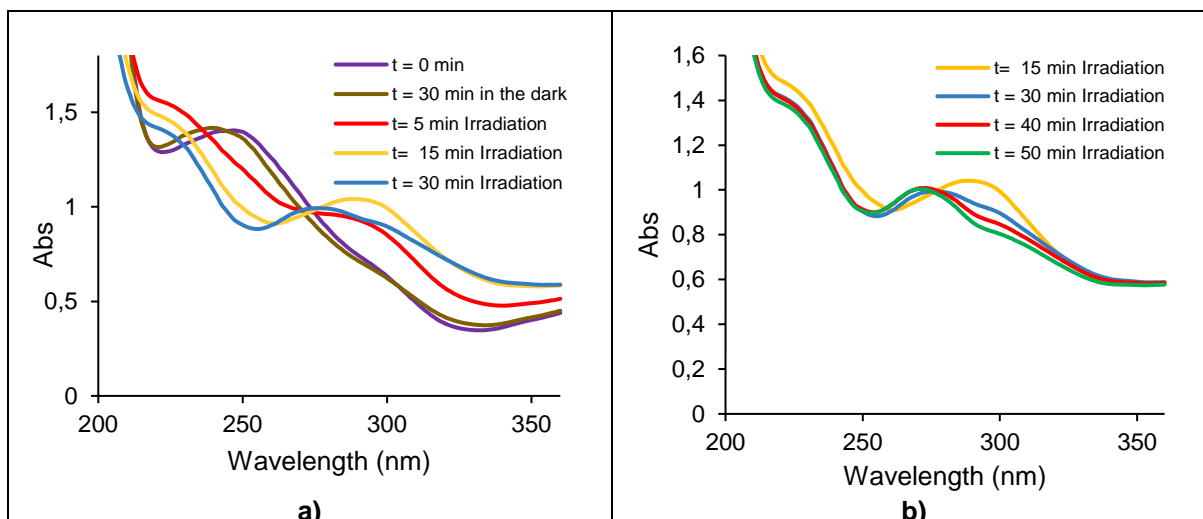


Figure 3.5. UV-Vis spectra of the reaction mixture of paracetamol (130 μM , 20 ppm) and $\text{H}_2\text{TPP}(\text{COOH})_4$ (**3**) (13 μM , 10% molar ratio) with pH = 8.5 and the respective samples analyzed after predetermined periods of irradiation with white light (18 mW/cm^2), for **a**): the first 30 minutes of irradiation; and **b**): the last 35 minutes of irradiation.

Some previously reported intermediates of the photodegradation of paracetamol are benzoquinone, hydroquinone, *p*-aminophenol and *p*-nitrophenol.^{103,106} For this reason, these compounds were chosen to be analyzed as possible sub products of the oxidation of paracetamol in the presence of the porphyrin $\text{H}_2\text{TPP}(\text{COOH})_4$ (**3**).

The four possible products were analyzed by UV-Vis spectroscopy with the objective of trying to match their respective spectra with the results of our studies for the photodegradation of paracetamol with $\text{H}_2\text{TPP}(\text{COOH})_4$ (**3**). To that end, aqueous solutions of hydroquinone (20 ppm), benzoquinone (10 ppm), *p*-aminophenol (20 ppm) and *p*-nitrophenol (20 ppm) were prepared and analyzed by UV-Vis (**Figure 3.6**), for further comparison.

Both hydroquinone's and *p*-aminophenol's spectra are a possible match to P1's. These products have two absorption bands at approximately 222 nm and 288 nm for hydroquinone, and 232 nm and 296 nm for *p*-aminophenol which is very similar to P1. On the other hand, none of the products analyzed seems to be a match to P2.

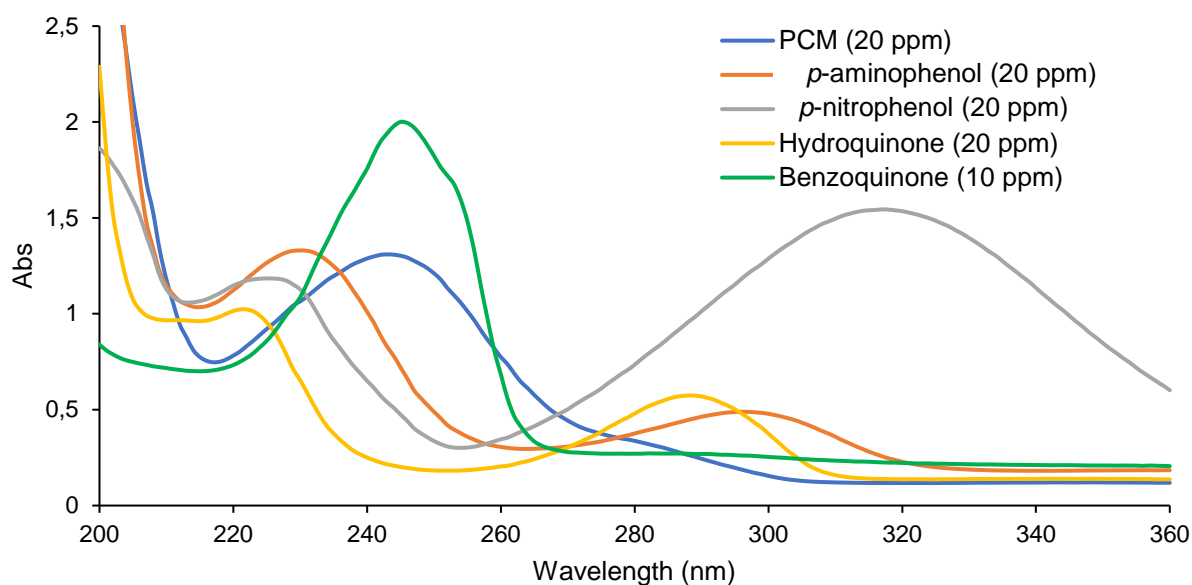


Figure 3.6. UV-Vis spectra of aqueous solutions of paracetamol (20 ppm), *p*-aminophenol (20 ppm), *p*-nitrophenol (20 ppm), hydroquinone (20 ppm) and benzoquinone (10 ppm).

This information allowed us to form a few conclusions regarding the possible degradation mechanism taking place during the reaction. Previous studies have reported a reaction mechanism starting with the attack of $\bullet\text{OH}$ radicals onto the aromatic ring of paracetamol, that can either be in the *ortho*- or *para*- positions, regarding the position of the OH group.^{107,108} The attack onto the *meta*- position is insignificant.¹⁰³ When the attack occurs in the *para*- position the next step is the elimination of the acetamide radical and formation of hydroquinone, which can be further oxidized to either benzoquinone (**Figure 3.7**) or 1,2,4-trihydroxibenzene. Both these compounds will then be oxidized to different simple dicarboxylic acids. Based on our results, this could be the reaction mechanism taking place. The reaction solution has an alkaline pH which means $\bullet\text{OH}$ radicals are available, and hydroquinone represents an intermediate which is later oxidized, similarly to P1.

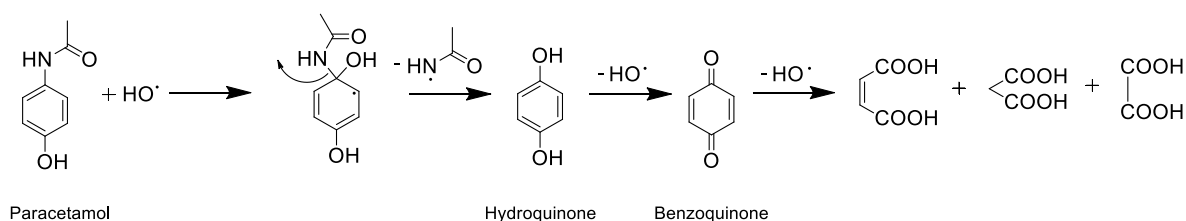


Figure 3.7. Paracetamol oxidation mechanism by photocatalysis.^{107,108}

Another possibility corresponds to the mechanism proposed by Edgar Moctezuma *et al.*¹⁰³ in 2012. It consists of a deacylation mechanism (**Figure 3.8**) in which paracetamol would be oxidized to *p*-aminophenol which would in turn be very easily oxidized to *p*-nitrophenol. The sequence of oxidative

reactions would continue with the oxidation of *p*-nitrophenol to hydroquinone, ending in the same way as the mechanism from **Figure 3.7**. Assuming P1 is hydroquinone this could also be the mechanism taking place in our reaction, based on the same criteria. However, if one were to assume P1 is *p*-aminophenol instead, then the likelihood of this being the correct mechanism for our reaction is significantly reduced. This conclusion is justified by the fact that Moctezuma and co-workers reported that the oxidation of *p*-aminophenol is extremely fast and so, it is only detected in trace amounts.¹⁰³ This observation is not in accordance with our results since P1 is in the reaction mixture for approximately 15 minutes.

Despite this evaluation, without further and more detailed studies of identification of intermediate and final subproducts of the degradation of paracetamol it is not possible to affirm with certainty what reaction mechanism takes place.

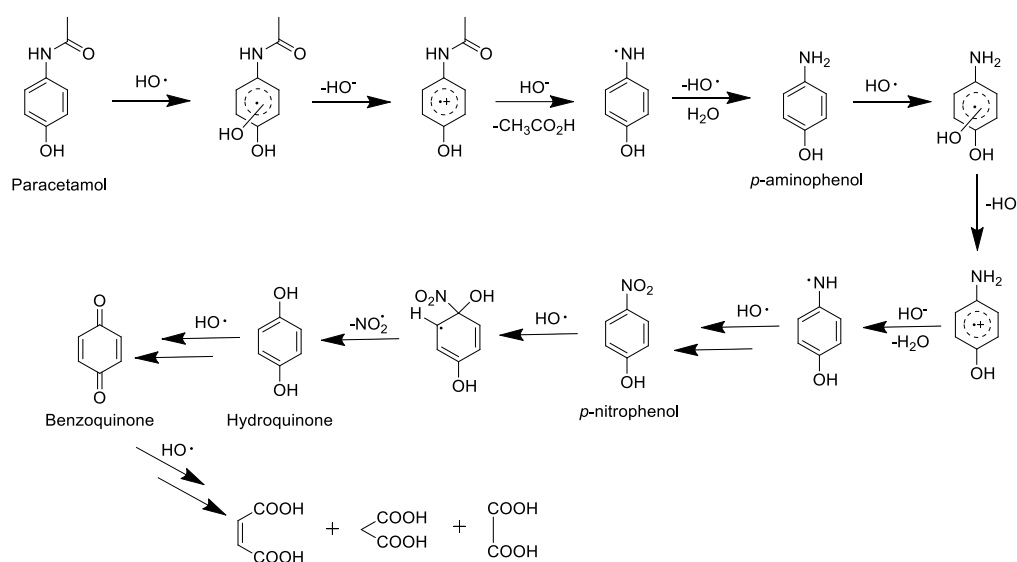


Figure 3.8. Adapted deacylation paracetamol oxidation mechanism by photocatalysis, proposed by Edgar Moctezuma *et al.*¹⁰³

The final catalytic study involving PCM and porphyrin **H₂TPP(COOH)₄ (3)** focused on the effect of the pH in the oxidation of the pharmaceutical. Previous studies of photodegradation of paracetamol promoted by a TiO₂/UV system have shown that the optimum pH for degradation of paracetamol is between 9 and 9.5.^{104,106} As such, we decided to investigate a range of pH values, including 9.5, to attest the possible effect in PCM's photooxidation with our catalyst.

As previously mentioned, the stock solution of the porphyrin was prepared with a mixture of distilled water and an aqueous saturated solution of potassium bicarbonate (9:1) and had a pH of 10.68. This fact obviously had an impact on the pH of the reaction solution. The first time the reaction was performed for 50 minutes (**Figure 3.5**) the initial pH of the reaction mixture was 8.90, but during the

reaction changed to 8.82. Other pH values were explored, namely: 2.5, 5.5, 7.0, 9.5 and 11.0, however now under pH buffer conditions, using Britton-Robson buffer solutions.

Degradation of the pharmaceutical substrate was only verified in the reactions with alkaline pH. However, the reactions at initial pH value of 9.5 and 11.0 had similar photodegradation profiles (**Figure 3.9**), that deviated slightly from what had been observed at initial pH 8.90. The first intermediate product, P1, was decomposed after only 20 and 10 minutes of irradiation, for the reactions at pH 9.5 and 11, respectively, whereas at pH 8.90 it took approximately 30 minutes to oxidize P1. After that, the sub product with λ_{max} at ca. 270 nm is formed and remains in solution for the remaining of the experiment.

The experiments at acid and neutral pH revealed no degradation of PCM (**Figure 3.10**). In addition, the catalyst was not stable under pH = 2.5 conditions, since there is a depletion of the porphyrin's characteristic Soret Band at $\lambda_{max} \sim 414$ nm, even in the dark (**Figure 3.11**).

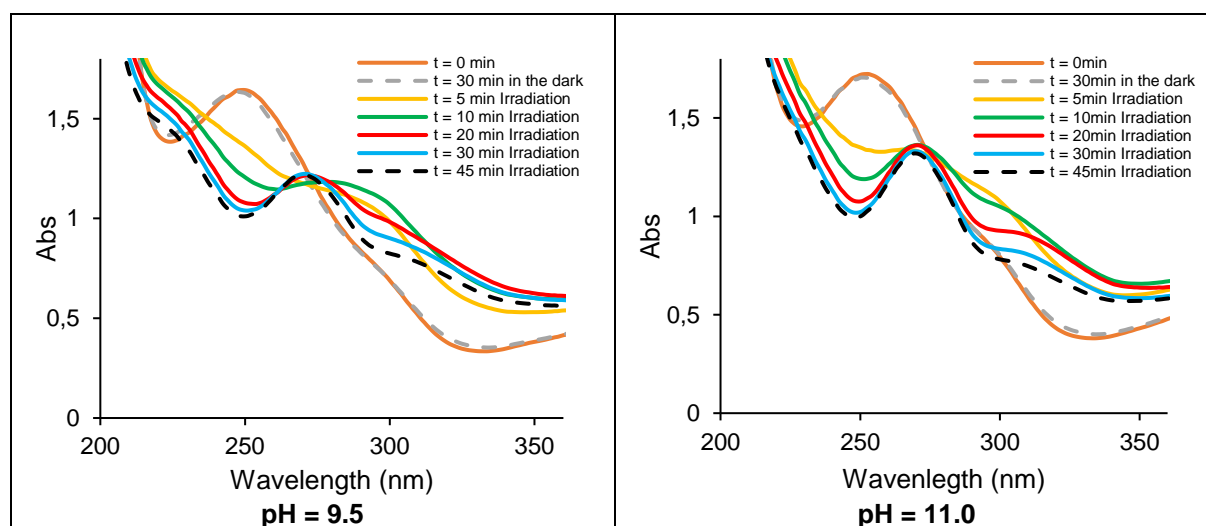


Figure 3.9. UV-Vis spectra of aqueous solutions of paracetamol (130 μ M, 20 ppm) and $H_2TPP(COOH)_4$ (**3**) (13 μ M, 10% molar ratio) with pH = 9.5 and pH = 11 and the samples analyzed at different times of irradiation with white light (18 mW/cm²).

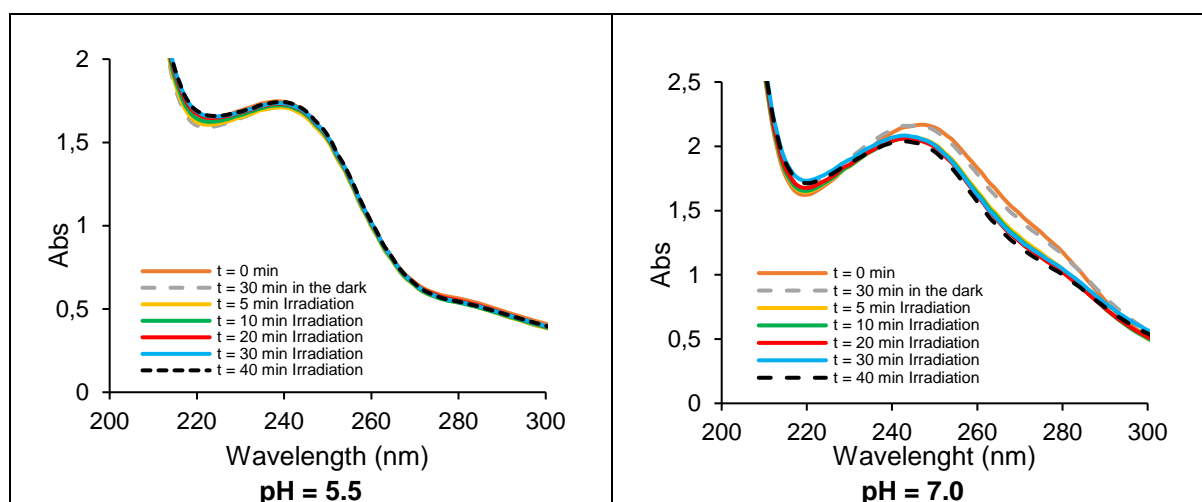


Figure 3.10. UV-Vis spectra of paracetamol (130 μM , 20 ppm) and $\text{H}_2\text{TPP}(\text{COOH})_4$ (**3**) (13 μM , 10% molar ratio) in solutions with pH = 5.5 and pH = 7.0 and of the samples analyzed at different times of irradiation with white light (18 mW/cm^2).

This study on the effect of pH in the photodegradation of paracetamol showed that at acidic or neutral values of pH the catalyst is not able to promote the degradation of the substrate, whereas, at alkaline values oxidation was verified. Previously reported worked has established that alkaline values of pH can contribute to the formation of $\bullet\text{OH}$ radicals.^{109–111} Bearing this in mind, it is possible to theorize that the oxidation of PCM is more dependent on the presence of $\bullet\text{OH}$ radicals than oxygen singlet, since only under conditions in which the first is likely to be more available, is the oxidation of PCM verified.

In addition, between the different alkaline values of pH used in the reactions, the only difference in results was how quickly the intermediate product, P1, was depleted. The reaction performed at pH 11.0 showed complete depletion of this intermediate product in only 10 minutes, whereas the reactions with pH values of 8.9 and 9.5 completed this depletion in 30 and 20 minutes, respectively. These results indicate that with porphyrin $\text{H}_2\text{TPP}(\text{COOH})_4$ (**3**) as homogeneous (photo)catalyst, the higher the solution's pH, the faster the substrates are oxidized. **Table 3.1** summarizes the main results of the reactions of the photooxidation of PCM with porphyrin $\text{H}_2\text{TPP}(\text{COOH})_4$ (**3**) performed at different pH.

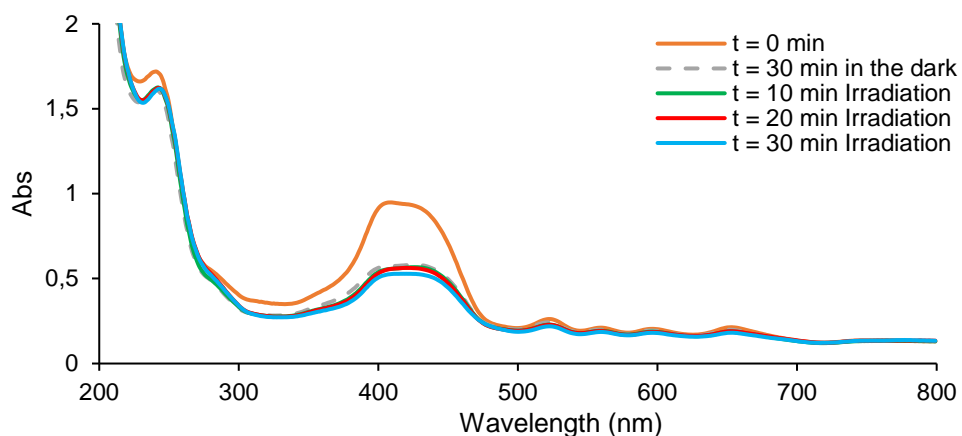


Figure 3.11. UV-Vis spectra of paracetamol (130 μM , 20 ppm) and $\text{H}_2\text{TPP}(\text{COOH})_4$ (**3**) (13 μM , 10% molar ratio) in a solution with $\text{pH}=2.5$ and of the samples analyzed at different times of irradiation with white light (18 mW/cm^2).

Table 3.1. Values of pH before and after irradiation for each study, as well as the main results from each reaction.

Initial pH	Final pH	Catalyst stability	PCM degradation
2.53	2.57	No	No
5.71	6.2	Yes	No
7.40	7.45	Yes	No
8.9	8.82	Yes	Yes
9.45	9.48	Yes	Yes
10.92	10.46	Yes	Yes

3.3.2 Photooxidation of paracetamol with MOF $\text{H}_2\text{TPP}(\text{COOH})_4\text{Zr}_4$

The study of photooxidation of paracetamol using $\text{H}_2\text{TPP}(\text{COOH})_4\text{Zr}_4$ MOF consisted in multiple different experiments, in pursue of the optimum reactions conditions. Firstly, the effect of catalyst concentration was evaluated. Then, the addition of an oxidant agent was attested and finally the effect of pH in heterogeneous catalysis was also investigated. **Table 3.2** summarizes the main reaction conditions present in each study as well as the main results (for detailed descriptions of the reactions refer to **Chapter 6: Experimental Section**).

The effect of the load of catalyst on the efficiency of PCM photodegradation was studied utilizing two different values of concentration: 12.96 μM and 65.05 μM (**Figure 3.12**). The experiments showed that under the reaction conditions the MOF catalyst was not able to oxidize the substrate, regardless of the load utilized. This conclusion is based on the fact that PCM's characteristic peak of absorption did not disappear, nor did it suffer a decrease.

Table 3.2. Main reaction conditions and results of the photocatalytic studies for PCM degradation performed with the MOF catalyst $\text{H}_2\text{TPP}(\text{COOH})_4\text{Zr}_4$.

Tested reaction condition	Reaction Conditions	Main results
Model Reaction	Catalyst concentration: 12.96 μM (10% of the molar concentration of the substrate)	No oxidation of the substrate was verified in the UV-Vis spectra.
Load of Catalyst	Catalyst concentration: 65.05 μM (50% of the molar concentration of the substrate)	No oxidation of the substrate was verified in the UV-Vis spectra.
Effect of oxidant (H_2O_2)	Catalyst concentration: 12.96 μM (10% of the molar concentration of the substrate) H_2O_2 concentration: $1.3 \times 10^{-3} \text{ M}$ (10 times the molar amount of substrate in solution)	No oxidation of the substrate was verified in the UV-Vis spectra.
	Catalyst concentration: 65.05 μM (50% of the molar concentration of the substrate) H_2O_2 concentration: $1.3 \times 10^{-3} \text{ M}$ (10 times the molar amount of substrate in solution)	No oxidation of the substrate was verified in the UV-Vis spectra.
Effect of pH	Catalyst concentration: 65.05 μM (50% of the molar concentration of the substrate) pH of the reaction solution: 8	Oxidation of the substrate was verified in the UV-Vis spectra, as well as possible formation of sub products. Loss of stability of the MOF catalyst was also verified.
	Catalyst concentration: 65.05 μM (50% of the molar concentration of the substrate) pH of the reaction solution: 11	Complete loss of the stability of the catalyst was verified.

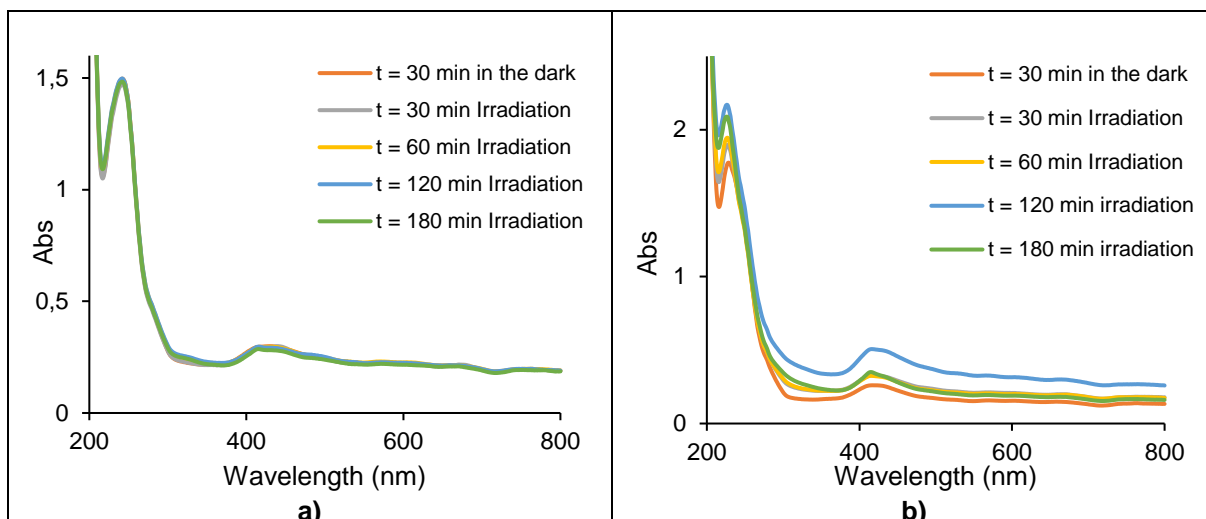


Figure 3.12. UV-Vis spectra of the aqueous solutions of paracetamol (130 μM , 20 ppm) and the MOF catalyst $\text{H}_2\text{TPP}(\text{COOH})_4\text{Zr}_4$: **a)** 12.96 μM (10% molar ratio) and **b)** 60,05 μM (50% molar ratio) and the samples analyzed after predetermined periods of irradiation with white light (18 mW/cm^2).

The next step of this study was to investigate the effect of the load of catalyst combined with the addition of H_2O_2 as oxidant. For that, the MOF catalyst $\text{H}_2\text{TPP}(\text{COOH})_4\text{Zr}_4$ (12.96 μM and 60.05 μM) and hydrogen peroxide (1.3×10^{-3} M) were added to aqueous solutions of paracetamol (130 μM). The results were very similar to those obtained in the reactions without the addition of an oxidant agent, as PCM's characteristic peak of absorption did not suffer a decrease during the reaction time (**Figure 3.13**). The objective with the addition of H_2O_2 was to increase the availability of $\cdot\text{OH}$ radicals in the solution. This is accomplished with the breakup of the relatively weak oxygen-oxygen single bond and yields $\cdot\text{OH}$ radicals (**Equation 7**).¹¹² However, the combined effect of the catalyst and the light did not result in the break of the aforementioned bond, therefore the availability of $\cdot\text{OH}$ radicals did not increase significantly, and no oxidation was verified.



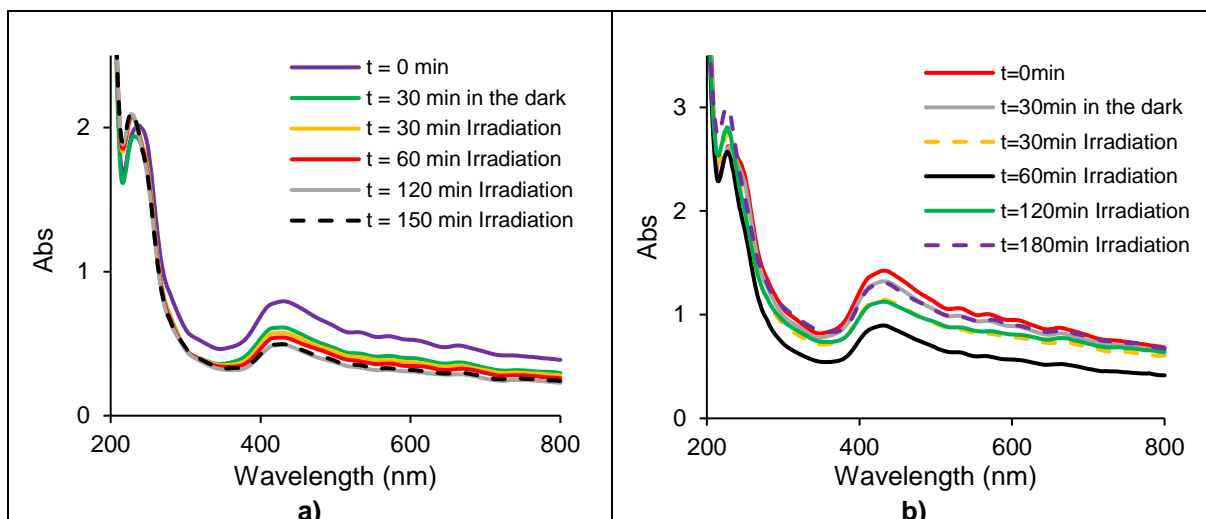


Figure 3.13. UV-Vis spectra of the aqueous solutions of paracetamol (130 μM , 20 ppm), the MOF catalyst $\text{H}_2\text{TPP}(\text{COOH})_4\text{Zr}_4$: **a)** 12.96 μM (10% molar ratio) and **b)** 60,05 μM (50% molar ratio); and H_2O_2 (1.3×10^{-3} M) and the samples analyzed after predetermined periods of irradiation with white light (18 mW/cm^2).

The last study conducted with the MOF catalyst $\text{H}_2\text{TPP}(\text{COOH})_4\text{Zr}_4$ was to access the effect of pH on the efficiency of PCM's photodegradation. The first studies were conducted with no regulation of pH hence, the reaction solution had a close pH of distilled water, in this case 7.25. However, considering the results relative to our studies of the effect of pH in the homogeneous photooxidation of paracetamol, as well as previously reported results of similar studies, it was clear that with alkaline values pH better results of degradation of paracetamol were obtained.^{104,106} With that in mind, two different values of pH were explored namely: 8 and 11. The pH was regulated using the same Britton-Robson buffer solutions that had been previously used in the homogeneous studies. In addition, the concentration of catalyst was 60.05 μM for both reactions.

The results from the reaction at pH = 8 lead us to believe that the substrate was oxidized, due to the fact that a new peak of absorption was formed at $\lambda \sim 317 \text{ nm}$ (**Figure 3.14**), which corresponds to the formation of an intermediate product. However, mineralization was not achieved since PCM's characteristic peak of absorption did not fully disappear. Furthermore, the Por-MOF was not completely stable under the tested conditions. Over time, it began to dissolve into the solution. This was verified both visually and by the increase in absorbance and definition of the Soret band characteristic of the base porphyrin.

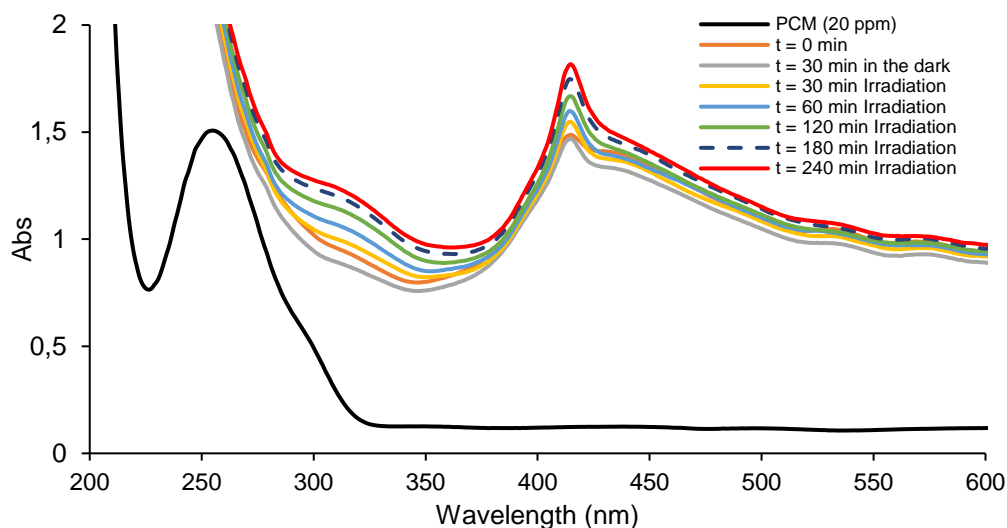


Figure 3.14. UV-Vis spectra of the aqueous solution (pH = 8) of paracetamol (130 μM , 20 ppm) and the MOF catalyst $\text{H}_2\text{TPP}(\text{COOH})_4\text{Zr}_4$ (60,05 μM , 50% molar ratio) and the samples analyzed after predetermined periods of irradiation with white light (18 mW/cm^2).

The fact that the MOF began to dissolve into its core porphyrin raises the question of whether or not there was a combined effect of both homogeneous and heterogeneous photocatalysis. Nevertheless, the contribution of the heterogeneous catalysis should be more significant based on the fact that the concentration of MOF in the solution was significantly superior to the concentration of base porphyrin. As a consequence, it also demonstrates that the MOF has the capacity to promote the photooxidation of PCM and under better reaction conditions it could even be recovered and used in multiple cycles.

The alkaline conditions promoted the photodegradation of PCM but hindered the MOF's stability. This was even more of an issue during the reaction at pH = 11. The MOF was completely dissolved in the reaction mixture after just a few minutes of irradiation, which made it impossible to draw any conclusions from this study.

This concludes the section regarding the photocatalytic studies for PCM degradation. The photodegradation of 17 β -estradiol (E2) with these catalysts will be described in the next section.

3.4 Photooxidation of 17 β -estradiol

The photocatalytic studies using 17 β -estradiol (E2) as substrate started by testing the catalytic activity of porphyrin **H₂TPP(COOH)₄ (3)**, followed by testing the respective Por-MOF. Unlike the studies with PCM however, this time, the studies focused on a quantitative analysis of the oxidation of the substrate. For that high performance liquid chromatography (HPLC) analysis were performed, in addition to following each reaction by UV-Vis spectroscopy.

Before the photocatalytic reactions, E2's photostability was investigated, similarly to what had been done at the beginning of the PCM studies. To that end, a solution of the substrate was prepared in methanol (147 μ M, 40 ppm) and irradiated for 3 h with white light at the used fluence rate (18 mW/cm²). The results of the stability test (**Figure 3.15**) clearly indicate that the substrate is stable under these conditions since its characteristic peak of absorption at approximately 281 nm did not suffer any depletion.

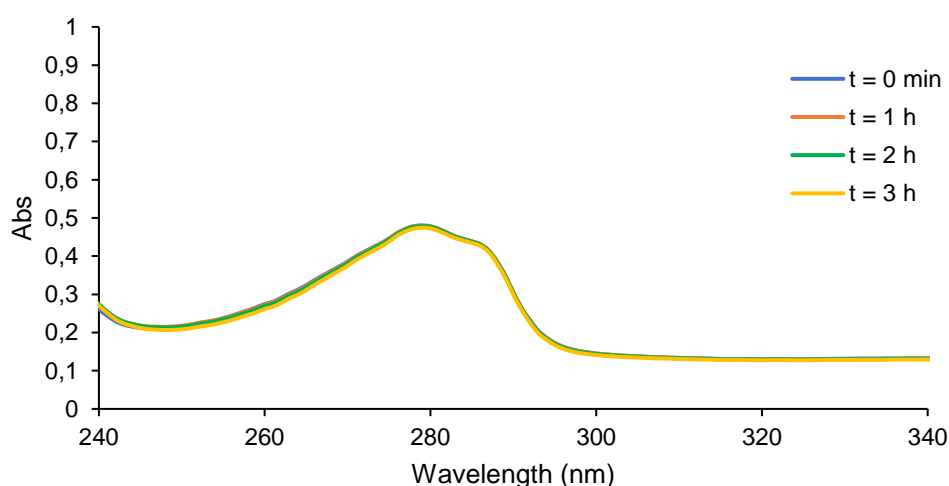


Figure 3.15. UV-Vis spectra of a methanol solution of 17 β -estradiol (E2) (147 μ M, 40 ppm) under white light (18 mW/cm²) and the respective samples analyzed after predetermined periods of irradiation.

3.4.1 Photooxidation of 17 β -estradiol with H₂TPP(COOH)₄

The photocatalytic performance of porphyrin **H₂TPP(COOH)₄ (3)** in the degradation of E2 was tested by irradiating with white light (18 mW/cm²), a reaction mixture consisting of both reagents dissolved in methanol for 180 minutes. The reaction was controlled by UV-Vis spectroscopy and samples were analyzed at predetermined periods of time (**Figure 3.16**).

The results show that after 30 minutes of irradiation, E2 is significantly oxidized given that its absorbance band is all but depleted. In addition, a new band was formed at approximately 232 nm, with

increasing intensity along the time (**Figure 3.16.a**). These two data points indicate that E2 must be oxidized with formation of a new product. In order to follow the degradation of E2 over time, this reaction was repeated using shorter irradiation intervals, with samples being analyzed, both by UV-Vis spectroscopy and HPLC, every 5 minutes, for the first 45 minutes of the reaction. The HPLC analysis reveals that the period the solution was left in dark conditions resulted in a slight decrease in E2 concentration (only 5%). Once the solution was irradiated, photodegradation occurred, with approximately 45% of E2 being oxidized (**Figure 3.16.b**).

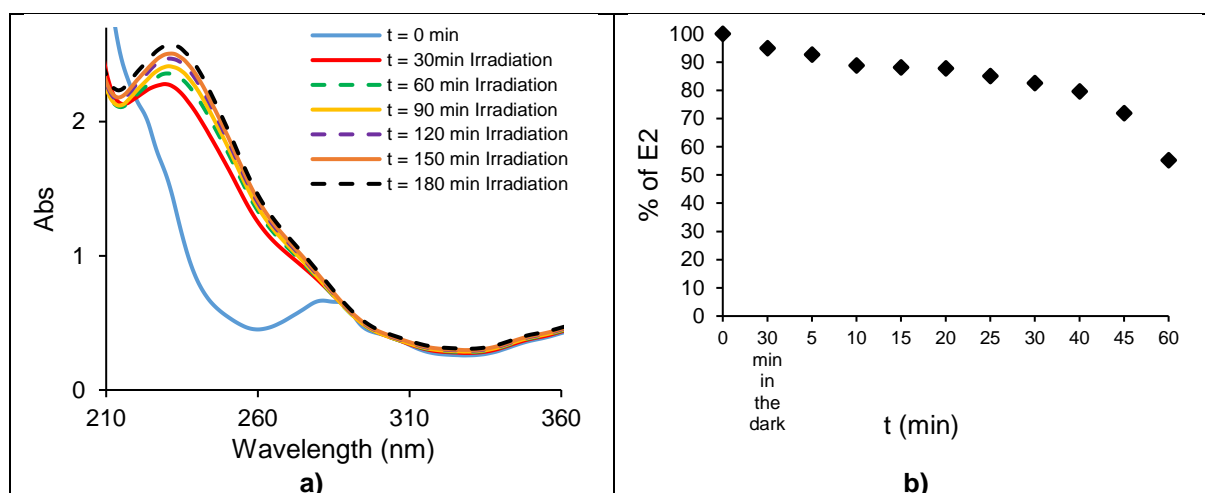


Figure 3.16. a): UV-Vis spectra of the reaction mixture of E2 (147 μM , 40 ppm) and $\text{H}_2\text{TPP}(\text{COOH})_4$ (**3**) (14.7 μM , 10% molar ratio) under white light irradiation (18 mW/cm^2), for 180 minutes, and the samples analyzed after predetermined periods of time; **b):** Evolution of the concentration of E2 in the reaction mixture over time, based on HPLC data.

The identification of sub products of E2 was not performed, contrary to what had been done during the PCM studies. Nevertheless, the analysis of the HPLC reports shows that two sub products with retention times ca. 3.6 minutes and 3.9 minutes were formed, circled in red in **Figure 3.18**. These products are less polar than E2 which has a retention time of ca. 10.7 minutes.

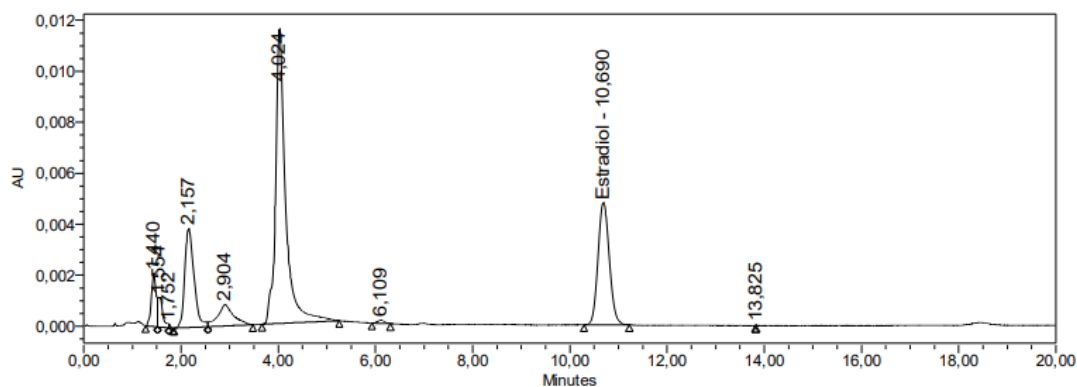


Figure 3.17. HPLC results from the sample of the reaction mixture consisting of a methanol solution of E2 (147 μM) and the porphyrin $\text{H}_2\text{TPP}(\text{COOH})_4$ (**3**) (14.7 μM , 10% molar ratio) analyzed before irradiation ($t = 0$ minutes).

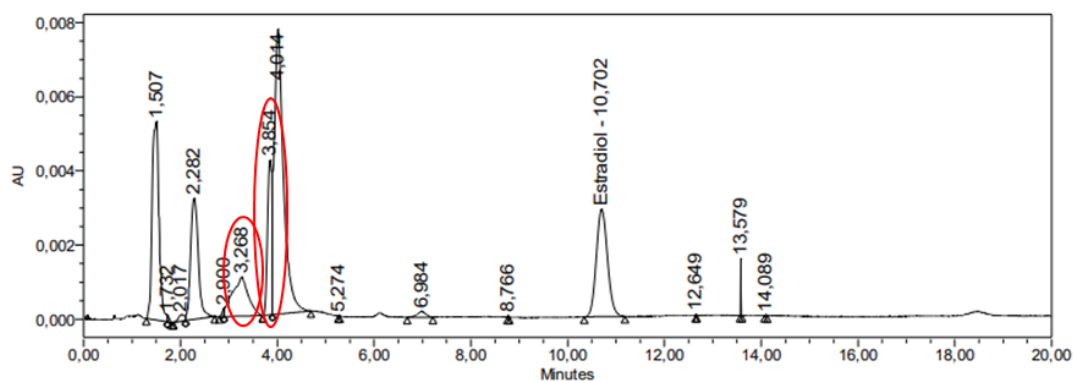


Figure 3.18. HPLC results from the sample of the reaction mixture consisting of a methanol solution of E2 (147 μM) and the porphyrin $\text{H}_2\text{TPP}(\text{COOH})_4$ (**3**) (14.7 μM , 10% molar ratio) analyzed after 60 minutes of irradiation. The red circles indicate the possible sub products of the oxidation of E2.

3.4.2 Photooxidation of 17β -estradiol with MOF $\text{H}_2\text{TPP}(\text{COOH})_4\text{Zr}_4$

After studying the photooxidation of 17β -estradiol with the homogeneous catalyst it was time to study how effective the MOF based on this porphyrin was as a photocatalyst in the degradation of E2. Once again, multiple studies were performed, in search for the optimum catalytic conditions, investigating the influence of the same parameters previously tested during the photocatalytic studies for PCM degradation (**Table 3.3**).

The first reaction was performed using a 1:10 catalyst:substrate molar ratio (the same amount as in the homogeneous studies). The reaction was under white light irradiation (18 mW/cm^2) for 270 minutes, and was controlled by UV-Vis spectroscopy with samples being analyzed at predetermined periods of time. The results of this study suggest that there was no significant photooxidation of E2

during the reaction (**Figure 3.19.a**). Given this result a higher load of catalyst was applied in a new reaction, this time correspondent to 1:2 catalyst:substrate molar ratio (**Figure 3.19.b**).

Table 3.3. Main reaction conditions and results of the photocatalytic studies for E2 degradation performed with the MOF catalyst $\text{H}_2\text{TPP}(\text{COOH})_4\text{Zr}_4$.

Tested reaction condition	Reaction Conditions	Main results
Model Reaction	Catalyst concentration: 14.70 μM (10% of the molar concentration of the substrate)	No oxidation of the substrate was verified in the UV-Vis spectra.
Load of Catalyst	Catalyst concentration: 73.50 μM (50% of the molar concentration of the substrate)	No oxidation of the substrate was verified in the UV-Vis spectra.
Effect of an oxidant agent (hydrogen peroxide)	Catalyst concentration: 73.50 μM (50% of the molar concentration of the substrate) H_2O_2 concentration: $1.47 \times 10^{-3} \text{ M}$ (10 times the molar amount of substrate in solution)	No oxidation of the substrate was verified in the UV-Vis spectra.
Effect of pH	Catalyst concentration: 73.5 μM (50% of the molar concentration of the substrate) pH of the reaction solution: 8	Oxidation of the substrate was verified in the UV-Vis spectra, as well as possible formation of sub products. Loss of stability of the MOF catalyst was also verified.

Once again, the results indicate that the photooxidation of E2 did not occur based on the presence of its absorbance band. These results lead to the conclusion that, in these reaction conditions, the catalyst is not able do oxidize the substrate even with loads of catalyst up to 50% molar the amount of substrate.

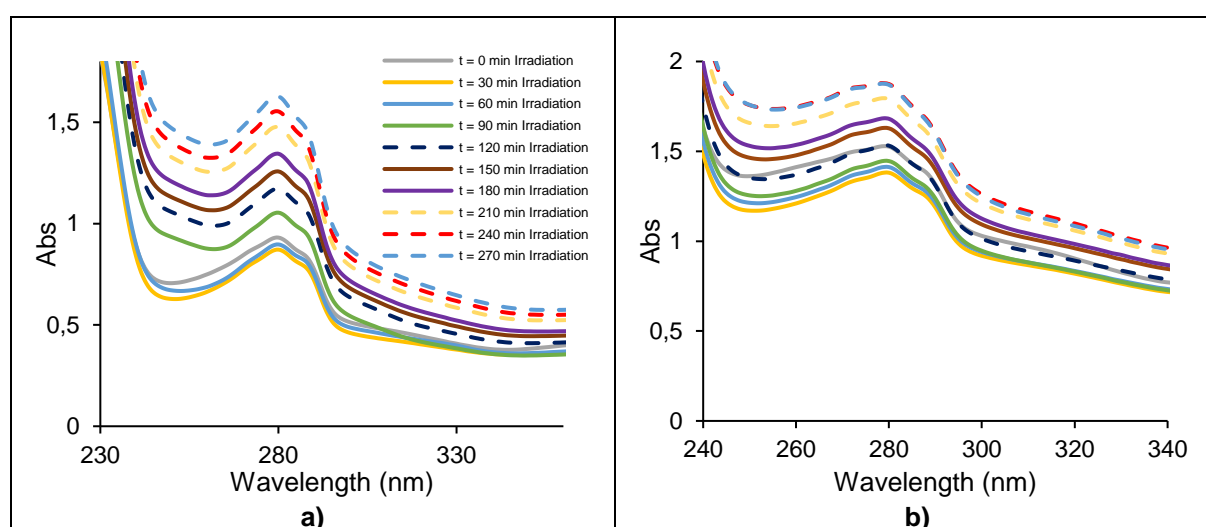


Figure 3.19. UV-Vis spectra of the reaction mixture of E2 (147 μM , 40 ppm) and $\text{H}_2\text{TPP}(\text{COOH})_4\text{Zr}_4$: **a)** 14.7 μM , 10% molar ratio and **b)** 73.5 μM , 50% molar ratio; under white light irradiation (18 mW/cm^2), for 270 minutes, and the respective samples analyzed after predetermined periods of time.

The effect of an oxidant agent in the photodegradation of E2 with the MOF catalyst **H₂TPP(COOH)₄Zr₄** was attested by adding H₂O₂ (1.47×10⁻³ M, correspondent to ten times the number of moles of substrate) to a solution containing the MOF and the substrate in the molar ratio 1:2. Then, the reaction mixture was irradiated with white light (18 mW/cm²) for 90 minutes and during this time, there was no decrease in absorbance of E2's band (**Figure 3.20**). As it had been verified during the PCM studies, once again the addition of H₂O₂ combined with irradiation and the MOF catalyst had no significant effect in the oxidation of the pharmaceutical substrate. Since the reaction conditions applied in this case were very similar to the ones applied in the same study with PCM, it is acceptable to conclude that the same reasons justify the lack of oxidation in this case.

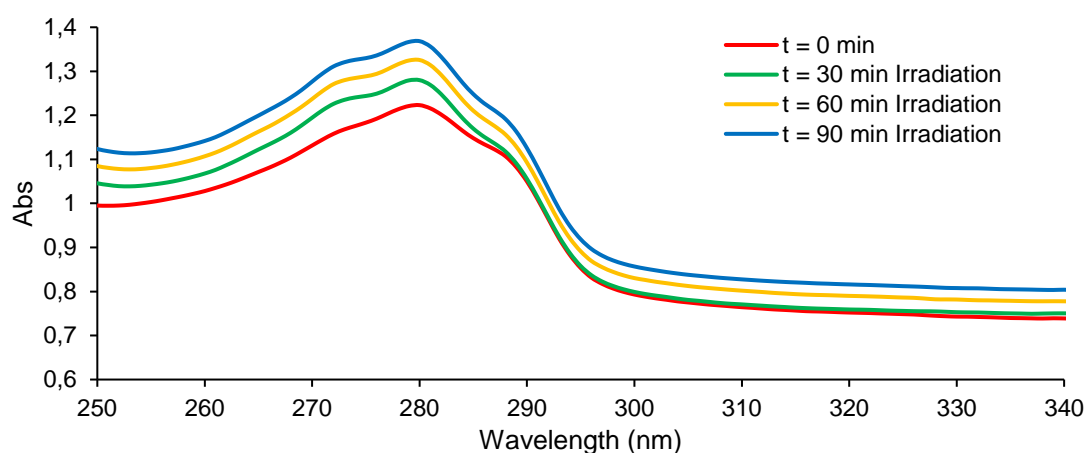


Figure 3.20. UV-Vis spectra of the reaction mixture of E2 (147 µM, 40 ppm), **H₂TPP(COOH)₄Zr₄** (73.5 µM, 50% molar ratio) and H₂O₂ (1.47×10⁻³ M) under white light irradiation (18 mW/cm²), for 90 minutes, and the respective samples analyzed after predetermined periods of time.

The results of the different heterogeneous catalytic studies for degradation of E2 had been, so far, in accordance with what was verified during the equivalent studies for degradation of PCM. In light of that information, we predicted that the effect of the pH could behave in a similar way, thereby testing the reaction of photooxidation of E2 with the MOF catalyst **H₂TPP(COOH)₄Zr₄** at pH ~ 8. The same reaction at pH = 11 was not tested since it had been established the MOF's lack of stability under such alkaline conditions.

The reaction mixture's pH was regulated with a Britton-Robson buffer solution with pH value 8 and the study followed the same general protocol used for the previous catalytic studies (for details please refer to **Chapter 6: Experimental Section**).

Once more, the results concerning the heterogeneous photocatalysis of both pharmaceutical compounds are in accordance, since with alkaline pH the MOF catalyst was able to oxidize the substrate even if not completely. It is possible to see how after 180 minutes of irradiation, E2's characteristic absorbance band loses its shape which indicates its photodegradation (**Figure 3.21.a**).

Moreover, HPLC results indicate that by the end of the reaction most of the substrate has been decomposed with a degradation of E2 up to 83% (**Figure 3.21.b**). It is also possible to verify that before the start of the irradiation, the concentration of the substrate in the solution has dropped approximately 42%. This can be explained by adsorption of the E2 by the MOF catalyst. This result is on pair with previous studies of heterogeneous photooxidation of E2 with MOFs.^{28,102,113}

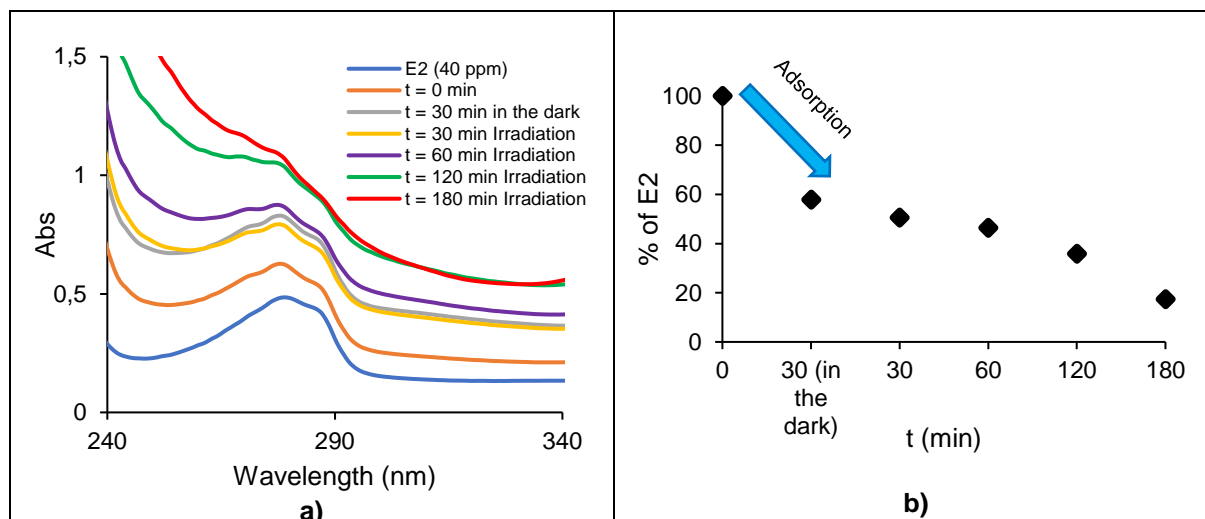


Figure 3.21. a): UV-Vis spectra of the reaction mixture of E2 (147 μM , 40 ppm) and $\text{H}_2\text{TPP}(\text{COOH})_4\text{Zr}_4$ (73.5 μM , 50% molar ratio) (pH \sim 8) under white light irradiation (18 mW/cm^2), for 180 minutes, and the respective samples analyzed after predetermined periods of time; **b):** Evolution of the concentration of E2 in the reaction mixture over time, based on HPLC data.

In terms of formation of sub products of the photodegradation of E2, similarly to the study in homogeneous conditions, the identification of sub products was not performed. However, looking at the HPLC reports it is possible to verify the formation of three sub products with retention times of ca. 1.9 minutes, 3.1 minutes, and 3.9 minutes (**Figure 3.22** and **Figure 3.23**). This means that while during the homogeneous photocatalysis of E2 only two sub products were verified by the HPLC reports this time three sub products were verified. In accordance with the homogeneous studies, however, is the fact that all the sub products are less polar then the E2.

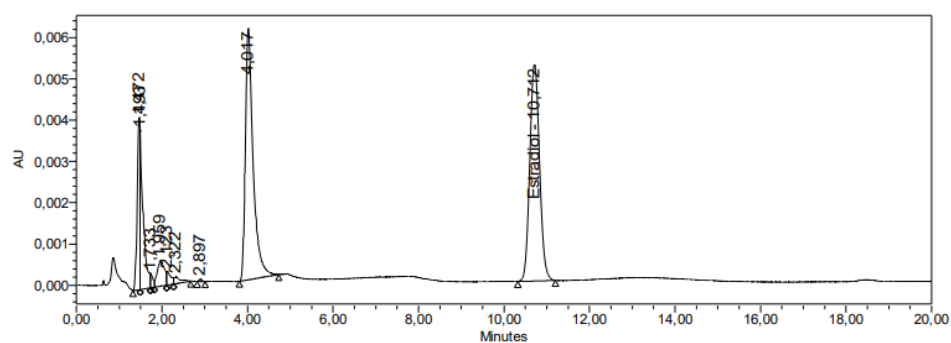


Figure 3.22. HPLC results from the sample of the reaction mixture consisting of a methanol solution of E2 (147 μM) and the MOF $\text{H}_2\text{TPP}(\text{COOH})_4\text{Zr}_4$ (73.5 μM), with pH \sim 8 analyzed before irradiation ($t = 0$ minutes).

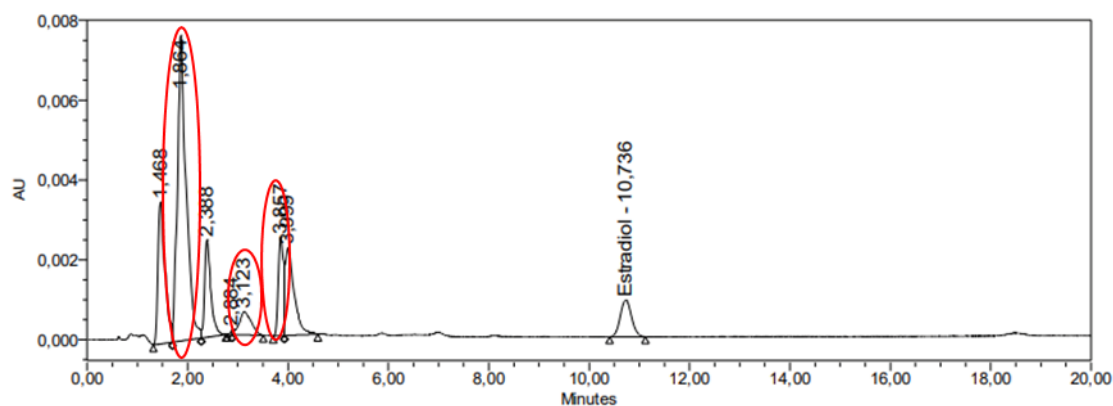


Figure 3.23. HPLC results from the sample of the reaction mixture consisting of a methanol solution of E2 (147 μM) and the MOF $\text{H}_2\text{TPP}(\text{COOH})_4\text{Zr}_4$ (73.5 μM), with pH \sim 8 analyzed after 180 minutes of irradiation. The red circles indicate the possible sub products of the oxidation of E2.

Despite the positive results with regards for the photodegradation of the pharmaceutical substrate, negative results were verified concerning the stability of the MOF under the tested reaction conditions. Over time, the MOF started to dissolve into its organic PBU, which can be attested by the increase in absorbance and definition of the porphyrin's Soret band, in the UV-Vis spectra (**Figure 3.24**). This result, which was also verified during the studies with PCM, points to the possibility of a combined effect of both homogeneous and heterogeneous photocatalysis. In addition, it prevents the recycling studies of the catalyst.

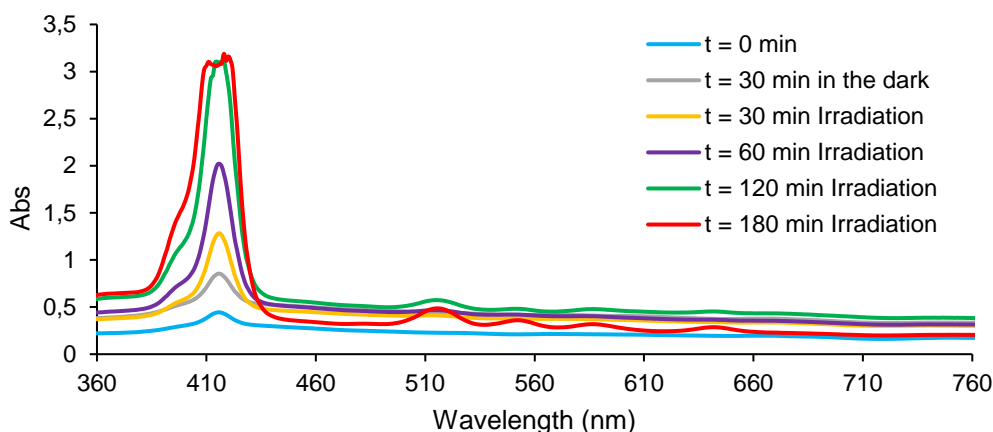


Figure 3.24. UV-Vis spectra of the MOF catalyst $\text{H}_2\text{TPP}(\text{COOH})_4\text{Zr}_4$ during the photooxidation of E2 at pH = 8.

The photocatalytic studies for degradation of PCM and E2 described in this chapter allow the formulation of a few conclusions. It was demonstrated, during the singlet oxygen assays that porphyrin $\text{H}_2\text{TPP}(\text{COOH})_4$ (**3**) is a good photosensitizer. This was an indicator of what was then later confirmed when testing its photocatalytic activity: the porphyrin has the capacity to act as a photocatalyst in the homogenous degradation of both pharmaceutical compounds. The results even allowed the formulation of possible reaction paths for the degradation of PCM, which included hydroquinone as a sub product which is originated during the reaction but ends up being oxidized along with the original PC. Furthermore, the studies with variation of pH pointed to the fact that the availability of $\cdot\text{OH}$ radicals was a determinant factor in the oxidation of PCM, since degradation was only verified when alkaline values of pH were registered.

Regarding the heterogeneous photocatalytic studies, it was clear that finding the optimum reaction conditions was no easy task. It was expected that the Por-MOF showed less photocatalytic activity than its porphyrin precursor and the results showed just that, with the studies with different loads of catalyst or with the oxidant agent, producing no positive results. However, it was possible to find conditions in which the photodegradation of each pharmaceutical was verified. Those conditions were once more related with alkaline values of pH, which is in alignment with the results from the homogeneous studies. Unfortunately, the Por-MOF was not completely stable under the tested conditions which hindered the possibility of evaluating its activity during multiple cycles. Nevertheless, if the optimum reaction conditions are found, it is expected that the effectiveness of the Por-MOF as a photocatalyst would improve significantly. Moreover, other metals than zirconium, which are perhaps more active, could also be employed in the process of making better MOF catalysts for this application.

This concludes the section covering the photocatalytic studies performed for this dissertation. The next section will cover the catalytic studies performed in the absence of irradiation with the MOF $\text{Mn}(\text{III})\text{TPP}(\text{COOH})_4\text{Zr}_4$ and its respective base metalloporphyrin $\text{Mn}(\text{III})\text{TPP}(\text{COOH})_4$ (**7**).

3.5 Oxidation of pharmaceuticals in dark conditions

The singlet oxygen assays performed with the MOF **Mn(III)TPP(COOH)₄Zr₄** and metalloporphyrin **Mn(III)TPP(COOH)₄** (**7**) showed the inability of these materials to generate ¹O₂. Nevertheless, manganese porphyrin complexes have been utilized as catalysts in oxidation reactions with success in previously reported work.^{55,98,114} Considering this information, the materials were tested in dark conditions (without light) and in the presence of an oxidant agent to access their catalytic activity. For these studies the same pharmaceutical compounds (PCM and E2) were tested.

The studies began by performing reactions in which the substrate was put under dark conditions, with stirring, with either the catalyst or the oxidant agent in order to see if either of these had an effect. As expected, there was no degradation of PCM nor E2 during these tests (see **Appendix C** for the detailed results).

Once the aforementioned reactions were finished the studies of oxidation with both homogeneous and heterogeneous catalysts combined with an oxidant agent were performed. The procedure consisted in adding the catalyst and the oxidant to the aqueous solution of PCM (130 μM, 20 ppm) and to the solution of E2 (40 ppm, 147 μM) in methanol. The reaction solution would then be left in the dark with stirring and samples would be analyzed by UV-Vis spectroscopy in pre-determined intervals. The reaction mixtures had a catalyst/substrate molar ratio of 0.1 for the stock solution (the same solution utilized in the photocatalytic studies) of porphyrin **Mn(III)TPP(COOH)₄** (**7**) and of 0.5 for the MOF **Mn(III)TPP(COOH)₄Zr₄**. Hydrogen peroxide was the oxidant agent with an oxidant/substrate molar ratio of 10.

The results of the reactions with the porphyrin as catalyst show that under the described conditions the porphyrin is oxidized, whereas the substrate is not. This can be concluded based on the fact that while the absorbance band of the pharmaceutical substrates suffered no significant decrease, the Soret Band, characteristic of the porphyrin, suffered a very significant decrease over time (**Figure 3.25**).

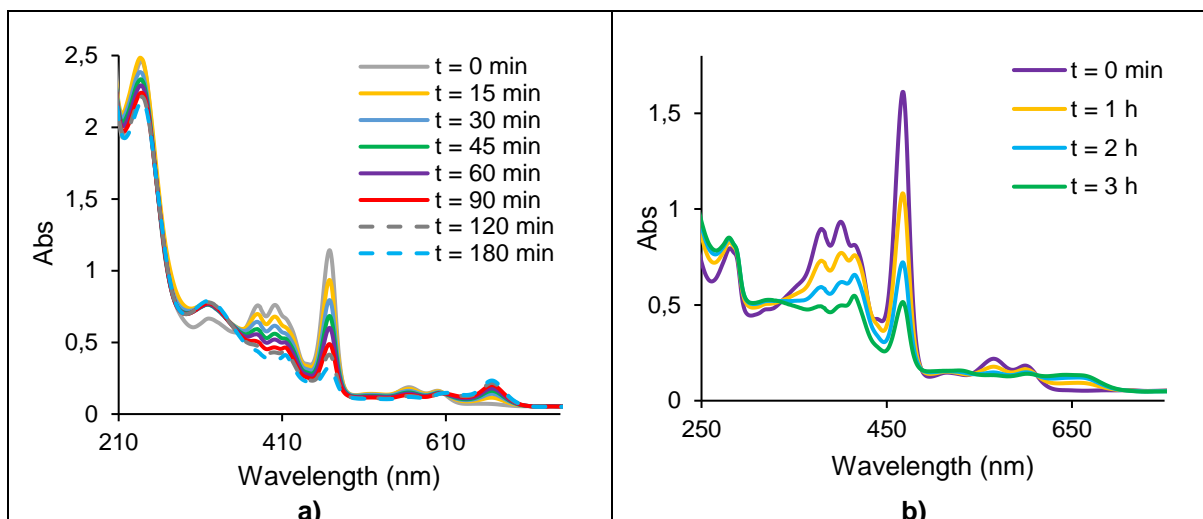


Figure 3.25. UV-Vis spectra of the reaction mixture of **Mn(III)TPP(COOH)₄ (7)** (molar ratio catalyst/substrate = 0.1) and H₂O₂ (molar ratio oxidant/substrate = 10) and **a)** PCM (130 μM, 20 ppm), **b)** E2 (40 ppm, 147 μM). The reactions were left in the dark with stirring for 180 min and the respective samples analyzed after predetermined periods of time.

The reactions performed in the presence of the Por-MOF as heterogeneous catalyst showed the latter's stability under the reaction conditions. However, it is also possible to conclude that under the tested reaction conditions the catalyst was not able to oxidize neither PCM nor E2 (**Figure 3.26**). These results were somewhat unexpected. Despite not being able to generate singlet oxygen, manganese metalloporphyrins have shown catalytic activity in dark conditions in the oxidation of alkanes⁹³, in the oxidation of (*Z*)-cyclooctene, cyclohexane and heptane⁹⁴ and in the degradation of the pharmaceutical compound trimethoprim⁹⁸, to cite a few previously reported reactions. This leads us to believe that the conditions under which the reactions were conducted were not ideal for the degradation of the pharmaceutical pollutants.

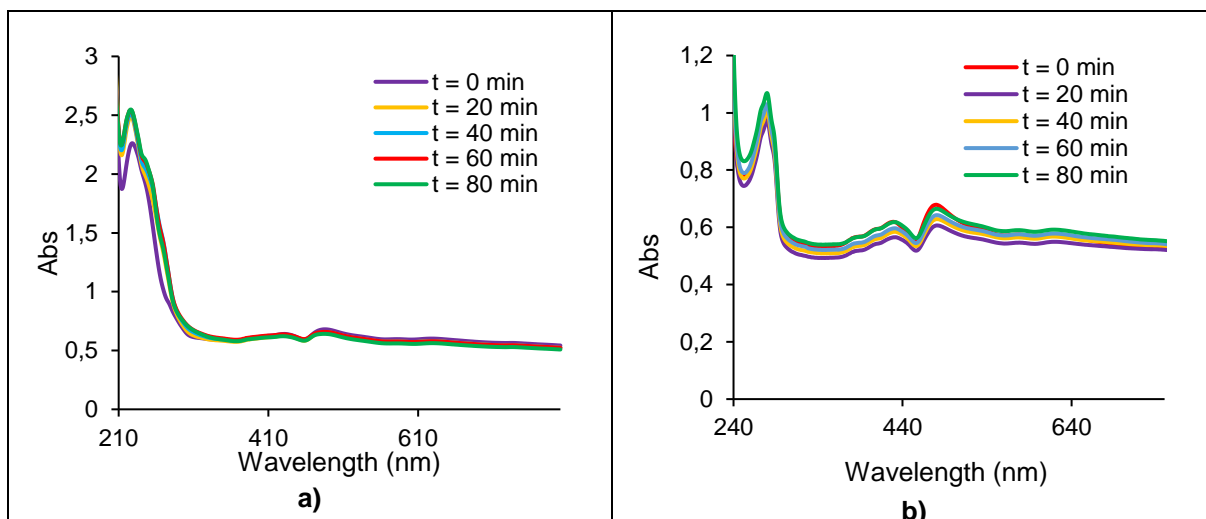


Figure 3.26. UV-Vis spectra of the reaction mixture of **Mn(III)TPP(COOH)₄Zr₄** (catalyst/substrate molar ratio = 0.5) and H₂O₂ (oxidant/substrate molar ratio = 10) and **a)** PCM (130 μM, 20 ppm), **b)** E2 (40 ppm, 147 μM). The reactions were left in the dark with stirring for 80 min and the respective samples analyzed after predetermined periods of time.

These studies in dark conditions had negative results with no degradation of either pharmaceutical being verified. As it was previously mentioned this is somewhat surprising but can, perhaps, be explained by the fact that the zirconium, is seemingly not very catalytically active. Furthermore, the fact that the manganese ion might not be significantly available as a catalytic center, due to the structure of the MOF, also helps to explain the negative results obtained in these studies.

4. Preparation of tetra-pyridyl and tetra-S-pyridyl based MOFs as catalysts for microwave-assisted oxidation of secondary alcohols

4.1 General Overview

While developing the previously described materials and performing the catalytic studies which constituted the main focus of this dissertation, tetra-pyridyl and tetra-S-pyridyl based MOFs were also prepared with the goal of complementing a different project. The intent of this project was to develop porphyrin based MOFs which could then be utilized as catalysts for micro-wave assisted oxidation of secondary alcohols. The oxidation of alcohols is one of the most important types of reactions in industrial processes and organic chemistry, since they allow the obtention of a wide range of aliphatic compounds.^{115,116} As a result, there is great interest in finding and developing “greener” methods for performing these reactions and that is where microwave-assisted oxidation with Por-MOFs comes in.

In an initial phase, the objective was to prepare metalloporphyrin based MOFs with 5,10,15,20-tetrakis(4-pyridyl)porphyrin (**H₂TPyP**, **11**) and 5,10,15,20-tetrakis[2,3,5,6-tetrafluoro-4-(4-pyridylsulfanyl)phenyl]porphyrin (**H₂TPPF₁₆(SPy)₄**, **12**) as organic linkers with a combination of copper and zinc, as metal ions. Additionally single metal, copper-copper Por-MOFs of these two porphyrins were also attempted. The structures and designations of the explored porphyrins are shown in **Figure 4.1**.

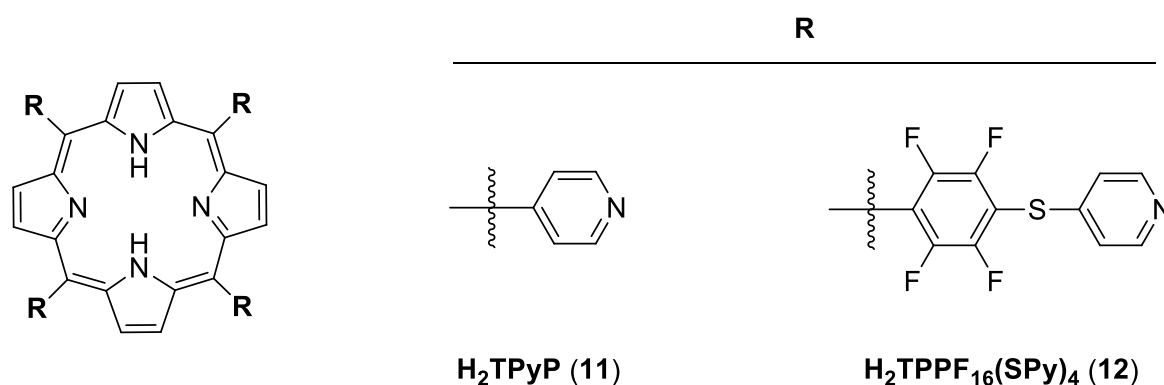
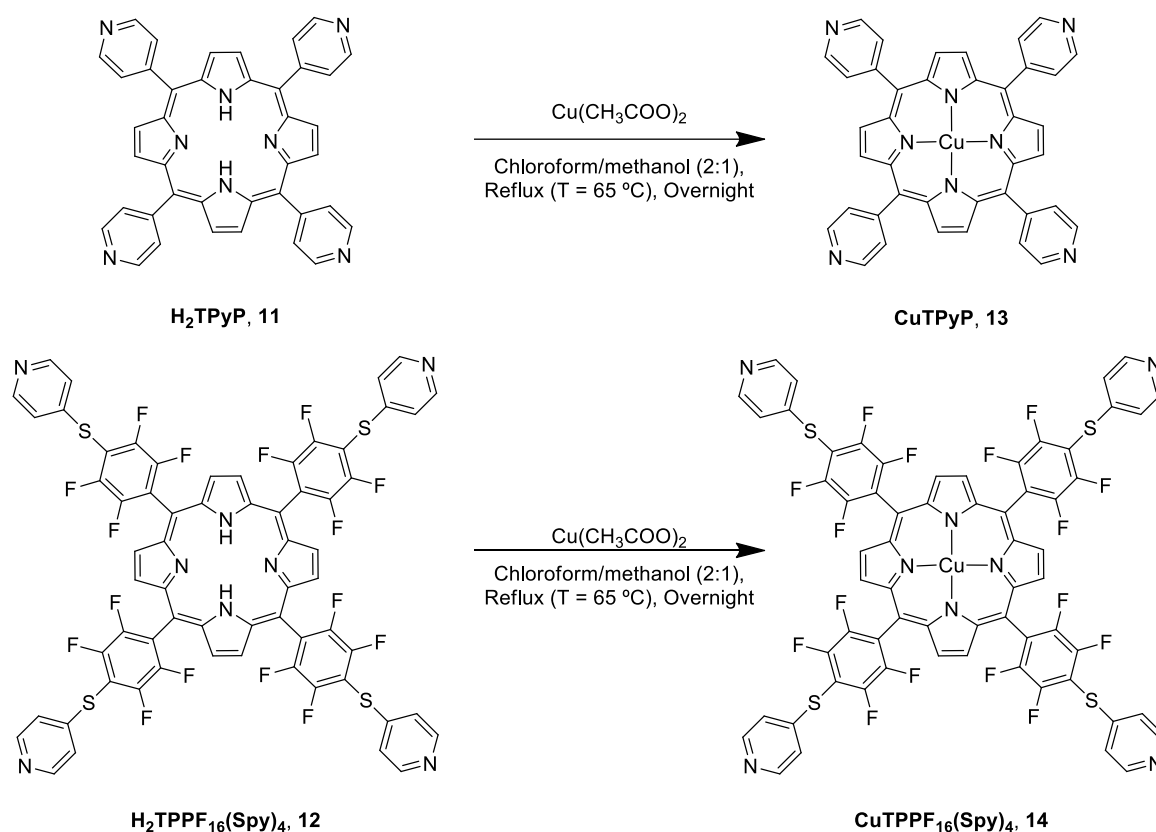


Figure 4.1. Structure and designation of the porphyrins explored in this section.

4.2 Synthesis of copper porphyrin complexes

Copper metal porphyrin complexes of both **H₂TPyP (11)** and **H₂TPPF₁₆(Spy)₄ (12)** were synthesized not only to then be used in the preparation of MOFs but also to be tested as homogeneous catalysts. The synthesis of both complexes (**Scheme 4.1**) followed the procedure reported by Castro, Kelly *et al.* (2017).¹¹⁷ The reactions were controlled by TLC and the complexes were obtained in quantitative yields. Both metallic complexes were characterized by UV-Vis spectroscopy and the results are in alignment with what can be found in the literature (See **Appendix D** for details).¹¹⁷



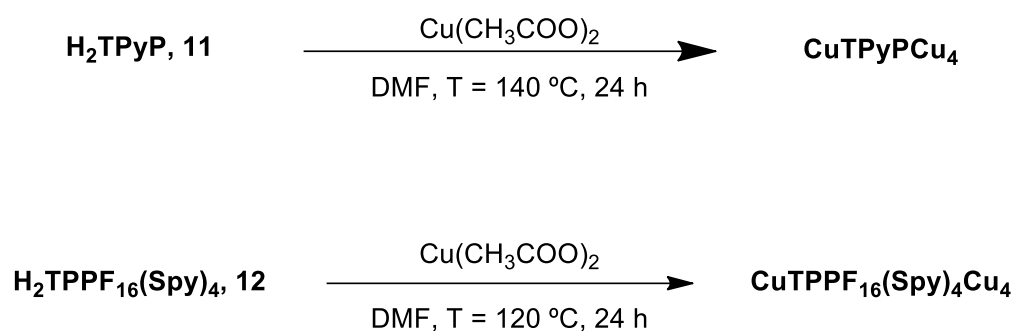
Scheme 4.1

4.3 Preparation of tetra-pyridyl and tetra-S-pyridyl based MOFs

In this section the preparation of the MOFs based of porphyrins **H₂TPyP (11)** and **H₂TPPF₁₆(Spy)₄ (12)** will be described, both the successful and the unsuccessful attempts. The characterization of the materials will also be shown. The MOFs described in this section were prepared via the same solvothermal method described in **Chapter 2**. The generic procedures utilized were adapted from Ohmura, Tetsushi *et al.* (2006)¹¹⁷ and Castro, Kelly *et al.* (2017)¹¹⁸. The precautions taken

in the preparation of MOFs described in **Chapter 2** with the dissolution of the materials before starting the reaction, using the ultrasonic bath, as well as the thorough wash of the materials once the reaction was completed were also taken during the preparation of these MOFs. The solvent utilized during the washes was a mixture of dichloromethane/methanol (85:15) since it is the solvent which better dissolves the starting porphyrins **H₂TPyP (11)** and **H₂TPPF₁₆(SPy)₄ (12)**.

The first MOFs to be prepared were the single metal MOFs with copper as the metallic PBU (**Scheme 4.2**).



Scheme 4.2

After 24 h the reactions were stopped, the materials collected and washed and then characterized by Powder XRD (**Figure 4.2** and **Figure 4.3**). The analysis showed the materials had crystalline character, which indicates the success of the synthesis.

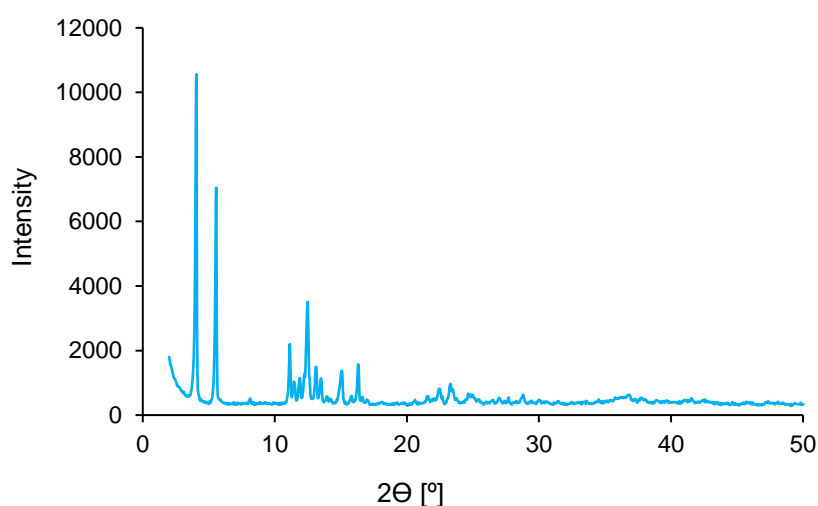


Figure 4.2. Powder X-ray diffraction data of MOF **CuTPyPCu₄**

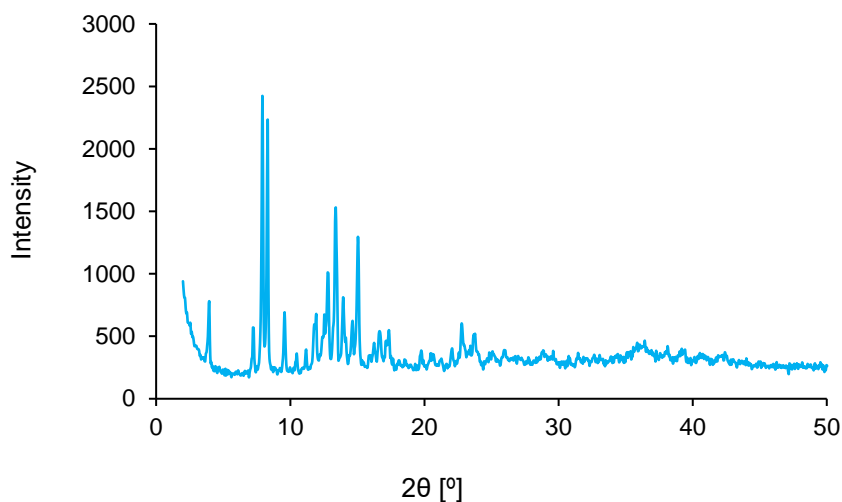
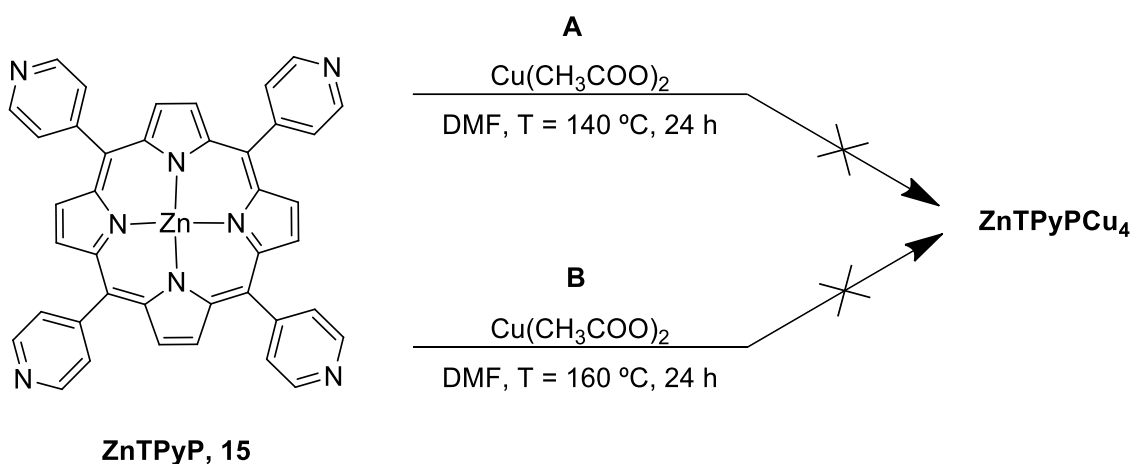


Figure 4.3. Powder X-ray diffraction data of MOF **CuTPPF₁₆(Spy)₄Cu₄**.

For the preparation of **ZnTPyPCu₄** two different reaction pathways (A and B) were attempted (**Scheme 4.3**). Pathway A was performed under the same conditions described in **Scheme 4.2**, for **H₂TPyP (11)**, whereas pathway B was performed at 160 °C instead of 140 °C. Both reactions had as their starting material the metallic complex **ZnTPyP (15)**, which was not synthesized during this project, instead it was kindly provided by master engineer Daniela Fonte.

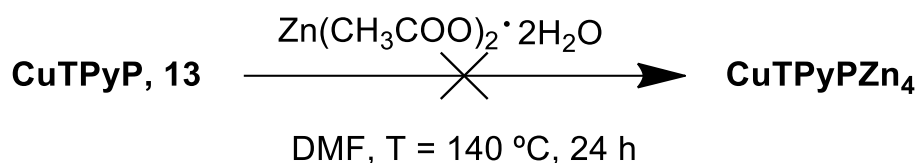


Scheme 4.3

Neither of the tested reaction pathways yielded the desired MOF. A solid was obtained from reaction pathway A, which after being thoroughly washed was analyzed by Powder XRD. The result of the analysis showed that the material was not crystalline. The solid was then put through another cycle of washing and analyzed by Powder XRD a second time. Nevertheless, the result was similar, and the

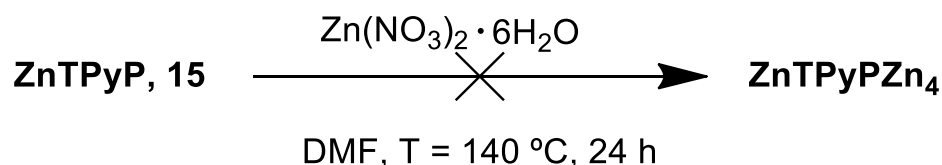
material was deemed as not being a MOF. From reaction pathway B resulted a solid which was mostly dissolved during the washing process, which means that this pathway was unsuccessful as well.

The preparation of MOF **CuTPyPZn₄** was attempted as well (**Scheme 4.4**), however, the obtained solid dissolved almost completely in the solution of dichloromethane/methanol (85:15) which meant that the obtained material was either not a Por-MOF or at least not a stable one.



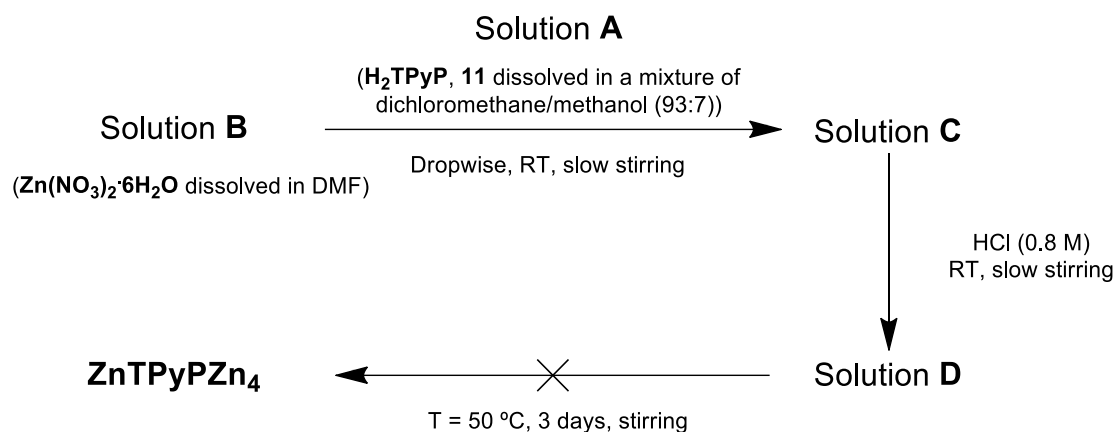
Scheme 4.4

Finally, the preparation of a Por-MOF with just the metal zinc was attempted (**ZnTPyPZn₄**). Firstly, we tried to prepare the MOF using the same general solvothermal method (**Scheme 4.5**). The starting material was the metallic complex **ZnTPyP (15)**. The result of the reaction was a solid which was completely dissolved during the washing process hence, it was not considered a MOF, or at least not a stable one for subsequent use in catalytic studies.



Scheme 4.5

A second attempt was performed with a completely different procedure adapted from Xie, Ming-Hua *et al.* (2011).⁸⁴ According to this procedure the free base porphyrin **H₂TPyP (11)** was dissolved in a solution of dichloromethane/methanol (93:7) (solution A). Another solution (B) was made, which consisted in dissolving zinc nitrate hexahydrate in DMF. Solution A was then added, dropwise, to solution B at room temperature, with slow agitation (solution C). A third step was to add HCl (0.8M) to solution C, also at room temperature, with slow agitation (solution D). The reaction mixture was then left stirring at 50 °C for 3 days, after which, a solid was formed (**Scheme 4.6**). The solid was collected and washed but dissolved completely during the process, therefore, this pathway was unsuccessful for the preparation of the desired MOF **ZnTPyPZn₄**.



Scheme 4.6

This concluded the attempts at preparation of tetra pyridyl and tetra-S-pyridyl based MOFs. It is clear that it was not possible to successfully synthesize a Por-MOF involving the zinc metal, during the period this dissertation was developed. The difficulties associated with the preparation of porphyrin or metalloporphyrin based MOFs are well documented, specially the issues regarding the MOF materials retaining their stability and crystallinity upon solvent removal.^{80,119} In fact, in the specific case of Por-MOFs, solvent molecules are usually a crucial part of building stable SBUs and so, washing of these materials can, oftentimes, be enough to collapse their structure. We suspect this is the main reason for the complete solubility of the solid materials obtained in the multiple synthesis in the washing solvent, hence being deemed unstable or not a MOF crystalline structure. Performing the washes with a mixture of dichloromethane/methanol (85:15) had the goal of completely remove unreacted porphyrin or metalloporphyrin which could have potentially remained in solution, this way minimizing the chances of having a powder consisting of a mixture of the MOF material and its precursor. However, by trying to avoid one potential problem another one was inadvertently created. Furthermore, it is our belief that zinc based SBUs are more labile, which directly contributes to the fact that the zinc based MOFs are significantly more prone to lose their structural integrity and collapse upon solvent removal. This is also in alignment with the empirical data demonstrated in this chapter, with multiple zinc based potential MOFs being dissolved upon washing, whereas the same was not verified with the copper-copper single metal materials.

5. Conclusions and Outlook

The main objective of this dissertation consisted of preparing zirconium Por-MOFs utilizing 5,10,15,20-tetrakis(4-carboxyethylthio-2,3,5,6-tetrafluorophenyl)porphyrin ($\text{H}_2\text{TPPF}_{16}(\text{SC}_2\text{H}_4\text{COOH})_4$, **1**), 5,10,15,20-tetrakis(4-carboxyphenylthio-2,3,5,6-tetrafluorophenyl)porphyrin ($\text{H}_2\text{TPPF}_{16}(\text{SC}_6\text{H}_4\text{COOH})_4$, **2**) and tetrakis(4-carboxyphenyl)porphyrin ($\text{H}_2\text{TPP}(\text{COOH})_4$, **3**) as organic linkers. Besides preparing MOFs from these free-base porphyrins there was also interest in preparing mixed metal Por-MOFs, thereby, the synthesis of zinc, iron, and manganese metalloporphyrins was successfully performed. These metalloporphyrins were characterized by UV-Vis spectroscopy. Unfortunately, we were not able to prepare MOFs with porphyrin $\text{H}_2\text{TPPF}_{16}(\text{SC}_2\text{H}_4\text{COOH})_4$ (**1**). Porphyrin $\text{H}_2\text{TPPF}_{16}(\text{SC}_6\text{H}_4\text{COOH})_4$ (**2**) yielded a MOF but it was not possible to obtain a reproducible reaction pathway that consistently yielded this material. However, two zirconium Por-MOFs were prepared with quantitative yields, from the free base porphyrin $\text{H}_2\text{TPP}(\text{COOH})_4$ (**3**) and its respective manganese metallic complex. These materials were characterized by Powder X-Ray diffraction and UV-Vis spectroscopy.

The capacity of the synthesized Por-MOFs and their respective porphyrin precursors to produce singlet oxygen was tested and $\text{H}_2\text{TPP}(\text{COOH})_4\text{Zr}_4$ as well as $\text{H}_2\text{TPP}(\text{COOH})_4$ (**3**) were able to produce the reactive oxygen species. On the other hand, $\text{Mn(III)TPP}(\text{COOH})_4\text{Zr}_4$ and the manganese metalloporphyrin were not able to produce $^1\text{O}_2$. These results informed the decision on how to conduct the catalytic studies for degradation of both paracetamol and 17β -estradiol.

The photocatalytic studies for degradation of paracetamol with porphyrin $\text{H}_2\text{TPP}(\text{COOH})_4$ (**3**) revealed the homogeneous catalyst's ability to decompose the pharmaceutical substrate in an aqueous solution under white light irradiation. The studies also allowed us to infer possible reaction mechanisms for the degradation of the drug, which included hydroquinone as an intermediate sub product. Regarding the (photo)catalytic activity of the Por-MOF, the studies revealed that only under alkaline conditions of pH was the MOF catalyst capable of decomposing the pharmaceutical substrate. However, the MOF revealed to be slightly unstable in the alkaline reaction mixture which hindered the possibility of studying its activity over multiple catalytic cycles.

After completing the catalytic studies with 17β -estradiol, we concluded that porphyrin $\text{H}_2\text{TPP}(\text{COOH})_4$ (**3**) was capable of oxidizing approximately 45% of the pharmaceutical present in the methanol reaction mixture, after 60 minutes of irradiation with white light. These results were obtained by HPLC analysis. The Por-MOF $\text{H}_2\text{TPP}(\text{COOH})_4\text{Zr}_4$ was also capable of oxidizing the pharmaceutical pollutant, with a reduction of 83% of the substrate's initial concentration being verified, after 3 hours of irradiation with white light. However, once more, alkaline conditions of pH were necessary for oxidation to be verified, which meant that the stability problem noticed during the paracetamol studies was also verified this time.

The results of the photocatalytic studies lead to the conclusion that the availability of •OH radicals, in alkaline reaction solutions, is of extreme relevance. This explains why the best oxidation results, both in homogeneous and heterogeneous catalysis, were obtained during the reactions with alkaline values of pH.

The catalytic studies with the manganese materials were performed in dark conditions with addition of an oxidant agent but did not result in the oxidation of the pharmaceutical substrates. Besides the reaction conditions, which might not have been ideal, we suspect that the manganese ion was not significantly available as an active site, due to the structure of the MOF, which largely contributed for the lack of catalytic activity of this heterogeneous catalyst.

Preparing mixed metal and single metal, copper and zinc, Por-MOFs based on tetra-pyridyl and tetra-S-pyridyl porphyrins was an additional goal of this dissertation. Unfortunately, mixed metal MOFs were not successfully synthesized during the duration of this project. The fact that zinc based SBUs are so much more labile, as well as the fact that the materials were washed with a solvent in which the precursors were extremely soluble probably contributed for the removal of solvent molecules from the SBUs, leading to the collapse of the solids structural integrity. On the other hand, single metal copper-copper MOFs were obtained from both porphyrins with quantitative yields. These materials were characterized by Powder X-Ray diffraction and will be utilized in a different project, as catalysts for microwave assisted oxidation of secondary alcohols.

The results and conclusions present in this dissertation further reinforce the potential of porphyrin based MOFs to be utilized as photocatalysts in advanced oxidation processes for the mineralization of pharmaceutical pollutants present in wastewaters. Nevertheless, this is a field in relative infancy and will benefit immensely from further research. Regarding the work presented in this dissertation, some avenues are worth continued exploration.

Porphyrins **H₂TPPF₁₆(SC₂H₄COOH)₄** (1) and **H₂TPPF₁₆(SC₆H₄COOH)₄** (2) have unique properties and their immobilization as zirconium Por-MOFs would certainly allow their utilization in interesting applications. During this dissertation we were close to the synthesis of a zirconium MOF based on porphyrin **H₂TPPF₁₆(SC₆H₄COOH)₄** (2). However, a reproducible synthetic pathway was not achieved. If more synthetic pathways were explored, with systematic alteration of reaction conditions, such as the temperature, the acid utilized or the reaction time, the probability of obtaining these materials would increase significantly. This is something worth exploring.

Additionally, the Por-MOF **H₂TPP(COOH)₄Zr₄** demonstrated to be capable of oxidizing both pharmaceuticals studied. However, the optimum reaction conditions, in which oxidation of the substrate is verified, as well as the stability of the heterogeneous catalyst were not found. Exploring other ways of controlling the reaction's pH so that the catalyst is stable but maintaining the availability of •OH radicals would be essential. Finding these conditions would be extremely interesting since it would allow for the study of the catalyst's activity in multiple catalytic cycles. This would be a massive step into introducing **H₂TPP(COOH)₄Zr₄** as viable photocatalyst for industrial applications.

6. Experimental Section

6.1 Materials and Equipment

The commercial reagents and solvents were obtained from multiple brands and used without any purification with exception for porphyrin **H₂TPPF₂₀ (4)** which was purified using a chromatography column with silica gel 60 (70-230 mesh ASTM) as its stationary phase and a mixture of petroleum ether and dichloromethane (75:25 (v/v)) as the mobile phase.

The multiple reactions of synthesis were controlled by TLC using pre-coated plastic silica gel 60 sheets.

Powder X-Ray diffraction data was collected with a D8 Advance Bruker AXS θ -2 θ diffractometer, with a copper radiation source (Cu K α , λ = 1.5406 Å) and a secondary monochromator, operated at 40 kV and 40 mA.

The absorption spectra of liquid and suspension samples were recorded using either an Agilent Technologies Cary 60 UV-Vis photometer or a Perkin Elmer model Lambda 35 UV-Vis spectrometer.

The irradiation system used was a Lumacare source, model LC-122A, consisting of a 250 W halogen lamp coupled with an optic fiber beam of red light (20-750 nm). In the singlet oxygen essays a LongPass color filter for wavelengths inferior to 500 nm from THORLABS GmbH was utilized. The radiation power was measured with a sensor model S302C coupled to a power meter model PM100D from THORLABS GmbH.

The HPLC analysis was conducted on a Waters Alliance e2695 Separations Module, with 2489 UV/Vis detector which is also from Waters. For the chromatographic separation a Bondapak™ C18 column (3.9 mm x 300 mm, 10 μ m) was utilized. The mobile phase was mixture of acetonitrile, methanol, and water (23:24:53 (v/v)). The injection volume was 10 μ L and E2 was detected at wavelength 225 nm.

6.2 Synthesis of porphyrins and metallic porphyrin complexes

6.2.1 Synthesis of 5,10,15,20-tetrakis(4-carboxyethylthio-2,3,5,6-tetrafluorophenyl)porphyrin

Porphyrin $\text{H}_2\text{TPPF}_{20}$ (**4**) (49.99 mg, 0.05 mmol, 1 eq) and 3-mercaptopropionic acid (0.02 mL, 0.22 mmol, 4.4 eq) were dissolved in 1.5 mL of DMF. Afterwards potassium carbonate (K_2CO_3) was added (52.44 mg, 0.38 mmol, 7.4 eq) and the reaction mixture was left stirring under an argon atmosphere, at room temperature for 1 h. The reaction was neutralized with a few drops of citric acid which led to the porphyrin's precipitation. The solid was filtrated and recrystallized in a mixture of methanol and chloroform. The porphyrin $\text{H}_2\text{TPPF}_{16}(\text{SC}_2\text{H}_4\text{COOH})_4$ (**1**) was obtained with a yield of 96.6% (65.33 mg, 0.05 mmol).

6.2.2 Synthesis of 5,10,15,20-tetrakis(4-carboxyphenylthio-2,3,5,6-tetrafluorophenyl)porphyrin

Porphyrin $\text{H}_2\text{TPPF}_{20}$ (**4**) (200.93 mg, 0.21 mmol, 1 eq) and 4-mercaptopbenzoic acid (139.20 mg, 0.90 mmol, 4.4 eq) were dissolved in 6 mL of DMF. Afterwards potassium carbonate (K_2CO_3) was added (209.90 mg, 1.52 mmol, 7.4 eq) and the reaction mixture was left stirring under an argon atmosphere, at room temperature for 1 h. The reaction was neutralized with a few drops of citric acid which led to the porphyrin's precipitation. The solid was filtrated and recrystallized in a mixture of methanol and chloroform. The porphyrin $\text{H}_2\text{TPPF}_{16}(\text{SC}_6\text{H}_4\text{COOH})_4$ (**2**) was isolated with a yield of 68.9%. (214.80 mg, 0.14 mmol).

6.2.3 Synthesis of metal porphyrin $\text{ZnTPPF}_{16}(\text{SC}_2\text{H}_4\text{COOH})_4$

Porphyrin $\text{H}_2\text{TPPF}_{16}(\text{SC}_2\text{H}_4\text{COOH})_4$ (**1**) (100.10 mg, 0.08 mmol, 1 eq) was mixed with zinc acetate anhydrous (21.60 mg, 0.12 mmol, 1.5 eq) in 50 mL of methanol. The reaction was left at reflux (oil around 70 °C) for 4 h, under vigorous stirring. The reaction was controlled by TLC and, once it was finished, a liquid-liquid extraction was performed with distilled water as aqueous phase and dichloromethane/methanol as organic phase. The organic phase was collected and concentrated by evaporation. The metal porphyrin was crystalized in a mixture of methanol and petroleum ether. The desired metallic complex was obtained with a yield of 66.7% (69.87 mg, 0.05 mmol):

6.2.4 Synthesis of metal porphyrin Mn(III)TPP(COOH)₄

Porphyrin **H₂TPP(COOH)₄ (3)** (61.00 mg, 0.08 mmol, 1 eq), manganese (II) acetate tetrahydrate (27.90 mg 0.11 mmol, 1.5 eq) and sodium acetate trihydrate (51.60 mg, 0.38 mmol, 5 eq) were mixed in 2.4 mL of acetic acid. The reaction occurred in suspension for 2 h and 30 min with strong agitation at 100 °C, with reflux. Afterwards ethyl acetate was added which immediately promoted the solid's precipitation. The solid was filtrated and washed with water until neutral pH. Metal porphyrin **Mn(III)TPP(COOH)₄ (7)** was obtained with a yield of 75.5% (52.60 mg, 0.06 mmol).

6.2.5 Synthesis of metal porphyrin Mn(III)TPPF₁₆(SC₆H₄COOH)₄

Porphyrin **H₂TPPF₁₆(SC₆H₄COOH)₄ (2)** (50.85 mg, 0.03 mmol, 1 eq) and manganese (II) acetate tetrahydrate (12.17 mg, 0.05 mmol, 1.5 eq) were mixed in 8.3 mL of DMF in a glass reactor. The glass reactor was closed under argon atmosphere. The reaction took place in suspension, overnight, with stirring, at 120 °C. Afterwards the reaction was left open to air for 24 h with stirring. After that more manganese (II) acetate tetrahydrate (12.17 mg, 0.05 mmol, 1.5 eq) was added and the reaction mixture was left open to air, with stirring, at 140 °C with reflux, for 2 h. The obtained solid was filtrated and dissolved in methanol. A few drops of HCl were added to precipitate the metal porphyrin **Mn(III)TPPF₁₆(SC₆H₄COOH)₄ (8)** which was then filtrated and collected with a yield of 35.2% (19.23 mg, 0.01mmol).

6.2.6 Synthesis of metal porphyrin Fe(III)CITPPF₁₆(SC₂H₄COOH)₄

Porphyrin **H₂TPPF₁₆(SC₂H₄COOH)₄ (1)** (100.40 mg, 0.08 mmol, 1 eq) and iron (II) chloride tetrahydrate (22.60 mg, 0.11 mmol, 1.5 eq) were mixed in 20 mL of acetic acid. The reaction was left stirring at reflux, under an argon atmosphere for 5 h. Afterwards, distilled water was added to precipitate the reaction product. The solid was filtrated and then redissolved in acetone. The acetone was then removed in a rotavapor and finally the product was crystalized from a mixture of dichloromethane/methanol (75:15) with a few drops of petroleum ether. Metal porphyrin **Fe(III)CITPPF₁₆(SC₂H₄COOH)₄ (9)** was obtained with a yield of 62.0% (66.45 mg, 0.05 mmol).

6.3 Preparation of porphyrin based MOFs

6.3.1 Preparation of MOF $\text{H}_2\text{TPP}(\text{COOH})_4\text{Zr}_4$

The free base porphyrin $\text{H}_2\text{TPP}(\text{COOH})_4$ (**3**) (50.57 mg; 0.06 mmol; 1 eq), was mixed with zirconium chloride anhydrous (78.00 mg; 0.33 mmol; 5.15 eq) and benzoic acid (2.70 g; 22.11 mmol; 340.1 eq) in 8 mL of DMF in a glass reactor. Before the reaction all the reagents were thoroughly dissolved by putting the reactor in an ultrasonic bath for a few seconds. For the reaction the glass reactor was put in an oil bath at approximately 120 °C, with slow agitation for approximately 19 hours. The obtained solid was washed with ethanol 4 times and once with acetone being centrifuged and filtrated after each wash. The MOF $\text{H}_2\text{TPP}(\text{COOH})_4\text{Zr}_4$ was obtained with quantitative yield (90.39 mg, 0.08 mmol).

6.3.2 Preparation of MOF $\text{Mn}(\text{III})\text{TPP}(\text{COOH})_4\text{Zr}_4$

The metal porphyrin $\text{Mn}(\text{III})\text{TPP}(\text{COOH})_4$ (**7**) (51.19 mg; 0.06 mmol; 1 eq), was mixed with zirconium chloride anhydrous (66.01 mg; 0.28 mmol; 5.15 eq) and benzoic acid (2.28 g; 18.71 mmol; 340.1 eq) in 4 mL of DMF in a glass reactor. Before the reaction all the reagents were thoroughly dissolved by putting the reactor in an ultrasonic bath for a few seconds. For the reaction the glass reactor was put in an oil bath at approximately 140 °C, with slow agitation for approximately 20 hours. The obtained solid was washed with ethanol 4 times and once with acetone being centrifuged and filtrated after each wash. The MOF $\text{Mn}(\text{III})\text{TPP}(\text{COOH})_4\text{Zr}_4$ was obtained with a yield of 96.0% (70.97 mg, 0.05 mmol).

6.4 Catalytic Studies

6.4.1 Preparation of catalyst stock solutions, photostability tests and $^1\text{O}_2$ production assay

For the preparation of homogeneous catalyst stock solutions, the porphyrins $\text{H}_2\text{TPP}(\text{COOH})_4$ (**3**) and $\text{Mn}(\text{III})\text{TPP}(\text{COOH})_4$ (**7**) (3.95 mg, 5×10^{-6} mol and 4.51 mg, 5×10^{-6} mol, respectively) were dissolved in 10 mL of a solution of distilled water and an aqueous saturated solution of potassium bicarbonate (90:10). Both solutions had concentrations of 500 μM and the pH value of each stock solution was 10.68 and 9.38, respectively

For the photostability tests, 20 μL (2.5 μM) of the stock solution were added to open glass vials with 4 mL of distilled water. The mixture was exposed to visible white light (18 mW/cm^2), with stirring for periods up to 4 hours. The results were analyzed by UV-Vis spectroscopy.

For the singlet oxygen assays 25 mL of a stock solution of DPBF (0.68 mg, 25×10^{-6} mol) were prepared in a mixture of DMF and distilled water (90:10). Stock solutions (100 μM) of the homogeneous catalysts porphyrins **H₂TPP(COOH)₄ (3)** (0.79 mg, 1 mmol) and **Mn(III)TPP(COOH)₄ (7)** (0.9 mg, 1 mmol) were prepared in the same mixture of DMF and distilled water (90:10). Five solutions of DPBF (16.5 μM) were prepared in a mixture of DMF and distilled water (9:1). To four of them were added the four catalysts studied: porphyrins **H₂TPP(COOH)₄ (3)** and **Mn(III)TPP(COOH)₄ (7)** (0.67 μM) and the MOFs **H₂TPP(COOH)₄Zr₄** (0.1 mg, 20.9 μM) and **Mn(III)TPP(COOH)₄Zr₄** (0.1 mg, 19.0 μM) and the remaining solution was the control with just DPBF. These 5 solutions were irradiated at room temperature, for a period of 21 minutes, with filtered white light (18 mW/cm^2). The light was filtered through a cut-off filter for wavelengths inferior to 550 nm. The reactions were controlled by UV-Vis in pre-determined intervals of time.

6.4.2 Photocatalytic oxidation of paracetamol

The catalytic studies were performed in small glass vials opened to the air. The reactions started by mixing the aqueous stock solution of PCM (130 μM , 20 ppm) with the catalyst. For the homogeneous catalytic studies, porphyrin **H₂TPP(COOH)₄ (3)** (13 μM) was added, and the mixture was homogenized for a few seconds and then a UV-Vis analysis was performed, corresponding to $t = 0$ min. After that the solutions were left with vigorous stirring, in the dark for 30 minutes after which another UV-Vis analysis was performed. Finally, the solutions were exposed to white light (18 mW/cm^2) for periods of time ranging between 45 and 180 minutes. Samples of the solutions were analyzed by UV-Vis spectroscopy at pre-determined periods of time. For the heterogeneous catalytic studies, the MOF **H₂TPP(COOH)₄Zr₄** was added (12.96 μM or 65.05 μM) and the solution was put in an ultrasonic bath for a few seconds in order to break the MOF grains into smaller particles, favoring the homogenization of the mixture. At this moment the solution was analyzed by UV-Vis, correspondent to $t = 0$ min. Afterwards the studies were performed following the same procedure as for the homogeneous studies. For the studies with the addition of hydrogen peroxide, the concentration of oxidant in the reaction mixture was 1.3×10^{-3} M. For the studies with variation of pH, the pH of each reaction solution was controlled with Britton-Robson buffer solutions of the pretended pH. The pH was measured before the start of the reaction and at the end.

6.4.3 Photocatalytic oxidation of 17 β -estradiol

The catalytic studies were performed in small glass vials opened to the air. The reactions started by mixing the methanol stock solution of E2 (147 μ M, 40 ppm) with the catalyst. For the homogeneous catalytic studies, porphyrin **H₂TPP(COOH)₄ (3)** (14.7 μ M) was added, and the mixture was homogenized for a few seconds and then a UV-Vis analysis was performed, correspondent to t = 0 min. After that the solutions were left with vigorous stirring, in the dark for 30 minutes after which another UV-Vis analysis was performed. Finally, the solutions were exposed to visible white light (18 mW/cm²) for periods of time ranging between 45 and 270 minutes. Samples of the solutions were analyzed by UV-Vis spectroscopy at pre-determined periods of time. For the heterogeneous catalytic studies, the MOF **H₂TPP(COOH)₄Zr₄** was added (14.7 μ M or 73.5 μ M) and the solution was put in an ultrasonic bath for a few seconds in order to break the MOF grains into smaller particles, favoring the homogenization of the mixture. At this moment the solution was analyzed by UV-Vis, correspondent to t = 0 min. Afterwards the studies were performed following the same procedure as for the homogeneous studies. The samples analyzed by HPLC were collected at the same moment samples were analyzed by UV-Vis. For the studies with the addition of hydrogen peroxide, the concentration of oxidant in the reaction mixture was 1.47 \times 10⁻³ M. For the studies with variation of pH, the pH of each reaction solution was controlled with Britton-Robson buffer solutions of the pretended pH. The pH was measured before the start of the reaction and at the end.

6.4.4 Oxidation of pharmaceuticals in dark conditions

The catalytic studies were performed in small glass vials opened to the air. The reactions started by mixing either the aqueous stock solution of PCM (130 μ M, 20 ppm), or the methanol stock solution of E2 (147 μ M, 40 ppm) with the catalyst. The homogeneous catalyst **Mn(III)TPP(COOH)₄ (7)** had concentration of 13.0 μ M and 14.7 μ M, in the reaction solutions, for the studies with PCM and E2 respectively. These concentrations correspond to a catalyst:substrate molar ratio of 0.1. The heterogeneous catalyst, MOF **Mn(III)TPP(COOH)₄Zr₄**, had concentration of 65.0 μ M and 73.5 μ M in the reaction solutions, for the studies with PCM and E2 respectively. These concentrations correspond to a catalyst:substrate molar ratio of 0.5.

After the addition of the catalyst an UV-Vis analysis was performed, correspondent to t = 0 min. Then hydrogen peroxide was added (1300 μ M and 1470 μ M, for the studies with PCM and E2 respectively) with an oxidant:substrate molar ratio of 10. Afterwards the reaction mixture was left under dark conditions, with vigorous stirring, for periods of time between 80 min and 180 min. Samples were collected and analyzed by UV-Vis spectroscopy at pre-determined periods of time.

6.5 Synthesis of tetra-pyridyl and tetra-S-pyridyl metallic porphyrin complexes

6.5.1 Synthesis of metal porphyrin CuTPyP

Porphyrin **H₂TPyP (11)** (50.13 mg, 0.08 mmol, 1 eq) was mixed with copper (II) acetate anhydrous (20.43 mg, 0.11 mmol, 1.5 eq) in 20 mL of a mixture of chloroform and methanol (67:33). The mixture was left with vigorous stirring, at reflux (oil around 65 °C), overnight. Once the reaction was finished a liquid-liquid extraction was performed with distilled water as aqueous phase and a mixture of dichloromethane and methanol (85:15) as organic phase. The organic phase was collected and concentrated by evaporation. The metal porphyrin was crystalized in a mixture of dichloromethane and methanol (85:15) and petroleum ether. The desired metallic complex was obtained with quantitative yield (58.13 mg, 0.09 mmol):

6.5.2 Synthesis of metal porphyrin CuTPPF₁₆(Spy)₄

Porphyrin **H₂TPPF₁₆(Spy)₄ (12)** (51.03 mg, 0.04 mmol, 1 eq) was mixed with copper (II) acetate anhydrous (7.48 mg, 0.04 mmol, 1.1 eq) in 20 mL of a mixture of chloroform and methanol (67:33). The mixture was left with vigorous stirring, at 65 °C, with reflux, overnight. Once the reaction was finished a liquid-liquid extraction was performed with distilled water as aqueous phase and a mixture of dichloromethane and methanol (85:15) as organic phase. The organic phase was collected and concentrated by evaporation. The metal porphyrin was crystalized in a mixture of dichloromethane and methanol (85:15) and petroleum ether. The desired metallic complex was obtained with a yield of 99.9% (53.32 mg, 0.04 mmol):

6.6 Preparation of tetra-pyridyl and tetra-S-pyridyl Por-MOFs

6.6.1 Preparation of MOF CuTPyPCu₄

Porphyrin **H₂TPyP (11)** (50.39 mg, 0.08 mmol, 1 eq), was mixed with copper (II) acetate anhydrous (136.5 mg; 0.80 mmol; 10 eq) in 12.5 mL of DMF in a glass reactor. Before the reaction all reagents were thoroughly dissolved by putting the reactor in an ultrasonic bath for a few seconds. For the reaction the glass reactor was put in an oil bath at 140 °C, with slow agitation for 24 hours. The obtained solid was then washed four times with a solution of dichloromethane and methanol (85:15) and

centrifuged and filtrated after each wash. MOF **CuTPyPCu₄** was obtained with quantitative yield (92.82 mg, 0.11 mmol).

6.6.2 Preparation of MOF **CuTPPF₁₆(Spy)₄Cu₄**

Porphyrin **H₂TPPF₁₆(Spy)₄ (12)** (50.79 mg, 0.04 mmol, 1 eq), was mixed with copper (II) acetate anhydrous (68.02 mg; 0.40 mmol; 10 eq) in 12.5 mL of DMF in a glass reactor. Before the reaction all the reagents were thoroughly dissolved by putting the reactor in an ultrasonic bath for a few seconds. For the reaction the glass reactor was put in an oil bath at 120 °C, with slow agitation for 24 hours. The obtained solid was then washed four times with a solution of dichloromethane and methanol (85:15) and centrifuged and filtrated after each wash. MOF **CuTPPF₁₆(Spy)₄Cu₄** was obtained with a yield of 70.1% (58.01 mg, 0.03 mmol).

7. References

1. Boreen, A. L., Arnold, W. A. & McNeill, K. Photodegradation of pharmaceuticals in the aquatic environment: A review. *Aquat. Sci.* **65**, 320–341 (2003).
2. Jones, O. A. H., Voulvoulis, N. & Lester, J. N. Human pharmaceuticals in wastewater treatment processes. *Crit. Rev. Environ. Sci. Technol.* **35**, 401–427 (2005).
3. Ebele, A. J., Abou-Elwafa Abdallah, M. & Harrad, S. Pharmaceuticals and personal care products (PPCPs) in the freshwater aquatic environment. *Emerg. Contam.* **3**, 1–16 (2017).
4. Richmond, E. K. *et al.* Pharmaceuticals and personal care products (PPCPs) are ecological disrupting compounds (EcoDC). *Elementa* **5**, (2017).
5. Sui, Q. *et al.* Occurrence, sources and fate of pharmaceuticals and personal care products in the groundwater: A review. *Emerg. Contam.* **1**, 14–24 (2015).
6. Gheorghe, S., Petre, J., Lucaci, I., Stoica, C. & Nita-Lazar, M. Risk screening of pharmaceutical compounds in Romanian aquatic environment. *Environ. Monit. Assess.* **188**, (2016).
7. Fent, K., Weston, A. A. & Caminada, D. Ecotoxicology of human pharmaceuticals. *Aquat. Toxicol.* **76**, 122–159 (2006).
8. Bound, J. P. & Voulvoulis, N. Pharmaceuticals in the aquatic environment - A comparison of risk assessment strategies. *Chemosphere* **56**, 1143–1155 (2004).
9. Al Aukidy, M., Verlicchi, P., Jelic, A., Petrovic, M. & Barcelò, D. Monitoring release of pharmaceutical compounds: Occurrence and environmental risk assessment of two WWTP effluents and their receiving bodies in the Po Valley, Italy. *Sci. Total Environ.* **438**, 15–25 (2012).
10. Pal, P. Treatment and Disposal of Pharmaceutical Wastewater: Toward the Sustainable Strategy. *Sep. Purif. Rev.* **47**, 179–198 (2018).
11. Michael, I. *et al.* Urban wastewater treatment plants as hotspots for the release of antibiotics in the environment: A review. *Water Res.* **47**, 957–995 (2013).
12. Schwartz, T., Kohnen, W., Jansen, B. & Obst, U. 2003 Fems Schwartz Et Al Detection of Antibiotic Resistant Bacteria and Their Resistance Genes in Wastewater, Surface Water and Drinking Water Biofilms.Pdf. *FEMS Microbiol. Ecol.* **43**, 325–335 (2003).
13. Kümmerer, K. Antibiotics in the aquatic environment - A review - Part I. *Chemosphere* **75**, 417–434 (2009).
14. Kümmerer, K. Antibiotics in the aquatic environment - A review - Part II. *Chemosphere* **75**, 435–441 (2009).

15. Bartolomeu, M., Neves, M. G. P. M. S., Faustino, M. A. F. & Almeida, A. Wastewater chemical contaminants: remediation by advanced oxidation processes. *Photochem. Photobiol. Sci.* **17**, 1573–1598 (2018).
16. Pei, M. *et al.* State of the art of tertiary treatment technologies for controlling antibiotic resistance in wastewater treatment plants. *Environ. Int.* **131**, 105026 (2019).
17. Gupta, V. K., Ali, I., Saleh, T. A., Nayak, A. & Agarwal, S. Chemical treatment technologies for waste-water recycling - An overview. *RSC Adv.* **2**, 6380–6388 (2012).
18. Wang, J. & Wang, S. Removal of pharmaceuticals and personal care products (PPCPs) from wastewater: A review. *J. Environ. Manage.* **182**, 620–640 (2016).
19. Miklos, D. B. *et al.* Evaluation of advanced oxidation processes for water and wastewater treatment – A critical review. *Water Res.* **139**, 118–131 (2018).
20. Dewil, R., Mantzavinos, D., Poulios, I. & Rodrigo, M. A. New perspectives for Advanced Oxidation Processes. *J. Environ. Manage.* **195**, 93–99 (2017).
21. Ma, D. *et al.* Critical review of advanced oxidation processes in organic wastewater treatment. *Chemosphere* **275**, (2021).
22. Xu, Y. *et al.* Advances in technologies for pharmaceuticals and personal care products removal. *J. Mater. Chem. A* **5**, 12001–12014 (2017).
23. Oppenländer, T. *Photochemical Purification of Water and Air: Advanced Oxidation Processes (AOPs) - Principles, Reaction Mechanisms, Reactor Concepts.* (2003 Wiley-VCH Verlag GmbH & Co. KGaA, 2002).
24. Ibhaddon, A. O. & Fitzpatrick, P. Heterogeneous photocatalysis: Recent advances and applications. *Catalysts* **3**, 189–218 (2013).
25. Andreozzi, R., Caprio, V., Insola, A. & Marotta, R. Advanced oxidation processes (AOP) for water purification and recovery. *Catal. Today* **53**, 51–59 (1999).
26. Chan, S. H. S., Wu, T. Y., Juan, J. C. & Teh, C. Y. Recent developments of metal oxide semiconductors as photocatalysts in advanced oxidation processes (AOPs) for treatment of dye waste-water. *Journal of Chemical Technology and Biotechnology* vol. 86 1130–1158 (2011).
27. Granados-Oliveros, G., Páez-Mozo, E. A., Ortega, F. M., Ferronato, C. & Chovelon, J. M. Degradation of atrazine using metalloporphyrins supported on TiO₂ under visible light irradiation. *Appl. Catal. B Environ.* **89**, 448–454 (2009).
28. Fernández, L. *et al.* Nanomagnet-photosensitizer hybrid materials for the degradation of 17 β -estradiol in batch and flow modes. *Dye. Pigment.* **142**, 535–543 (2017).
29. Huang, H., Song, W., Rieffel, J. & Lovell, J. F. Emerging applications of porphyrins in photomedicine. **3**, 1–15 (2015).

30. Alves, E. *et al.* An insight on bacterial cellular targets of photodynamic inactivation. *Future Med. Chem.* **6**, 141–164 (2014).
31. Almeida, A. *et al.* Photodynamic inactivation of pathogenic microorganisms in the environment : an efficient , cost-effective and sustainable technology. *Soc. Port. Microbiol.* **2012**, 1–6 (2012).
32. Michelin, C. & Hoffmann, N. Photosensitization and Photocatalysis-Perspectives in Organic Synthesis. *Am. Chem. Soc. Catal.* 12046–12055 (2018).
33. DeRosa, M. C. & Crutchley, R. J. Photosensitized singlet oxygen and its applications. *Coord. Chem. Rev.* **233–234**, 351–371 (2002).
34. Silvestri, S., Fajardo, A. R. & Iglesias, B. A. *Supported porphyrins for the photocatalytic degradation of organic contaminants in water: a review.* *Environmental Chemistry Letters* (Springer International Publishing, 2021).
35. Mon, M., Bruno, R., Ferrando-Soria, J., Armentano, D. & Pardo, E. Metal-organic framework technologies for water remediation: Towards a sustainable ecosystem. *J. Mater. Chem. A* **6**, 4912–4947 (2018).
36. Yaghi, O. M., Li, G. & Li, H. Selective binding and removal of guests in a microporous metal–organic framework. *Nature* **378**, 703–706 (1995).
37. Rowsell, J. L. C. & Yaghi, O. M. Metal-organic frameworks: A new class of porous materials. *Microporous Mesoporous Mater.* **73**, 3–14 (2004).
38. Pereira, C. F., Simoes, M. Q., Tomé, J. P. C. & Paz, F. A. A. Porphyrin-based metal-organic frameworks as heterogeneous catalysts in oxidation reactions. *Molecules* **21**, (2016).
39. Seth, S. & Matzger, A. J. Metal-Organic Frameworks: Examples, Counterexamples, and an Actionable Definition. *Cryst. Growth Des.* **17**, 4043–4048 (2017).
40. Batten, S. R. *et al.* Terminology of metal-organic frameworks and coordination polymers (IUPAC recommendations 2013). *Pure Appl. Chem.* **85**, 1715–1724 (2013).
41. Paz, F. A. A. *et al.* Ligand design for functional metal–organic frameworks. *Chem. Soc. Rev.* **41**, 1088–1110 (2012).
42. Silva, P., Vilela, S. M. F., Tomé, J. P. C. & Almeida Paz, F. A. Multifunctional metal-organic frameworks: From academia to industrial applications. *Chem. Soc. Rev.* **44**, 6774–6803 (2015).
43. Li, B., Wen, H., Zhou, W. & Chen, B. Porous Metal – Organic Frameworks for Gas Storage and Separation: What, How, and Why? *J. Phys. Chem. Lett.* **5**, 3468–3479 (2014).
44. Myunghyun Paik Suh, Hye Jeong Park, T. K. P. Hydrogen storage in metal organic frameworks (thesis-Jie Yang). *Chem. Rev.* **112**, 782–835 (2012).
45. Ma, S. *et al.* Further investigation of the effect of framework catenation on hydrogen uptake in

- metal - Organic frameworks. *J. Am. Chem. Soc.* **130**, 15896–15902 (2008).
46. Lee, Y. G., Moon, H. R., Cheon, Y. E. & Suh, M. P. A comparison of the H₂ sorption capacities of isostructural metal-organic frameworks with and without accessible metal sites: [Zn₂(abtc)(dmf)₂]₃ and [Cu₂(abtc)(dmf)₂]₃ versus [Cu₂(abtc)]₃. *Angew. Chemie - Int. Ed.* **47**, 7741–7745 (2008).
 47. Loiseau, T. *et al.* MIL-96, a porous aluminum trimesate 3D structure constructed from a hexagonal network of 18-membered rings and μ -3-oxo-centered trinuclear units. *J. Am. Chem. Soc.* **128**, 10223–10230 (2006).
 48. Senkovska, I. & Kaskel, S. High pressure methane adsorption in the metal-organic frameworks Cu₃(btc)₂, Zn₂(bdc)₂dabco, and Cr₃F(H₂O)₂O(bdc)₃. *Microporous Mesoporous Mater.* **112**, 108–115 (2008).
 49. Peng, Y. *et al.* Simultaneously high gravimetric and volumetric methane uptake characteristics of the metal-organic framework NU-111. *Chem. Commun.* **49**, 2992–2994 (2013).
 50. Ma, S. *et al.* Metal-organic framework from an anthracene derivative containing nanoscopic cages exhibiting high methane uptake. *J. Am. Chem. Soc.* **130**, 1012–1016 (2008).
 51. Millward, A. R. & Yaghi, O. M. Metal-organic frameworks with exceptionally high capacity for storage of carbon dioxide at room temperature. *J. Am. Chem. Soc.* **127**, 17998–17999 (2005).
 52. Furukawa, H. *et al.* Ultrahigh porosity in metal-organic frameworks. *Science.* **329**, 424–428 (2010).
 53. Harbuzaru, B. V. *et al.* A miniaturized linear pH sensor based on a highly photoluminescent self-assembled Europium(III) metal-organic framework. *Angew. Chemie - Int. Ed.* **48**, 6476–6479 (2009).
 54. Mesbah, A., Jacques, S., Rocca, E., François, M. & Steinmetz, J. Compact metal-organic frameworks for anti-corrosion applications: New binary linear saturated carboxylates of zinc. *Eur. J. Inorg. Chem.* 1315–1321 (2011).
 55. Corma, A., García, H. & Llabrés I Xamena, F. X. Engineering metal organic frameworks for heterogeneous catalysis. *Chem. Rev.* **110**, 4606–4655 (2010).
 56. Gautam, S. *et al.* Metal oxides and metal organic frameworks for the photocatalytic degradation: A review. *J. Environ. Chem. Eng.* **8**, 103726 (2020).
 57. Ai, L., Zhang, C., Li, L. & Jiang, J. Iron terephthalate metal-organic framework: Revealing the effective activation of hydrogen peroxide for the degradation of organic dye under visible light irradiation. *Appl. Catal. B Environ.* **148–149**, 191–200 (2014).
 58. Gao, Y. *et al.* Integrated adsorption and visible-light photodegradation of aqueous clofibrilic acid and carbamazepine by a Fe-based metal-organic framework. *Chem. Eng. J.* **330**, 157–165

- (2017).
59. Wang, D. *et al.* Simultaneously efficient adsorption and photocatalytic degradation of tetracycline by Fe-based MOFs. *J. Colloid Interface Sci.* **519**, 273–284 (2018).
 60. Milgrom, L. R. *The colours of life — an introduction to the chemistry of porphyrins and related compounds*. vol. 22 (Oxford University Press Inc., 1997).
 61. Küster, W. Beiträge zur Kenntnis des Bilirubins und Hämins. *Hoppe. Seylers. Z. Physiol. Chem.* **82**, 463–483 (1912).
 62. Fischer, H. Von & Orth, H. *Die Chemie des Pyrrols*. (Akademische Verlagsgesellschaft, 1937).
 63. Moss, G. P. Nomenclature of tetrapyrroles (Recommendations 1986). *Pure Appl. Chem.* **59**, 779–832 (1987).
 64. SMITH, K. M. Syntheses and chemistry of porphyrins. *J. Porphyr. Phthalocyanines* **04**, 319–324 (2000).
 65. Tomé, A. C., Neves, M. G. P. M. S. & Cavaleiro, J. A. S. Porphyrins and other pyrrolic macrocycles in cycloaddition reactions. *J. Porphyr. Phthalocyanines* **13**, 408–414 (2009).
 66. Kadish, K. M., Smith, K. M. & Guillard, R. *Handbook of Porphyrin Science*. (World Scientific Publisher, 2010).
 67. Zheng, W., Shan, N., Yu, L. & Wang, X. UV-visible, fluorescence and EPR properties of porphyrins and metalloporphyrins. *Dye. Pigment.* **77**, 153–157 (2008).
 68. Gomes, A. T. P. C., Neves, M. G. P. M. S. & Cavaleiro, J. A. S. Cancer , Photodynamic Therapy and Porphyrin-Type Derivatives. *Acad. Bras. Ciências* **90**, 993–1026 (2018).
 69. Pereira, P. M. R. *et al.* The role of galectin-1 in in vitro and in vivo photodynamic therapy with a galactodendritic porphyrin. *Eur. J. Cancer* **68**, 60–69 (2016).
 70. Chou, J., Kosal, M. E., Nalwa, H. S., Rakow, N. A. & Suslick, K. S. Applications of Porphyrins and Metalloporphyrins to Materials Chemistry. in *The Porphyrin Handbook* vol. 6 43–131 (2000).
 71. Stich, M. I. J., Fischer, L. H. & Wolfbeis, O. S. Multiple fluorescent chemical sensing and imaging. *Chem. Soc. Rev.* **39**, 3102–3114 (2010).
 72. Higashino, T. & Imahori, H. Porphyrins as excellent dyes for dye-sensitized solar cells: Recent developments and insights. *Dalt. Trans.* **44**, 448–463 (2015).
 73. Li, L. L. & Diao, E. W. G. Porphyrin-sensitized solar cells. *Chem. Soc. Rev.* **42**, 291–304 (2013).
 74. Costa e Silva, R., da Silva, L. O., de Andrade Bartolomeu, A., Brocksom, T. J. & de Oliveira, K. T. Recent applications of porphyrins as photocatalysts in organic synthesis: Batch and continuous flow approaches. *Beilstein J. Org. Chem.* **16**, 917–955 (2020).
 75. Min Park, J., Lee, J. H. & Jang, W. D. Applications of porphyrins in emerging energy conversion

- technologies. *Coord. Chem. Rev.* **407**, 213157 (2020).
76. Nam, W. High-valent iron(IV)-oxo complexes of heme and non-heme ligands in oxygenation reactions. *Acc. Chem. Res.* **40**, 522–531 (2007).
 77. Nakagaki, S., Castro, K. A. D. F., Neves, M. da G. P. M. S., do Amparo Faustino, M. & Iamamoto, Y. The research on porphyrins and analogues in Brazil: A small review covering catalytic and other applications since the beginning at Universidade de São Paulo in Ribeirão Preto until the joint venture between Brazilian researchers and colleagues from Unive. *J. Braz. Chem. Soc.* **30**, 2501–2535 (2019).
 78. Abrahams, B. F., Hoskins, B. F. & Robson, R. A New Type of Infinite 3D Polymeric Network Containing 4-Connected, Peripherally Linked Metalloporphyrin Building Blocks. *J. Am. Chem. Soc.* **113**, 3606–3607 (1991).
 79. Huh, S., Kim, S. J. & Kim, Y. Porphyrinic metal-organic frameworks from custom-designed porphyrins. *CrystEngComm* **18**, 345–368 (2016).
 80. Gao, W. Y., Chrzanowski, M. & Ma, S. Metal-metalloporphyrin frameworks: A resurging class of functional materials. *Chem. Soc. Rev.* **43**, 5841–5866 (2014).
 81. Zhao, M., Ou, S. & Wu, C. De. Porous metal-organic frameworks for heterogeneous biomimetic catalysis. *Acc. Chem. Res.* **47**, 1199–1207 (2014).
 82. Chen, Y. & Ma, S. Biomimetic catalysis of metal-organic frameworks. *Dalt. Trans.* **45**, 9744–9753 (2016).
 83. Feng, D. *et al.* Zirconium-metalloporphyrin PCN-222: Mesoporous metal-organic frameworks with ultrahigh stability as biomimetic catalysts. *Angew. Chemie - Int. Ed.* **51**, 10307–10310 (2012).
 84. Xie, M. H., Yang, X. L., Zou, C. & Wu, C. De. A SnIV-porphyrin-based metal-organic framework for the selective photo-oxygenation of phenol and sulfides. *Inorg. Chem.* **50**, 5318–5320 (2011).
 85. Johnson, J. A., Zhang, X., Reeson, T. C., Chen, Y. S. & Zhang, J. Facile control of the charge density and photocatalytic activity of an anionic indium porphyrin framework via in situ metalation. *J. Am. Chem. Soc.* **136**, 15881–15884 (2014).
 86. Pereira, C. F. *et al.* Detoxification of a Mustard-Gas Simulant by Nanosized Porphyrin-Based Metal-Organic Frameworks. *ACS Appl. Nano Mater.* **2**, 465–469 (2019).
 87. Jiang, Z. W. *et al.* Controllable Synthesis of Porphyrin-Based 2D Lanthanide Metal–Organic Frameworks with Thickness- and Metal-Node-Dependent Photocatalytic Performance. *Angew. Chemie - Int. Ed.* **59**, 3300–3306 (2020).
 88. Thandu, M., Comuzzi, C. & Goi, D. Phototreatment of water by organic photosensitizers and comparison with inorganic semiconductors. *Int. J. Photoenergy* **2015**, 10–12 (2015).

89. Murphy, S. *et al.* Photocatalytic activity of a porphyrin/TiO₂ composite in the degradation of pharmaceuticals. *Appl. Catal. B Environ.* **119–120**, 156–165 (2012).
90. He, Y. *et al.* Construction of a new cascade photogenerated charge transfer system for the efficient removal of bio-toxic levofloxacin and rhodamine B from aqueous solution: Mechanism, degradation pathways and intermediates study. *Environ. Res.* **187**, 109647 (2020).
91. Carrasco, S., Sanz-Marco, A. & Martín-Matute, B. Fast and Robust Synthesis of Metalated PCN-222 and Their Catalytic Performance in Cycloaddition Reactions with CO₂. *Organometallics* **38**, 3429–3435 (2019).
92. Lourenço, L. M. O. *et al.* Synthesis, characterization and electrochemical properties of meso-thiocarboxylate-substituted porphyrin derivatives. *J. Porphyrins Phtalocyanines* **18**, 967–974 (2014).
93. Lindsay, J. R., Iamamoto, Y. & Vinhado, S. Oxidation of alkanes by iodosylbenzene (PhIO) catalysed by supported Mn(III) porphyrins: Activity and mechanism. *J. Mol. Catal. A Chem.* **252**, 23–30 (2006).
94. Castro, K. A. D. D. F. *et al.* Synthesis of new metalloporphyrin derivatives from [5,10,15,20-tetrakis(pentafluorophenyl)porphyrin] and 4-mercaptobenzoic acid for homogeneous and heterogeneous catalysis. *Appl. Catal. A Gen.* **503**, 9–19 (2015).
95. Takagi, S., Eguchi, M., Tryk, D. A. & Inoue, H. Porphyrin photochemistry in inorganic/organic hybrid materials: Clays, layered semiconductors, nanotubes, and mesoporous materials. *J. Photochem. Photobiol. C Photochem. Rev.* **7**, 104–126 (2006).
96. Vail, S. A. *et al.* Synthesis and fluorescence properties of a porphyrin-fullerene molecular wire. *J. Phys. Org. Chem.* **17**, 814–818 (2004).
97. Venkatramaiah, N., Pereira, C. F., Mendes, R. F., Paz, F. A. A. & Tomé, J. P. C. Phosphonate appended porphyrins as versatile chemosensors for selective detection of trinitrotoluene. *Anal. Chem.* **87**, 4515–4522 (2015).
98. Piccirillo, G. *et al.* Supported metalloporphyrins as reusable catalysts for the degradation of antibiotics: Synthesis, characterization, activity and ecotoxicity studies. *Appl. Catal. B Environ.* **282**, (2021).
99. Kobayashi, H., Higuchi, T., Kaizu, Y., Osada, H. & Aoki, M. Electronic Spectra of Tetraphenylporphyrinatoiron(III) Methoxide. *Bull. Chem. Soc. Jpn.* **48**, 3137–3141 (1975).
100. Xu, Q. *et al.* Manganese porphyrin-based metal-organic framework for synergistic sonodynamic therapy and ferroptosis in hypoxic tumors. *Theranostics* **11**, 1937–1952 (2021).
101. Mboula, V. M. *et al.* Photocatalytic degradation of estradiol under simulated solar light and assessment of estrogenic activity. *Appl. Catal. B Environ.* **162**, 437–444 (2015).

102. Mai, J., Sun, W., Xiong, L., Liu, Y. & Ni, J. Titanium dioxide mediated photocatalytic degradation of 17 β -estradiol in aqueous solution. *Chemosphere* **73**, 600–606 (2008).
103. Moctezuma, E., Leyva, E., Aguilar, C. A., Luna, R. A. & Montalvo, C. Photocatalytic degradation of paracetamol: Intermediates and total reaction mechanism. *J. Hazard. Mater.* **243**, 130–138 (2012).
104. Yang, L., Yu, L. E. & Ray, M. B. Degradation of paracetamol in aqueous solutions by TiO₂ photocatalysis. *Water Res.* **42**, 3480–3488 (2008).
105. Pasternack, R. F. *et al.* On the Aggregation of Meso-Substituted Water-Soluble Porphyrins. *J. Am. Chem. Soc.* **94**, 4511–4517 (1972).
106. Jallouli, N., Elghniji, K., Trabelsi, H. & Ksibi, M. Photocatalytic degradation of paracetamol on TiO₂ nanoparticles and TiO₂/cellulosic fiber under UV and sunlight irradiation. *Arab. J. Chem.* **10**, 3640–3645 (2017).
107. Vogna, D., Marotta, R., Napolitano, A. & Ischia, M. Advanced Oxidation Chemistry of Paracetamol. UV/H₂O₂-Induced Hydroxylation/Degradation Pathways and 15 N-Aided Inventory of Nitrogenous Breakdown Products. *J. Org. Chem.* **67**, 6143–6151 (2002).
108. Dalmázio, I., Alves, T. M. A. & Augusti, R. An Appraisal on the Degradation of Paracetamol by TiO₂/UV System in Aqueous Medium. Product Identification by Gas Chromatography-Mass Spectrometry (GC-MS). *J. Braz. Chem. Soc.* **19**, 81–88 (2008).
109. Zhang, Y., Zhou, J. L. & Ning, B. Photodegradation of estrone and 17 β -estradiol in water. *Water Res.* **41**, 19–26 (2007).
110. Galindo, C., Jacques, P. & Kalt, A. Photodegradation of the aminoazobenzene acid orange 52 by three advanced oxidation processes: UV/H₂O₂, UV/TiO₂ and VIS/TiO₂ Comparative mechanistic and kinetic investigations. *J. Photochem. Photobiol. A Chem.* **130**, 35–47 (2000).
111. Shourong, Z., Qingguo, H., Jun, Z. & Bingkun, W. A study on dye photoremoval in TiO₂ suspension solution. *J. Photochem. Photobiol. A Chem.* **108**, 235–238 (1997).
112. Woodard & Curran, I. 7 Methods for Treating Wastewaters from Industry. in *Industrial Waste Treatment Handbook* 149–334 (Butterworth-Heinemann, 2006).
113. Ohko, Y. *et al.* 17 β -estradiol degradation by TiO₂ photocatalysis as a means of reducing estrogenic activity. *Environ. Sci. Technol.* **36**, 4175–4181 (2002).
114. Xie, M. H. *et al.* Highly efficient C-H oxidative activation by a porous Mn III-porphyrin metal-organic framework under mild conditions. *Chem. - A Eur. J.* **19**, 14316–14321 (2013).
115. Kopylovich, M. N. *et al.* Catalytic Oxidation of Alcohols: Recent Advances. *Adv. Organomet. Chem.* **63**, 91–174 (2015).
116. Parmeggiani, C. & Cardona, F. Transition metal based catalysts in the aerobic oxidation of

- alcohols. *Green Chem.* **14**, 547–564 (2012).
117. Castro, K. A. D. F. *et al.* Copper–Porphyrin–Metal–Organic Frameworks as Oxidative Heterogeneous Catalysts. *ChemCatChem* **9**, 2939–2945 (2017).
118. Ohmura, T., Usuki, A., Fukumori, K., Ohta, T. & Ito, M. New Porphyrin-Based Metal–Organic Framework with High Porosity: 2-D Infinite 22.2-Å Square-Grid Coordination Network. *Inorg. Chem.* **45**, 1–3 (2010).
119. Castro, K. A. D. F. *et al.* Porphyrinic coordination polymer-type materials as heterogeneous catalysts in catechol oxidation. *Polyhedron* **158**, 478–484 (2019).

8. Appendices

8.1 Appendix A: characterization of porphyrins and metalloporphyrins

In this section can be found the UV-Vis spectra of the porphyrins synthesized during the development of this project, 5,10,15,20-tetrakis(4-carboxyethylthio-2,3,5,6-tetrafluorophenyl)porphyrin ($\text{H}_2\text{TPPF}_{16}(\text{SC}_2\text{H}_4\text{COOH})_4$, 1) (Figure 8.1) and 5,10,15,20-tetrakis(4-carboxyphenylthio-2,3,5,6-tetrafluorophenyl)porphyrin ($\text{H}_2\text{TPPF}_{16}(\text{SC}_6\text{H}_4\text{COOH})_4$, 2) (Figure 8.2), as well as of the metalloporphyrins prepared, $\text{ZnTPPF}_{16}(\text{SC}_2\text{H}_4\text{COOH})_4$ (5) (Figure 8.3), $\text{Mn(III)TPP}(\text{COOH})_4$ (7) (Figure 8.4), $\text{Mn(III)TPPF}_{16}(\text{SC}_6\text{H}_4\text{COOH})_4$ (8) (Figure 8.5) and $\text{Fe(III)CITPF}_{16}(\text{SC}_2\text{H}_4\text{COOH})_4$ (9) (Figure 8.6).

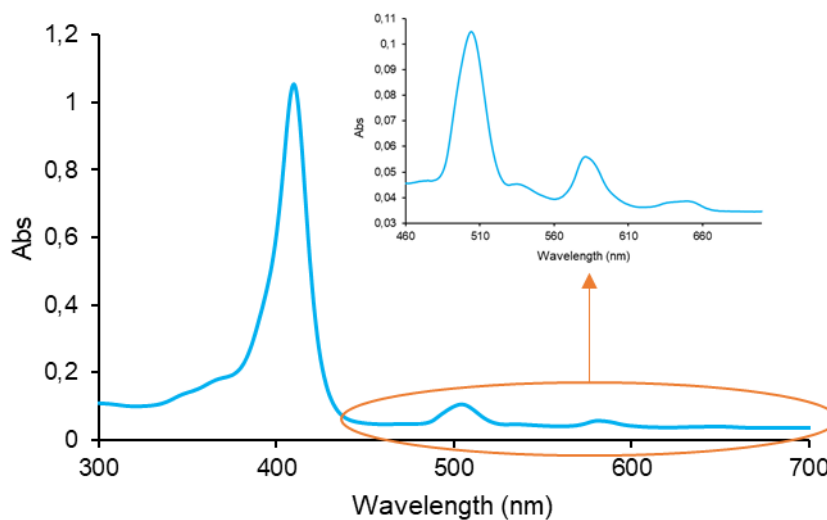


Figure 8.1. UV-Vis spectra of porphyrin $\text{H}_2\text{TPPF}_{16}(\text{SC}_2\text{H}_4\text{COOH})_4$ (1) in methanol.

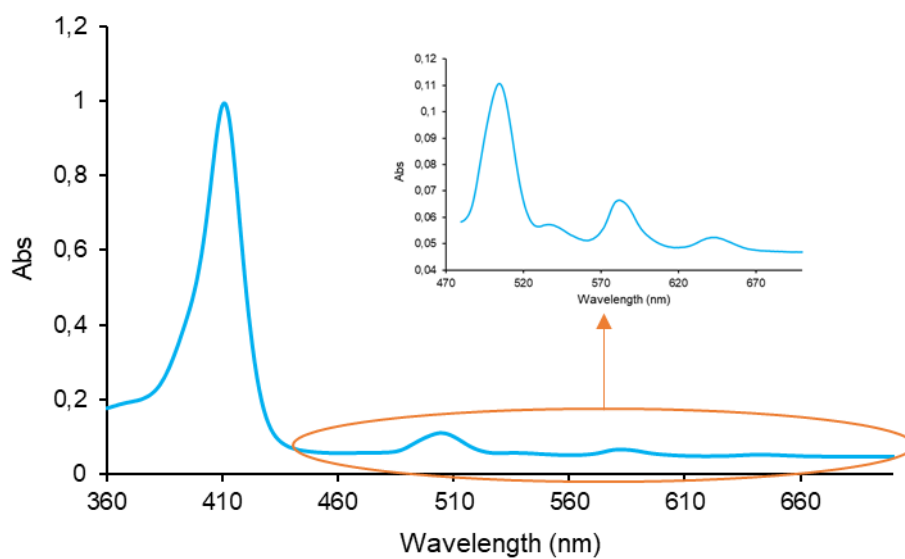


Figure 8.2. UV-Vis spectra of porphyrin $\text{H}_2\text{TPPF}_{16}(\text{SC}_6\text{H}_4\text{COOH})_4$ (**2**) in methanol.

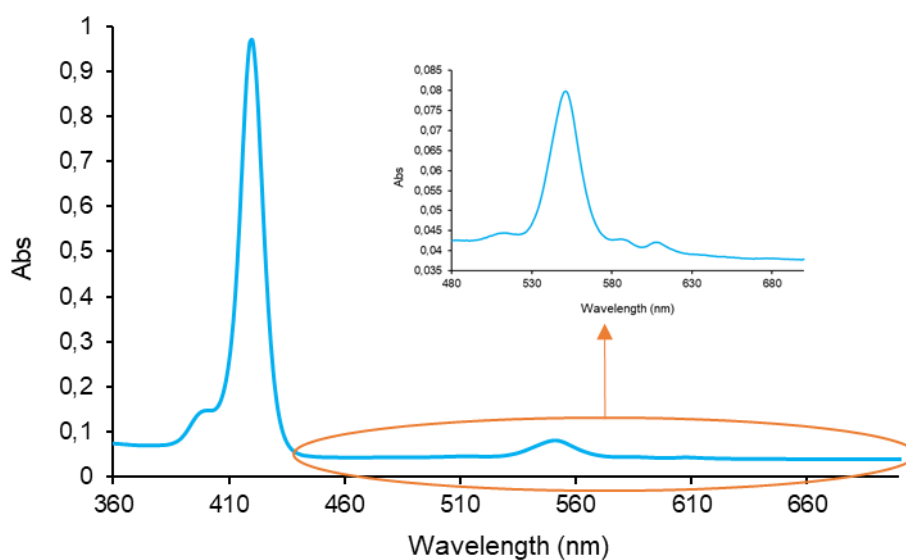


Figure 8.3. UV-Vis spectra of metalloporphyrin $\text{ZnTPPF}_{16}(\text{SC}_2\text{H}_4\text{COOH})_4$ (**5**) in methanol.

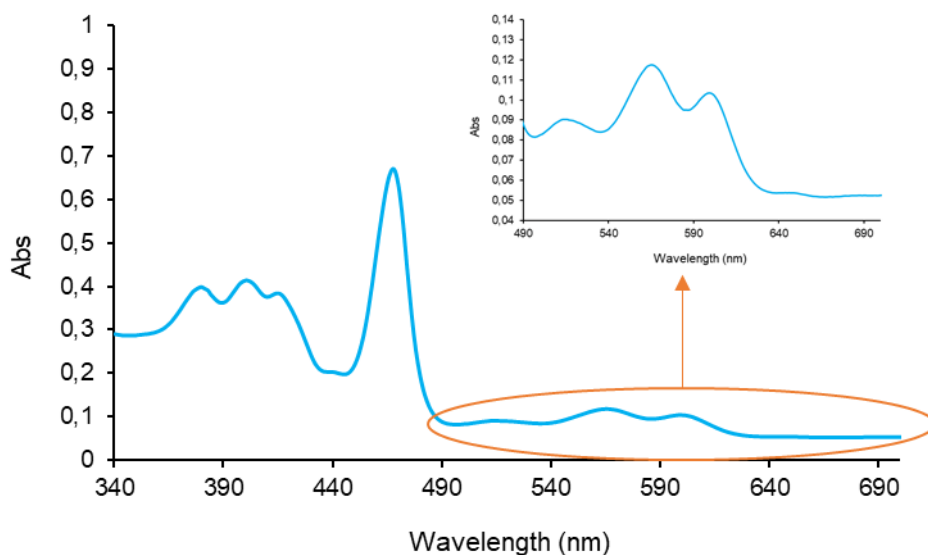


Figure 8.4. UV-Vis spectra of metalloporphyrin **Mn(III)TPP(COOH)₄ (7)** in methanol.

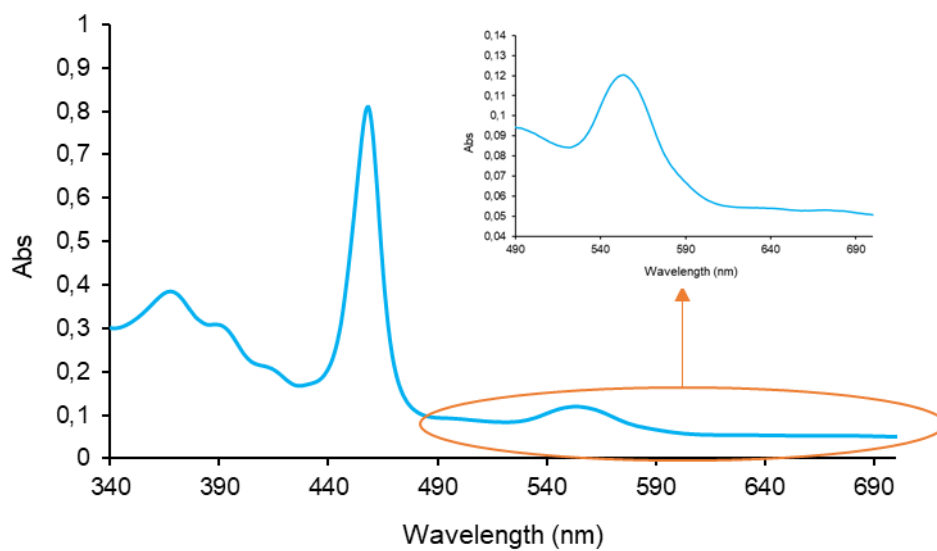


Figure 8.5. UV-Vis spectra of metalloporphyrin **Mn(III)TPPF₁₆(SC₆H₄COOH)₄ (8)** in methanol.

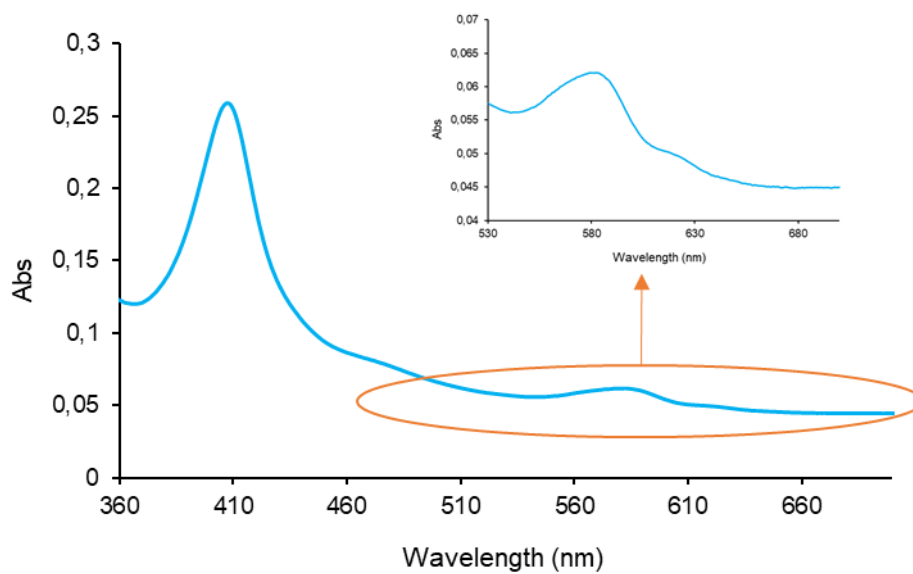


Figure 8.6. UV-Vis spectra of metalloporphyrin $\text{Fe(III)CITPPF}_{16}(\text{SC}_2\text{H}_4\text{COOH})_4$ (9) in methanol.

8.2 Appendix B: Photocatalytic studies with the metalloporphyrin Mn(III)TPP(COOH)₄ and its respective Por-MOF

The singlet oxygen assays with the manganese materials revealed that neither had the capability of generating ¹O₂. This way, the photocatalytic studies with these materials were performed as a control, only to compare them with the results of the free base porphyrin H₂TPP(COOH)₄ (3) and its respective zirconium Por-MOF.

The studies consisted in irradiating solutions of PCM (130 μM, 20 ppm) (Figure 8.7) or E2 (147 μM, 40 ppm) (Figure 8.8) with either the metalloporphyrin Mn(III)TPP(COOH)₄ (7) (13 μM or 14.7 μM, respectively) or the Por-MOF Mn(III)TPP(COOH)₄Zr₄ (13 μM or 14.7 μM, respectively) for maximum periods between 180 and 210 minutes. Before irradiation the solutions were left in dark conditions, with vigorous stirring for 30 minutes.

The results of these reactions confirmed our predictions. Neither the homogeneous photocatalysis nor the heterogeneous resulted in degradation of the pharmaceuticals. This confirms the hypothesis that the manganese materials were not photocatalytically active.

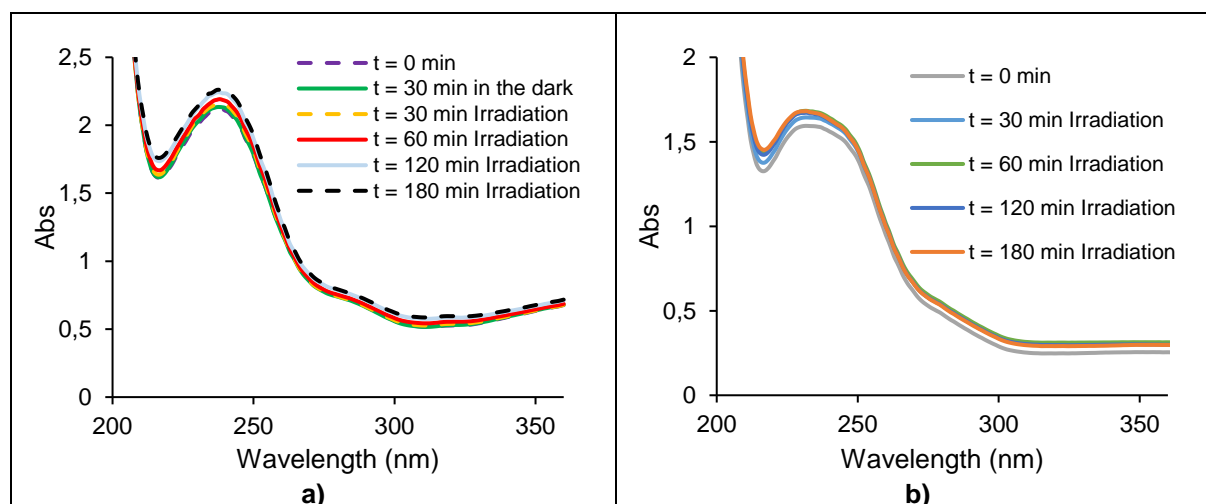


Figure 8.7. UV-Vis spectra of the reaction solutions with PCM (130 μM, 20 ppm) and a): the metalloporphyrin Mn(III)TPP(COOH)₄ (7) (13 μM) and b): the Por-MOF Mn(III)TPP(COOH)₄Zr₄ (13 μM). The solutions were irradiated for 180 minutes, and samples were analyzed at predetermined periods of time.

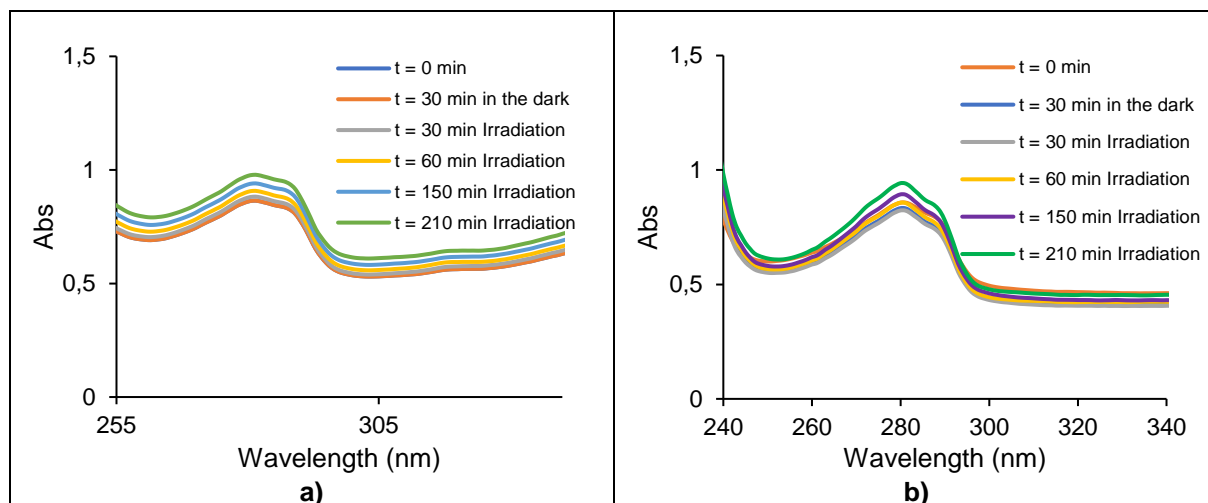


Figure 8.8. UV-Vis spectra of the reaction solutions with E2 (147 μM , 40 ppm) and **a)** the metalloporphyrin **Mn(III)TPP(COOH)₄ (7)** (14.7 μM) and **b)** the Por-MOF **Mn(III)TPP(COOH)₄Zr₄** (14.7 μM). The solutions were irradiated for 210 minutes, and samples were analyzed at predetermined periods of time.

8.3 Appendix C: Catalytic studies in dark conditions

At the beginning of the catalytic studies with metalloporphyrin **Mn(III)TPP(COOH)₄ (7)** and the Por-MOF **Mn(III)TPP(COOH)₄Zr₄**, four reactions were performed in order to attest whether the pharmaceutical substrates suffered any degradation with just the catalyst or the oxidant agent, under dark conditions with vigorous stirring for a predetermined period of time. As expected, the results of these reactions showed no degradation of the substrate.

The two reactions with PCM consisted in preparing reaction mixtures of PCM (130 μM , 20 ppm) with either the porphyrin catalyst **Mn(III)TPP(COOH)₄ (7)** (13 μM , molar ratio catalyst/substrate = 0.1) or H_2O_2 (1300 μM , molar ratio oxidant/substrate = 10) as oxidant agent (**Figure 8.9** and **Figure 8.10**, respectively). Then, the reaction mixture was left under vigorous stirring in dark conditions for 3 hours.

The two reactions with E2 consisted in preparing reaction mixtures of E2 (147 μM , 40 ppm) with either the porphyrin catalyst **Mn(III)TPP(COOH)₄ (7)** (14.7 μM , molar ratio catalyst/substrate = 0.1) or H_2O_2 (1470 μM , molar ratio oxidant/substrate = 10) as oxidant agent (**Figure 8.11** and **Figure 8.12**, respectively).

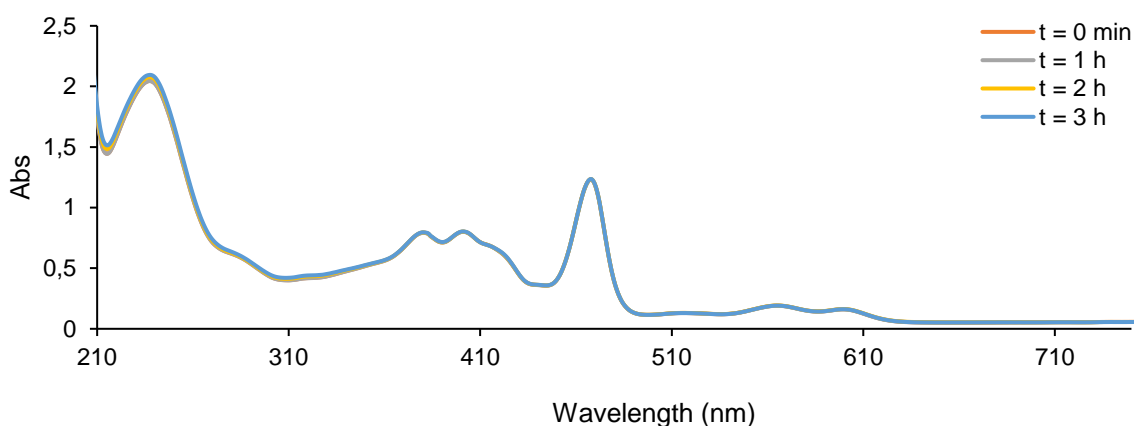


Figure 8.9. UV-Vis spectra of the reaction with PCM (130 μM , 20 ppm) and the porphyrin catalyst **Mn(III)TPP(COOH)₄ (7)** (13 μM , molar ratio catalyst/substrate = 0.1), left under vigorous stirring and dark conditions for 3 hours.

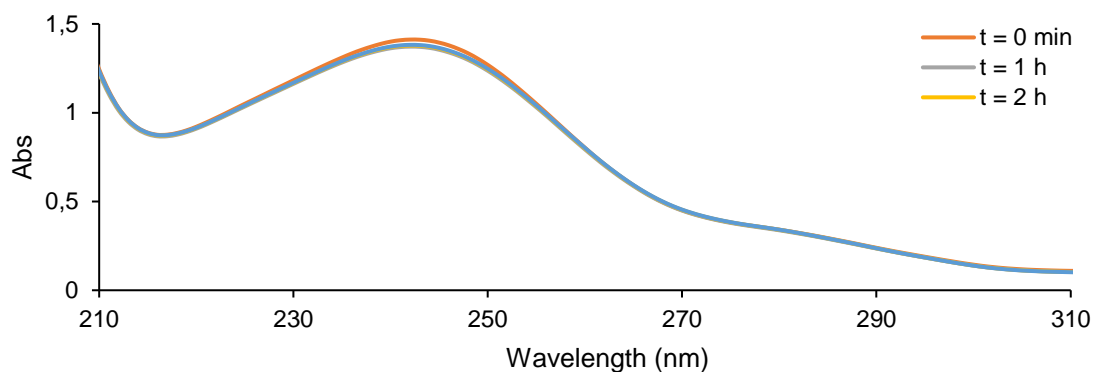


Figure 8.10. UV-Vis spectra of the reaction with PCM (130 μM, 20 ppm) and H₂O₂ (1300 μM, molar ratio oxidant/substrate = 10) as oxidant agent, left under vigorous stirring and dark conditions for 3 hours.

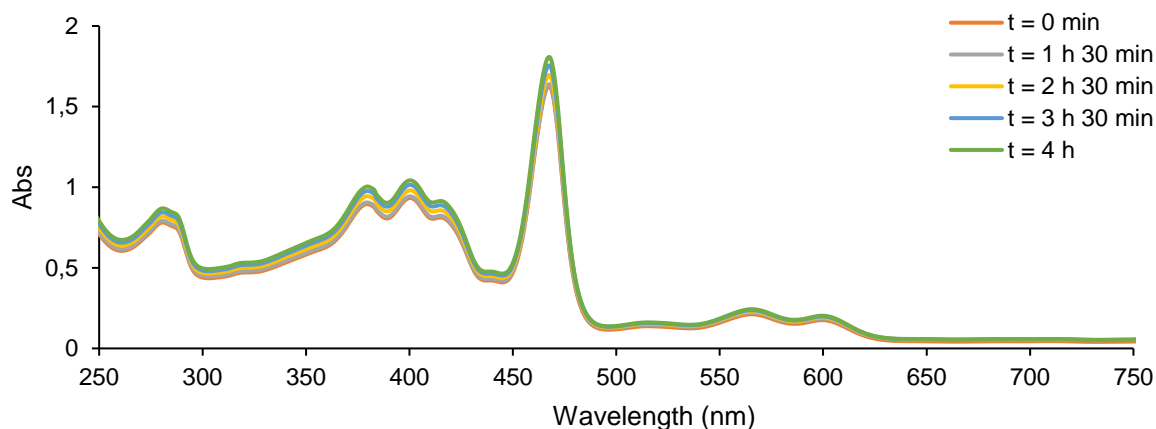


Figure 8.11. UV-Vis spectra of the reaction with E2 (147 μM, 40 ppm) and the porphyrin catalyst Mn(III)TPP(COOH)₄ (7) (14.7 μM, molar ratio catalyst/substrate = 0.1), left under vigorous stirring and dark conditions for 4 hours.

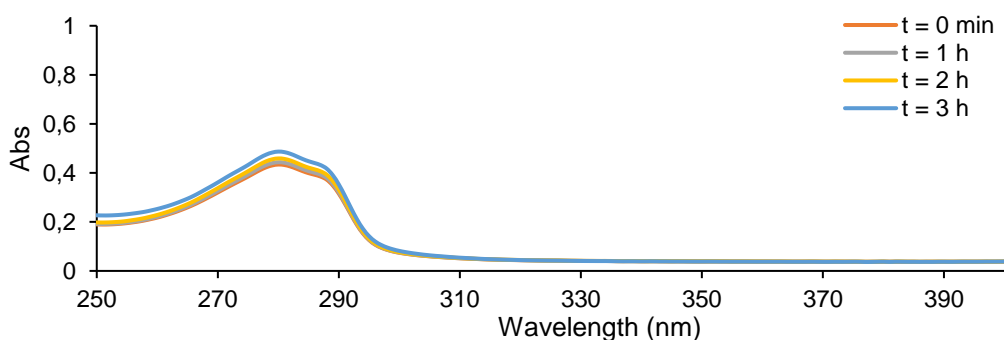


Figure 8.12. UV-Vis spectra of the reaction with E2 (147 μM, 40 ppm) and H₂O₂ (1470 μM, molar ratio oxidant/substrate = 10) as oxidant agent, left under vigorous stirring and dark conditions for 3 hours.

8.4 Appendix D: Characterization of tetra-pyridyl and tetra-S-pyridyl metalloporphyrins

The tetra-pyridyl and tetra-S-pyridyl copper metalloporphyrins synthesized during this project were characterized by UV-Vis spectroscopy. **Figure 8.13** shows the spectra referring to **CuTPyP (13)** while **Figure 8.14** presents the spectra of **CuTPPF₁₆(SPy)₄ (14)**.

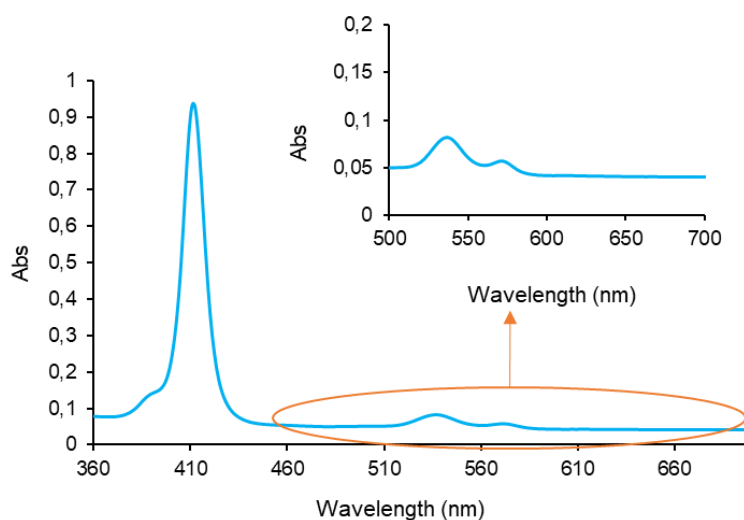


Figure 8.13. UV-Vis spectra of metalloporphyrin **CuTPyP (13)** in a mixture of dichloromethane and methanol (85:15).

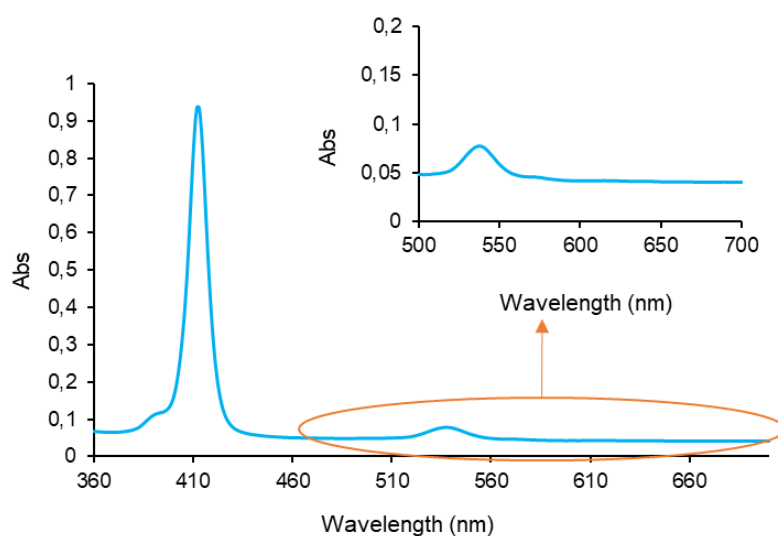



Figure 8.14. UV-Vis spectra of metalloporphyrin **CuTPPF₁₆(SPy)₄ (14)** in a mixture of dichloromethane and methanol (85:15).


8.5 Communications

Ribeiro, J. R. P., Figueira, F., Soliman, M. M. A., Fernandes, S. R. G., Guedes da Silva, M. F. C., Pombeiro, A. J. L., Almeida Paz, F. A., Alegria, E. C. B. A., Tomé, J. P. C., Pharmaceuticals photodegradation by zirconium-porphyrin MOF, Poster presentation, 1st edition of Iberian Symposium of Young Photochemists, Online, 18th-21st October 2021.



TÉCNICO LISBOA

Pharmaceuticals photodegradation by zirconium-porphyrin MOF




ISEL


João R. P. Ribeiro,^{1*} Flávio Figueira,² Mohamed M. A. Soliman,³ Sara R. G. Fernandes,¹ M. Fátima C. Guedes da Silva,¹ Armando J. L. Pombeiro,¹ Filipe A. Almeida Paz,² Elisabete C. B. A. Alegria,^{1,3} João P. C. Tomé¹

¹ CQE & Departamento de Engenharia Química, Instituto Superior Técnico, Universidade de Lisboa, 1049-001 Lisbon, Portugal
² CICECO - Aveiro Institute of Materials, Department of Chemistry, University of Aveiro, 3810-193 Aveiro, Portugal
³ Departamento de Engenharia Química, ISEL-Instituto Superior de Engenharia de Lisboa, 1959-007 Lisboa, Portugal.


* joao.policarpo.ribeiro@tecnico.ulisboa.pt



COE



FCT



Introduction

There are a wide range of pharmaceuticals used to treat many medical conditions. Though being a positive aspect of modern society when it comes to healthcare, it poses nevertheless a serious environmental problem as an increasing volume of pharmaceutical compounds are being detected as contaminants in wastewaters and, concomitantly, in water reserves.^{1,2} It is imperative to develop and implement effective and efficient ways to treat water by removing or, at least, transforming this type of pollutants into more environmental benign species. Advanced Oxidation Processes (AOPs) have shown to be an interesting solution to rapidly oxidize these organic pollutants to less hazardous products³, and porphyrin-based Metal-Organic Frameworks have been found to be effective as catalysts to this end.^{4,5} In this context we prepared PCN-224 and tested its photocatalytic activity in the degradation of paracetamol⁶.

Methods

Synthesis: The zirconium-porphyrin MOF was synthesized using a solvothermal method. The porphyrin H₂TPP(COOH)₄ was mixed with zirconium chloride and benzoic acid in DMF. The mixture was slowly stirred for 20 hours at 130 °C. The obtained solid was characterized by X-ray diffraction and the analysis showed its crystallinity as shown in Figure 1.

Photocatalytic studies:

- A stock solution of H₂TPP(COOH)₄ was added to an aqueous solution of paracetamol, 20ppm (130 μM). The concentration of catalyst was 13 μM. The solution was irradiated with white light for 30 minutes and samples were analysed by UV-Vis spectroscopy in intervals of 5 minutes.
- The photocatalytic studies with PCN-224 as photocatalyst have not been optimized yet.



Figure 1

Results

- Figure 2 shows the UV-Vis spectrum of the various samples analysed during the photocatalytic study of degradation of paracetamol. It is possible to see that only after 5 minutes of irradiation the paracetamol is completely depleted and that a subproduct is formed with a peak at approximately 290 nm. After 30 minutes of irradiation the previously formed subproduct is also depleted and a new subproduct is formed with its absorption peak being situated at approximately 270 nm.
- The fact the porphyrin H₂TPP(COOH)₄ is capable of the degradation of paracetamol is indicative that MOF PCN-224 should also be able to oxidize the substrate via AOP.

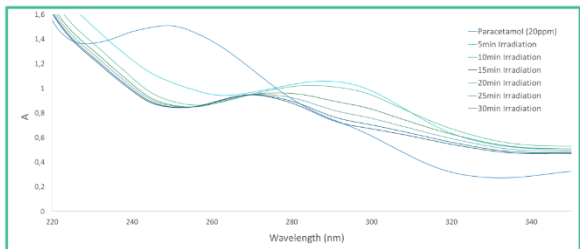


Figure 2

Future Work

- Optimize the conditions for photodegradation of paracetamol and other pharmaceuticals with the PCN-224 MOF.
- Perform multiple catalytic cycles to access the MOFs capacity to be recycled without losing activity.

Acknowledgements: We wish to thank FCT for the financial support to CQE (UIDB/00100/2020 and PTDC/QUI-QIN/29778/2017) and CICECO (UIDB/50011/2020 & UIDP/50011/2020) research units, through national funds and where applicable co-financed by FEDER, within the PT2020 Partnership Agreement. The research contract of FF (REF-168-89-ARI/2018) is funded by national funds (OE), through FCT, in the scope of the framework contract foreseen in nos. 4, 5 and 6 of article 23 of the Decree-Law 57/2016, of 29 August, changed by Law 57/2017, of 19 July.

References : [1] A. L. Boreen, W. A. Arnold, K. McNeill, *Aquatic Sciences*, **2003**, 65, 320-341. [2] M. Mon *et al.*, *J. Mater. Chem. A*, **2018**, 6, 4912. [3] Y. Xu, *et al.*, *J. Mater. Chem. A*, **2017**, 5, 12001. [4] P. Silva, *et al.*, *Chem. Soc. Rev.*, **2015**, 44, 6774. [5] C. F. Pereira, *et al.*, *Molecules*, **2016**, 21,1348. [6] D. Feng, *et al.*, *Angew. Chem. Int. Ed.*, **2012**, 51, 10307-10310